Evidence of change in the Sea of Okhotsk between 1949-1952 and 1993 from Hydrographic Data: Implications for the North Pacific.

by
Katherine Louise Hill
B.Sc.(Hons), University of Southampton, U.K. 1998.

A Thesis Submitted in Partial Fulfilment of the
Requirements for the Degree of

MASTER OF SCIENCE

in the School of Earth and Ocean Sciences

[redacted]

Dr. A. J. Weaver, Supervisor (School of Earth and Ocean Sciences).

[redacted]

Dr. H.J. Freeland, Member (Institute of Ocean Sciences).

[redacted]

Dr. J. Fyfe, Member (School of Earth and Ocean Sciences).

[redacted]

Dr. A. Bychkov, External Examiner (Institute of Ocean Sciences).

Supervisor: Dr A.J. Weaver.

Abstract

The Sea of Okhotsk holds substantial importance to North Pacific processes, as it is thought to be the major source region for North Pacific Intermediate water (NPIW). A cruise though this area in 1993, as part of the WOCE project has gone a long way to increasing understanding of the properties and underlying processes. In addition, recent publications have focused on the growing evidence of large-scale changes in water mass properties in the North Atlantic, and more recently, the North Pacific, in which large scale warming and freshening of intermediate waters has been noted. The Sea of Okhotsk is likely to play a key role in such changes due to its role in intermediate water formation.

Recently, ship data from 5 cruises have been made available from the period 1949 to 1952. This provides the opportunity to shed light on the physical properties of this region, and quantify how it has changed over 40 years by comparing this data with the WOCE P1W cruise. We made two significant conclusions. First, there has been a basinwide warming and freshening of the Sea of Okhotsk. This corroborates other studies suggesting a large scale freshening of intermediate water, attributed to an intensified high latitude hydrological cycle in response to global warming. Second, from salt flux

calculations, we concluded that the Sea of Okhotsk was capable of causing the freshening noted in the NPIW over the past half century under certain outflow conditions.

Examiners:

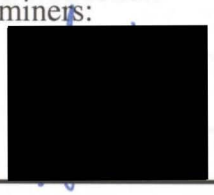

Dr. A. J. Weaver, Supervisor (School of Earth and Ocean Sciences).

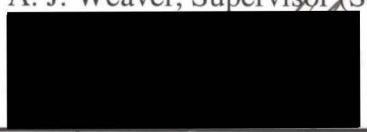

Dr. H.J. Freeland, Member (Institute of Ocean Sciences).

Dr. J. Fyfe, Member (School of Earth and Ocean Sciences).

Dr. A. Bychkov, External Examiner (Institute of Ocean Sciences).

Table of Contents

Abstract ii

Table of Contents iv

List of Tables vi

List of Figures vii

Acknowledgements x

1. Introduction

1.1. The Sea of Okhotsk and the global ocean. 1

1.2. The Pacific Ocean. 2

1.3. North Pacific Intermediate Water. 3

1.4. Mechanisms for forming NPIW. 4

1.5. Focus on the Sea of Okhotsk. 6

1.6. Okhotsk water mass production. 8

1.7. Interaction between the Okhotsk and the Pacific Ocean. 11

1.8. Monitoring changes. 14

1.9. The focus of this thesis. 18

2. Data and Processing.

2.1. The Data 39

2.1.1. The Vityaz dataset. 39

2.1.2. The WOCE P1W dataset. 40

2.1.3. NOAA-AVHRR data 40

2.2. Data Processing 41

2.2.1. Vityaz data 41

2.2.2. WOCE PIW data. 42

2.2.3. Flux through the Bussol Strait. 42

a. A Question of Geostrophy. 43

b. Hydraulic Control. 43

2.2.4. AVHRR data. 46

3. Results

3.1. Surface Properties: The AVHRR data. 54

3.2. Subsurface: Vityaz ship data. 55

3.3. Comparing Vityaz with WOCE along line P1W. 57

3.4. Flux Calculations. 59

4. Discussion.

4.1. Climatology of the Sea of Okhotsk. 81

4.2. Okhotsk structure in cross section. 82

4.3. Changes along the P1W transect. 83

4.4. Fluxes throught the sea of Okhotsk. 84

4.5. Caution: Long term change or variation? 85

5. References. 86

List of Tables

1.1 Comparing the Salinities of the Bussol Strait, South Subtropical Gyre, and the mean salinity, at NPIW reference densities. 13

2.1. Details of the *Vityaz* surveys. 39

3.1. Salt flux results under different outflow scenarios through the Bussol Strait. 60

List of Figures.

1.1. Bathymetry of the Sea of Okotsk, plotted using the ETOPO 5 dataset. 20

1.2. Schematic of thermohaline circulation. 21

1.3. Meridional transect of the Atlantic Basin. 22

1.4. a. Pacific surface temperature. 23

b. Pacific surface salinity. 24

1.5. Meridional transects through the Pacific of:

a. Temperature. 25

b. Salinity. 25

c. Potential Density. 26

1.6. Low salinity tongue in the North Pacific. 27

1.7. Major global surface currents. 28

1.8. Global occurrence of intermediate water masses. 29

1.9. The Kuroshio/Oyashio mixing zone. 30

1.10. Formation of NPIW: roles of OIW and GAIW. 31

1.11. Detailed map of the Sea of Okhtosk and relevant place names. 32

1.12. Water mass structure of the Sea of Okhotsk. 33

1.13. Schematic summarising the mixing in the Sea of Okhotsk. 34

1.14. a. Phases of the Pacific Decadal Oscillation (PDO). 35

b. PDO time series. 35

1.15. a. Phases of the North Atlantic Oscillation (NAO). 36

	b. NAO time series.	37
1.16.	The relationship between the NAO, the Labrador Sea, and Thermohaline Circulation.	38
2.1.	Station locations from theVityaz Cruises.	47
2.2.	Station locations from the WOCE P1W cruise.	48
2.3.	Schematic summarising principles of the Geostrophic Method.	49
2.4.	An example of Potential Density profiles used for calculating topographic outflow.	50
2.5.	Schematic summarising principles behind salt flux calculations.	51
2.6.	Comparing salinity in the central Okhotsk to the open Pacific in 1993.	52
2.7.	Map used to calculate the volume of NPIW.	53
3.1.	An example of winter time SST from satellite AVHRR data.	61
3.2.	An example of summer SST satellite AVHRR data.	62
3.3.a.	A 12 year time series of summer SST anomalies from the AVHRR.	63
3.3.b.	Detrended AVHRR SST anomalies plotted against the PDO index.	64
3.4.	Temperature climatology at 200m, produced by regridding Vityaz data (1949-1952) using objective analysis..	65
3.5.	Salinity climatology at 200m depth (1949-1952).	66
3.6.	Geostrophic flow patterns (1949-1952).	67
3.7.	Temperature transect across Bussol Strait (1949).	68
3.8.	Salinity transect across the Bussol Strait (1949).	69

3.9. Potential density across the Bussol Strait (1949). 70

3.10. Temperature along P1W transect (1993). 71

3.11. Salinity along P1W transect (1993). 72

3.12. Temperature along P1W transect (1949-1952). 73

3.13. Salinity along P1W transect (1949-1952). 74

3.14. Potential density along P1W transect (1993). 75

3.15. Potential Density along P1W transect (1949-1952). 76

3.16. Temperature changes between 1949-1952 and 1993 along P1W. 77

3.17. Salinity changes between 1949-1952 and 1993 along P1W. 78

3.18. Comparing depth averaged temperatures along line P1W. 79

3.19. Comparing depth averaged salinities along line P1W. 80

Acknowledgements

Many thanks are due to Andrew J. Weaver, my supervisor, and Howard Freeland for their assistance and guidance. Also worthy of mention are Edward W. Wiebe and Michael Roth for their patience and assistance with the rigours of computor processing, as well as other members of the Climate Group.

I must also mention my mother for her unconditional support, my brother for never forgetting how to enjoy life and my friend Trevor Baker for making sure my weekends are full of adventure!

I dedicate this thesis to my Father, who despite leaving this world some time ago, will always be by my side, and a part of every decision I make.

Mr David J. Hill

1947-1989

Chapter 1

Introduction

1.1. The Sea of Okhotsk and the Global Ocean

The Sea of Okhotsk is situated on the northwestern boundary of the Pacific Ocean, providing Russia an important link with the Pacific through their territorial waters. It is landlocked on 3 sides, and to the southeast, the Kuril Islands mark its boundary with the open North Pacific Ocean (see figure 1.1). The Sea is characterised by a wide shallow coastal shelf region to the north, and a deep basin to the south, bordering the Kuril Islands. The Sea of Okhotsk exhibits unique climate characteristics, as described in the book by Leonov (1960). He noted that near polar climatic conditions prevail due to the Siberian High – Aleutian Low pressure gradient, establishing strong northwesterly winds off the Asian continent throughout most of the year. Annual average temperatures hover around -6°C, several degrees lower than the latitudinal average, with very low precipitation levels. Due to the maritime influence, the southern Sea of Okhotsk was found to experience a milder, damper climate – see Preller & Hogan (1998) for more details.

Recent interests have been sparked in relation to its role in thermohaline circulation, and contribution to the water mass structure of the North Pacific. Before focussing in on the

Sea of Okhotsk, its role in shaping the structure and behaviour of the Pacific will be addressed.

1.2. The Pacific Ocean

Figure 1.2 shows an idealised representation of the global thermohaline circulation. The first thing to note is the asymmetry in the characteristics of the two main ocean basins, the Pacific and the Atlantic: predominantly the lack of deep-water formation in the Pacific. Deep-water formation is the process whereby surface water actively sinks to great depths through heat and freshwater exchange at the air-sea interface. There are two such regions of significance. First is the high latitude North Atlantic, which can be split into two zones: the Greenland Iceland Norway (GIN) Sea, which forms the principal component of North Atlantic Deep Water (NADW), and the Labrador Sea, which forms upper NADW. The second region is the Weddell & Ross Seas in the Southern Ocean, where Antarctic Bottom Water (AABW) is formed. Figure 1.3 is a meridional section of the Atlantic basin, showing the deep-water masses sinking at high latitudes to fill the deep ocean basins. The reason why there is no deep-water formation in the North Pacific has been the centre of many debates.

When the physical properties of the two ocean basins are addressed (Weaver *et al* 1999), the dominant difference is the asymmetry in surface salinity: the Pacific is significantly fresher than the Atlantic. This has been attributed to the net export of freshwater from the Atlantic to the Pacific through atmospheric transport patterns (Broecker *et al*, 1990). A second factor is the dense outflow of warm, salty waters from the Mediterranean

contributing to the surface waters of the Norwegian Sea, so elevating it's salinity. In the Pacific, the only marginal sea, which could conceivably serve a similar purpose, would be the Sea of Okhotsk on the northwestern seaboard; however, the Okhotsk outflow is actually defined by a salinity minimum.

Reid *et al* (1997) summarised the large-scale characteristics of the Pacific Ocean circulation. Figure 1.4 shows the potential temperature and salinity characteristics of the surface waters in the Pacific. There is a clear transition to higher salinity in surface waters on moving south through the ocean basin. This transition is also highlighted in a transect plot through the ocean (figure 1.5). The densest water is formed in the Ross Sea (South Pacific), which is characterised by 46.12 potential density, σ_4, -0.2° potential temperature, and salinities of 34.70-34.71 psu. The dramatic shoaling of isopycnals and isotherms indicates this formation region. Additionally, to the north, a distinct "tongue" of low salinity water originating in the northernmost region of the Pacific and spreading at depths of less than 1000m, is clearly visible in the intermediate waters (figure 1.6).

1.3. North Pacific Intermediate Water (NPIW)

North Pacific Intermediate Water is the densest water formed in the North Pacific, at 26.8 σ_θ (26.7-26.9), and is characterised by a salinity minimum at intermediate depths occupying the north subtropical gyre (figure 1.7) at depths of around 300-600m. When compared with the other major intermediate water masses (see figure 1.8) its common characteristics with Labrador Sea Water (LSW) are apparent in terms of climate and

geographic setting of formation regions and open ocean occurrence. It is clear that NPIW exhibits some unique features. The characteristics of this water mass are clearly defined, occupying an unusually narrow density signature. It is spatially confined, mainly to the subtropical gyre with it's formation region situated in the subpolar region, while AAIW occupies the Southern Hemisphere oceans, extending north of the Equator, and LSW is confined to the subarctic northern Atlantic only. It has also been noted that NPIW lacks a corresponding oxygen maximum, indicating sources that involve vigorous mixing, whereas LSW and AAIW are formed in direct contact with the atmosphere.

1.4. Mechanisms for forming NPIW.

The NPIW formation region is generally thought to be the mixed water region between the Kuroshio Extension and the Oyashio front (figure 1.9), fed by waters from the Oyashio, Kuroshio and Tsugaro warm current (figure 1.7) (Reid 1965 & 1973, Talley 1992 & 1995, Yasuda *et al* 1996 &1997). Although much of the early conclusions were speculative, Reid (1965) noted an interesting lack of surface outcrop at the NPIW density anywhere in the North Pacific.

Two potential source regions of such specific characteristics are discussed in the literature. First, the Okhotsk outflow (Wüst 1930, Kitani 1973, Alfultis & Martin 1987, Yasuda 1997, Talley, 1991, Talley & Nagata 1995), and second the Gulf of Alaska (Van Scoy *et al* 1991, You *et al* 2000). The latter has received less attention in recent years; as Van Scoy admitted herself, waters of 26.8 σ_θ have never been observed in the Alaskan

Gyre. Evidence shows that waters of 26.7-26.9 σ_θ are formed by direct ventilation beneath sea ice formation in the Sea of Okhotsk (Kitani 1973, Talley 1991, Ohtani 1989). Moreover, it is generally agreed that the mixed water region, where the Kuroshio and Oyashio meet at the western boundary is the principal site of lateral mixing, making the Okhotsk outflow a popular candidate for supplying the necessary mode water, simply through it's proximity and prevailing current direction. Following extensive ship surveys throughout the Pacific, Reid (1965) argued that NPIW resulted from vertical mixing of low salinity surface water throughout the subarctic region.

Given the availability of a comprehensive dataset available for the North Pacific from the World Ocean Circulation Experiment (WOCE), You *et al* (2000) undertook a study to quantify the roles of the Gulf of Alaska and the Sea of Okhotsk in forming NPIW. You *et al* used neutral density surfaces, identifying NPIW at σ_N 26.9. Two regions of double diffusion were identified; the Alaskan Gyre on σ_N 26.5 neutral surface, and the Sea of Okhotsk on σ_N 26.9, which indicate 2 different formation sources, and also different formation mechanisms. The Gulf of Alaska is characterised by high potential vorticity and lies at σ_N 26.2-26.5; this is shallower than in the Okhotsk Sea, which exhibits low potential vorticity. These contributors are named Gulf of Alaska Intermediate Water (GAIW) and Okhotsk Intermediate Water (OIW) respectively. It was found that GAIW contributes to upper NPIW in the eastern sector of the subtropical gyre, while OIW dominates the western and lower sectors. It was also noted that GAIW shows significant seasonal variability, with the bulk of formation occurring in winter. Figure 1.10 summarises the spreading regions of these two water masses.

1.5. Focus on the Sea of Okhotsk

With lower salinity and higher oxygen concentrations than anywhere in the North Pacific, the outflow from the Sea of Okhotsk has a significant influence on North Pacific characteristics. Figure 1.11 summarises the structure of the basin, and major place names. The basin is characterised by a large coastal shelf in the north, with depths of less than 400m, descending to depths of more than 3000m in the Kuril Basin to the south. With the Kamchatka Peninsula to the east, the string of Kuril Islands to the south-east mediate communication between the Sea of Okhotsk and the Pacific. The channels of principal importance are the Bussol Strait with a sill depth of around 2300m, and the Kruzenstern Strait (1900m). In addition, the Sea of Okhotsk is connected to the Japan Sea, by way of the Soya Strait (40m) and the Tartar Strait (10m).

In 1960 Leonov published a detailed discription of all aspects of the Sea of Okhotsk and later, Kitani (1973) published the results of extensive ship surveys in the region (summarised in figure 1.12). Examining the temperature-salinity characteristics of the Sea of Okhotsk and surrounding regions, it became apparent that the depth of maximum temperature (named *Mesothermal water* by Kitani) in the western North Pacific and the Bering Sea was much shallower than in the Sea of Okhotsk. One of the most important characteristics noted was the existence of cold-water layers beneath the summer surface water. One named *subsurface cold water*, is found at depths shallower than 100m and is thought to be the remains of winter surface cold water formed by thermal convection.

The other is called *lower cold water*, or *transitional water*, at depths of around 150-600m, and is slightly higher in temperature and salinity than those of the subsurface cold water. This is where mesothermal waters are found in the Bering Sea and subarctic western North Pacific.

The characteristics of transitional water are unique, not found in other subarctic regions such as the Bering Sea, and this water is thought to be a mixture of the cold saline bottom water and the western North Pacific mesothermal water. Kitani (1973) proposed that the cold saline water, formed in a polynya in the northern Okhotsk, sinks down following the continental shelf (Shelf Dense Water, SDW), and moves south along the western boundary. At the same time warm fresher water from the mesothermal western North Pacific moves northward along the eastern boundary, which infers a roughly cyclonic (anti clockwise) circulation, transporting warm water north, and cool water south. This forms a central region of intense horizontal mixing, with much of the vertical mixing taking place around the Kuril Islands. This resulting Transitional Water is cooler and fresher than the rest of the North Pacific and has since been named Okhotsk Intermediate Water (OIW).

The general circulation within the Sea of Okhotsk is generally agreed to be a cyclonic, cell (Leonov 1960, Yasuoka 1967&1968, Kitani 1973, and Favourite *et al* 1976) with inflow predominantly through the shallower Kruzenstern Strait, and out of the Bussol Strait. Transition water is thus formed by dense shelf water from the north mixing with water from the North Pacific in the central Sea of Okhotsk. Wakatsuchi & Martin (1991)

identified circulation in the southern Kuril basin as a large Anticyclonic cell, with associated seasonal anticyclonic eddies. These eddies have also been noted in Satellite Sea Ice and SST data (Kuzmina & Skymlarov, 1984; Hatakeyama et al, 1985; Wataksuchi & Martin, 1990) – see Talley & Nagata (1995) for a more comprehensive discussion. Tidal amplitudes are large in the Sea of Okhotsk, and tidal energy dissipation is estimated to be second largest in the world (Miller, 1966). This is likely to have a central role in the mixing dynamics of the region. Limited observations of tidal currents lead Suzuki and Kanari (1986) to develop a tidal model incorporating existing observations. Of particular interest was a cyclonic – anticyclonic circulation over the Kashevarov Bank. This becomes a region of oscillating convergence – divergence, depending on the direction of motion, and hence could be a region of intense tidal mixing.

1.6. Okhotsk water mass production

The Okhotsk's ability to produce dense water centres around the polinya over theNorthern Shelf and the Kashevarov Bank in winter (Kovshov, 1982). The Kashevarov Bank is a site of intense heat loss, thus dense water formation (Alfultis & Martin, 1987) related to the strong upwelling and vertical mixing discussed by Suzuki & Kanari (1986). With much dispute surrounding whether dense water is produced in sufficient quantities to form NPIW, Alfultis & Martin (1987) focussed on estimating the magnitude of this transitional water production: in particular, by estimating the production of dense shelf water. Mean annual dense water (>26.5 σ_θ) production was estimated to be approximately 0.5 Sv, which was believed sufficient to infer it as a source of intermediate waters of the

North Pacific. Gladyshev (1998a) presented direct estimates from CTD data for June 1996, which agreed well with that presented by Alfultis & Martin (1987) for a warm year. However, a sequence of abnormally warm winters in the early 1990's not only caused a decrease in dense water production on the shelf, but also a change in its composition. Estimates from the spring survey in 1995 and June 1996 (Gladyshev 1998a) suggested that the rate of formation of *very* dense water (> 26.8 σ_θ) was an order of magnitude lower than suggested by Alfultis & Martin.

Northern Shelf polynya are known to form between January/February and when air temperatures rise through 0°C around April (Gladyshev, 1998b). To obtain more reliable quantitative estimates, Martin *et al* (1998) performed winter surveys between 1990 and 1995. He used an algorithm developed for the SSM/I (Special Sensor Microwave/ Imager) to obtain the composition of ice / open water for each polynya, and a heat flux algorithm to derive ice production. Martin *et al* concluded that the 6-year average dense water production was approximately 0.2-0.4 Sv, in line with earlier estimates. However, the ice production on the northwest shelf was found to vary by a factor of 3. This can be attributed to the southwest-northeast trend of the coastline and the roughly parallel prevailing winds, which means that small variations in wind direction yield large changes in ice production.

Freeland *et al* (1998) undertook a detailed study of the physical properties of the northern Sea of Okhotsk. They examined the ability of the northern shelf polynya to produce the necessary density and volume of water required for SOIW production. Suggestions of

wind control by Martin *et al* were confirmed. It was found that local high winds could maintain polynya openings, elevating surface densities to higher than expected surface values. However, this dense water, identified as a temperature maximum within the Okhotsk basin, could only reach 27.05 potential density, and as such was only able to ventilate the shallower portion of SOIW. These findings raise the question of what additional processes elevate these densities and supply the deeper regions of this water mass.

As part of the same experiment, Wong *et al* (1998) used CFC's and temperature/salinity measurements to estimate ventilation rates for the Sea of Okhotsk. These data were used to calibrate a simple box model, and calculate flux rates in and out of the Sea of Okhotsk. It was concluded that 1.9 Sv of upper Sea of Okhotsk Intermediate Water (SOIW) and 0.8 Sv of lower SOIW are exported from the Sea of Okhotsk. The maximum export from the Sea of Okhotsk occurred at $26.8\sigma_\theta$, consistent with Yasuda *et al* (1997). These calculations support previous theories (Talley *et al* 1991, Yasuda *et al* 1996) that the Okhotsk is an important source of cold freshwater present in the NPIW. Wong *et al* calculated that the minimum export of SOIW requires a production rate of 0.9 Sv of SDW, higher than the value of 0.5± 0.2 Sv discussed in section 1.6. For these calculations it was assumed that increases in salinity and density were solely due to brine rejection during ice formation. The findings of Wong *et al* support Talley (1991), who proposed that salt fluxes through the shallow Soya and Tatar straits, which connect the Sea of Okhotsk to the Japan Sea, are important in the winter for increasing the salinity and density of self water. This would enhance SDW production. Aota (1975) noted

inflow, although with significant seasonal variability, through the Soya and Tartar straits from the Japan Sea.

1.7. Interaction between the Sea of Okhotsk and the Pacific.

Interaction between the Sea of Okhotsk and the open Pacific Ocean is limited to a number of narrow passages between the Kuril Islands. Of primary importance are the Bussol and Kruzenstern Straits, which are two of the deeper openings. In section 1.5 it was noted that the general flow structure for this region is in through the Kruzenstern and out through the Bussol Strait. The total exchange between the Okhotsk and the North Pacific has been estimated at 15 Sv (Kurashina *et al*, 1967). However, the specific details of this flow are still under much dispute. For instance, Leonov (1960) and Moroshkin (1966) both noted '2-sided' (bi-directional) currents in most passages.

Freeland *et al* (1998) discussed the vertical structure of the deep Sea of Okhotsk in terms of the nature of its communications with the Pacific using Silicon/Oxygen ratios (Si/O). The characteristics in the Bussol Strait suggest a two-layer flow, with properties down to 1700m coinciding with the Sea of Okhotsk, and below this depth, coinciding with the Pacific. It was also noted that water at depths of 3000m in the Kuril Basin exchange freely with water at depths of only 2000m in the Pacific. However, it could not be established with any certainty whether this represented a steady horizontal flow, or the survey caught a periodic deepwater renewal in the act.

Kurashina *et al* (1967) calculated flow through the two major straits by a combination of Geostrophic, GEK (Geomagnetic Electrokinetograph Instrument) and two current meter

measurements. In the Bussol Strait, flows were calculated as 4.8Sv in and 4.3Sv out, whereas flows in the Kruzenstern Strait were 3.6Sv in and 2.5Sv out. However, as Talley (1991) noted, only geostrophic measurements were used at the two main passages. Since non-geostrophic components are likely to be significant in the straits, errors are probably large. Wong *et al* (1998) used CFC tracer methods to conclude that the Kruzenstern Strait exhibited a dominant inflow, and to confirm a dominant outflow through the Bussol Strait (figure 1.13). There is still much uncertainty regarding the nature of flow through these straits, and the inter-basin relationship they mediate.

The Okhotsk Outflow enters the Pacific Ocean by combining with the Oyashio current, which flows southward from the Bering Sea (figure 1.7). Therefore, the influence of the Okhotsk outflow can be measured by monitoring the change in Oyashio characteristics as it flows along the Kuril Islands. Observations of these changes were carried out by Kono & Kawasaki (1997) who concentrated on how the Bussol Strait outflow modified the Oyashio using CTD measurements in August and September between 1989 and 1992. Although the outflow was found to be very weak, significant seasonal variability was noted. Water as cold as Okhotsk seawater was not found in the downstream region: therefore it was decided that the bulk of modification occurs as a result of water exchange between the Oyashio and the Okhotsk Sea in the region around and northeast of the Bussol Strait. This reinforces Kitani's (1973) findings discussed in section 1.5. It has been suggested that the Oyashio current exhibits significant seasonal variability (Sekine, 1988). Outside the summer season, Kono & Kawasaki suggest that the outflow from the Bussol Strait could be so significant that the Oyashio could carry the discharged Okhotsk

Sea water without mixing. However, such theories have no supporting evidence to date, highlighting the need for a wintertime survey of the region.

With the precise flow characteristics through the islands yet to be established, Talley (1991) used salt conservation to determine whether the SOIW was capable of producing observed patterns in the North Pacific. Talley considered the North Pacific in the region 26.7 – 27.65 σ_θ, assumed no vertical mixing, that 5Sv cycles through the Okhotsk, and that roughly the same amount of high salinity water cycles through the subtropical gyre. Under these assumptions, she inferred that if the Okhotsk was the main provider of freshwater to the North Pacific in this potential density range, then the mean salinity of these two regions should equate to the measured mean salinity for the signature densities.

Region	Salinity (psu)	
	δ_θ = 26.8	δ_θ = 27.3
South subtropical gyre	34.4 *	34.5 *
Bussol Strait	33.5 *	34.15 *
Mean Salinities	33.95	34.3

Table 1.2. Salinity values for south subtropical gyre and the Bussol Strait, and corresponding mean values for NPIW density range.

* Numbers extracted from Reid (1965)

The mean salinities Talley (1991) calculated were found to be close to those found on the maps of Reid (1965) for this density range. Values for the regions in question are summarised in table 1.2. While Talley herself admitted that this method is not rigorously quantitative, it does illustrate that the Okhotsk can produce enough low salinity water to form the observed salinity pattern. Its role is akin with the Mediterranean's influence on the North Atlantic, which significantly modifies properties in the North Atlantic without much mass exchange.

1.8. Monitoring Changes

A recent analysis of archived data by Levitus *et al* (2000) presents evidence of global mean warming of the World Ocean between 1948 and 1998. More significantly, substantial changes in the ocean heat content were discovered in the 300-1000m depth regions of each ocean, and deeper than 1000m in the North Atlantic. It was suggested that in convective regions such as the Greenland Iceland Norway (GIN) Sea and the Labrador Sea in the North Atlantic, the apparent warming indicated by sea surface temperatures (SST) might remain small, despite large increases in the heat flux from the atmosphere to the ocean. Moreover, these subsurface temperatures exhibit a global scale decadal variability, which is consistent with that found in the global surface temperature measurements. Surprisingly, subsurface changes were found to precede the SST patterns.

The high latitudes of the North Atlantic are arguably the most significant convective regions in the World Ocean, and therefore changes in this region are thought to dominate

thermohaline variability. Read & Gould (1992) concluded that the subpolar North Atlantic between Greenland and the United Kingdom has been cooling and freshening since the 1960's. They suggested that this was caused by the initiation of intermediate water formation in the Labrador Sea. When this change is considered in the context of theories from Levitus (2000) discussed above, such a change could have far reaching consequences in the global ocean. Bryden *et al* (1996) presented evidence for a consistent increase in North Atlantic salinity and temperature down to 2000 dbar since 1957 in a study of ocean properties along a section at 24°N, attributing this principally to changes in water mass characteristics.

There has been less work focussing on the North Pacific, although evidence of large-scale changes is building. Freeland *et al* (1997) presented evidence for a warming and freshening of the winter mixed layer in the Northeast Pacific. In addition, Wong *et al* (1999) presented evidence from ship surveys that there has been coherent basin wide freshening of intermediate waters between 1930 and 1985: specifically, a decrease of 0.1psu along 47°N in the North Pacific. Wong *et al* suggest elevated levels of high latitude precipitation, and thus an intensified hydrological cycle. This was found to be qualitatively consistent with model predictions of the hydrological cycle's response to global warming. However, changes in precipitation calculated by Wong et al (1999) from salinity changes are 3 times that shown in model responses for the same time period (Manabe *et al* 1990,1991, Gordon & O'Farrel 1997, Murphy & Mitchell 1995). This evidence would suggest a shift in the climate of source regions of the intermediate water masses, specifically sources of NPIW the dominant intermediate water mass in the North

Pacific. It also adds fuel to recent ideas from Levitus *et al* (2000) that changes are being communicated rapidly to the deep ocean, and highlights a need for increased climatic monitoring of deep ocean hydrography.

Pacific inter-annual variability is dictated by El Niño-Southern Oscillation. Lower-frequency variability in North Pacific climate is described by the Pacific Decadal Oscillation (PDO). Figure 1.14 shows the two main phases of the PDO, and it is apparent on first sight that it could significantly influence the surface waters of the Sea of Okhotsk. As yet, no evidence has been presented to such an effect. However, Overland & Salo (1999) suggested that while the PDO has an east-west character in temperature in the North Pacific, the salinity field signature has a NNW/SSE character, similar to the pattern of variability in precipitation. As the Sea of Okhotsk is a formation region of intermediate water masses, this could cause a subsurface PDO signature to propagate through the system, and therefore influence the characteristics of NPIW. Although little has been published on this hypothesis, parallels can be drawn from studies of the Labrador Sea region, with which the Sea of Okhotsk shares common physical and geographic characteristics (see figure 1.8). There is evidence to suggest that the North Atlantic Oscillation (NAO)/Arctic Oscillation (AO) (figure 1.15) has significant influence over the convection in the North Atlantic, and therefore the thermohaline circulation.

The first to observe such behaviour was Dickson *et al* (1988), who noted evidence of anomalously low salinity characteristics in the 1970's and dubbed it "The Great Salinity

Anomaly". But it wasn't until more recently that this anomalous behaviour was suggested to be a component of an oscillating system (Wohlleben & Weaver 1995, Dickson *et al* 1996, Belkin *et al* 1998). Dickson *et al* (1996) suggested a remote connection between A/NAO and the production the Labrador Sea Water (LSW). For example, during the NAO minimum of the 1960's, Dickson noted that freshwater transport to the Labrador Sea was enhanced, thus suppressing convection (and therefore deepwater formation). LSW production resumed in the early 1970's and since then the tendency has been towards increasing and deepening ventilation of the Labrador Sea (figure 1.16). Delworth & Dixon (2000) noted an overall enhancement in thermohaline circulation in response to the recent positive trend of the NAO. These examples suggest an intrinsic influence of both long-term climate change and surprisingly, what are often deemed predominantly short-term oscillations on deeper water characteristics.

Semi-enclosed basins such as the Sea of Okhotsk are also often used as indicators of change on basin to global scales. The continental influence, and smaller volume (and thus heat capacity) than the open ocean means they tend to respond quicker, and show more extreme responses than the open ocean. The Mediterranean is a popular candidate for such work (Bethoux et al 1999, Tragou & Garrett 1997, Gilman & Garrett 1994). Such amplification of signals could have far reaching effects when a region such as the Sea of Okhotsk is considered, as they will be communicated to intermediate depths throughout the open North Pacific through mechanisms of intermediate water formation.

Similarities between the Sea of Okhotsk and the Mediterranean can be drawn in terms of their volume and role in forming dense water and supplying it to the open ocean mediated by a small channel. However, the differences between these two basins are significant. First, the Mediterrranean supplies warm salty waters to the Atlantic whereas the Sea of Okhotsk supplies cool fresher water to the North Pacific. Second, mixing and dynamics of the Sea of Okhotsk is dominated by strong tidal mixing and sea ice dynamics, whereas the Mediterranean has very little tidal influence, and high evaporation rates.

1.9. The focus of this Thesis.

In summary, it is clear that the Sea of Okhotsk is an important region of study, if we are going to be able to monitor changes to the global ocean system. First, it provides a "laboratory" to monitor high latitude changes and variability. Second, evidence suggests that the deep ocean is highly responsive to surface forcing. Formation regions such as the Sea of Okhotsk provide a link to the deep ocean, allowing communication of surface changes. Last, the specific details of the Okhotsk's role in NPIW and North Pacific dynamics is not fully known. So far, this thesis has highlighted a number of questions yet to be answered regarding the behaviour of this region. First, the process by which water is formed to SOIW densities is yet to be fully established. Second, a question still hangs over the nature of the contribution of SOIW to NPIW. Lastly, can changes documented

in the North Pacific be traced back to changes in the Sea of Okhotsk? In this study, the last two questions will be tackled.

Until recently, there has been little archival data for the Sea of Okhotsk region to allow a detailed study of the Sea of Okhotsk. This meant that many of the theories presented to explain the role of the Sea of Okhotsk and underlying mechanisms were based on a considerable degree of speculation. However, a series of data from 5 ship cruises has recently come to light. These cruises took place over a period of 3 years, from 1949-1952 on the Russian research vessel, the *Vityaz*. It is the aim of this thesis, to utilise this data to quantify the contribution of the Sea of Okhotsk to North Pacific Intermediate Water and its role in North Pacific oceanography. In addition these archive results will be compared to those obtained during WOCE, line P1W surveyed in September 1993, to quantify changes in the characteristics of the deep-water structure of the Okhotsk over the 40 years. Satellite SST measurements from the NOAA-AVHRR instrument will be used to complement the ship data. These data will also allow a quantitative study of the nature of communication between the Okhotsk and the North Pacific.

Figure 1.1. The bathymetry of the Sea of Okhotsk. There is a clear transition from the wide shallow shelf in the north, to the deep basin in the south. This is enclosed by the shallow Kuril Shelf, along which runs the Kuril Island chain. This map was plotted using the ETOPO-5 bathymetric data set.

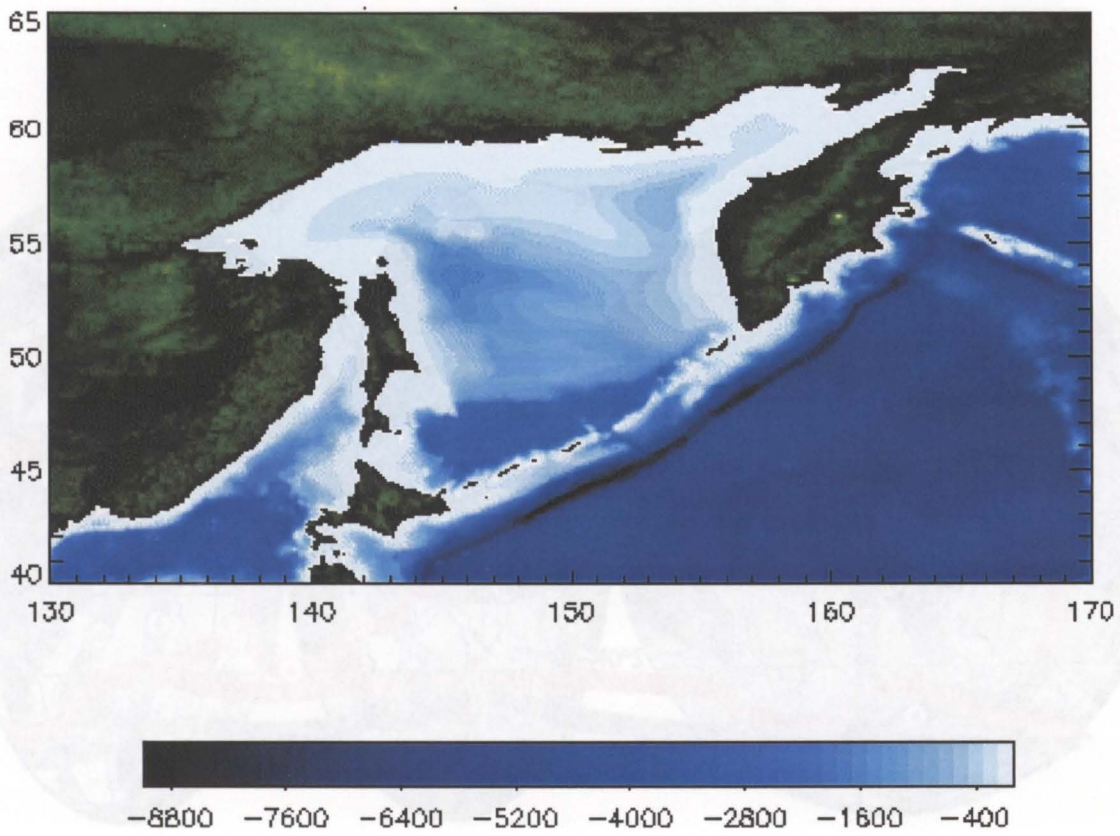

Figure 1.2. This schematic of Thermohaline Circulation highlights the differences between the two major ocean basins. Principally, the lack of deepwater formation in the North Pacific. Taken from Schmitz (1995)

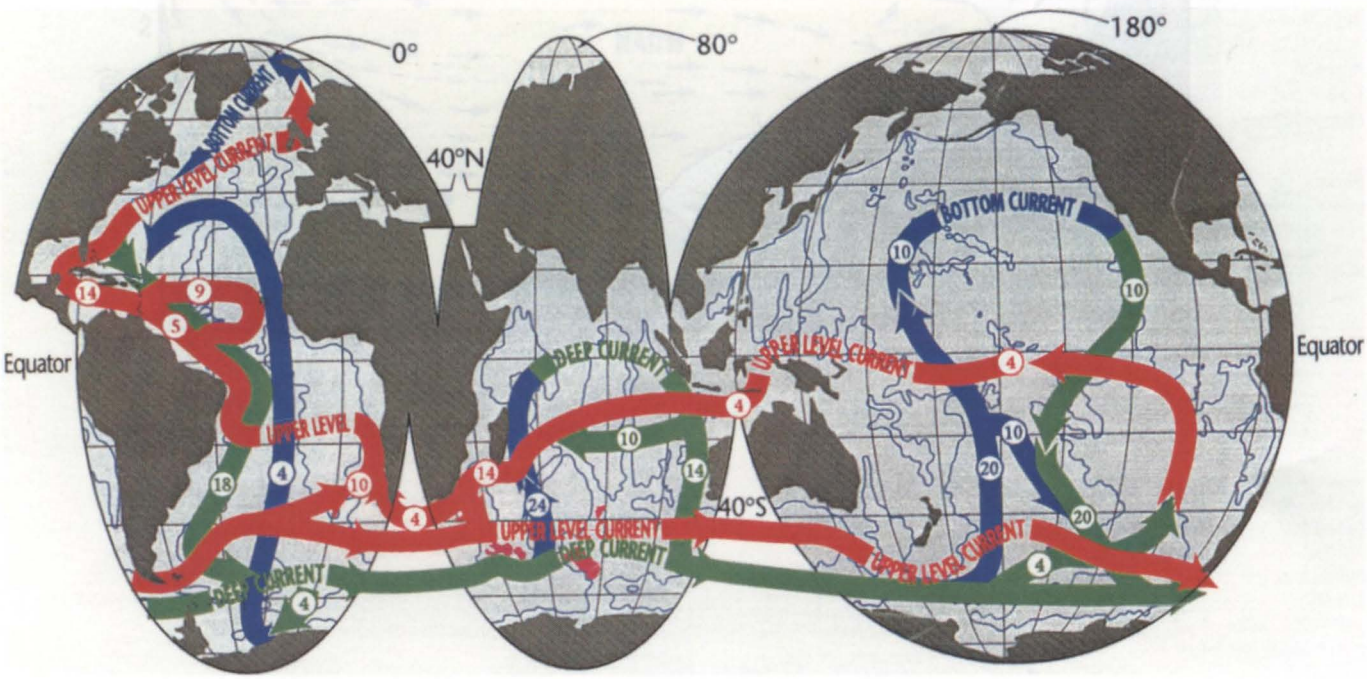

Figure 1.3. Meridional Transect of the Atlantic Basin, which contains the world's major deep-water formation zones, in addition to the Antarctic Intermediate water (AAIW). Taken from Bearman (1995)

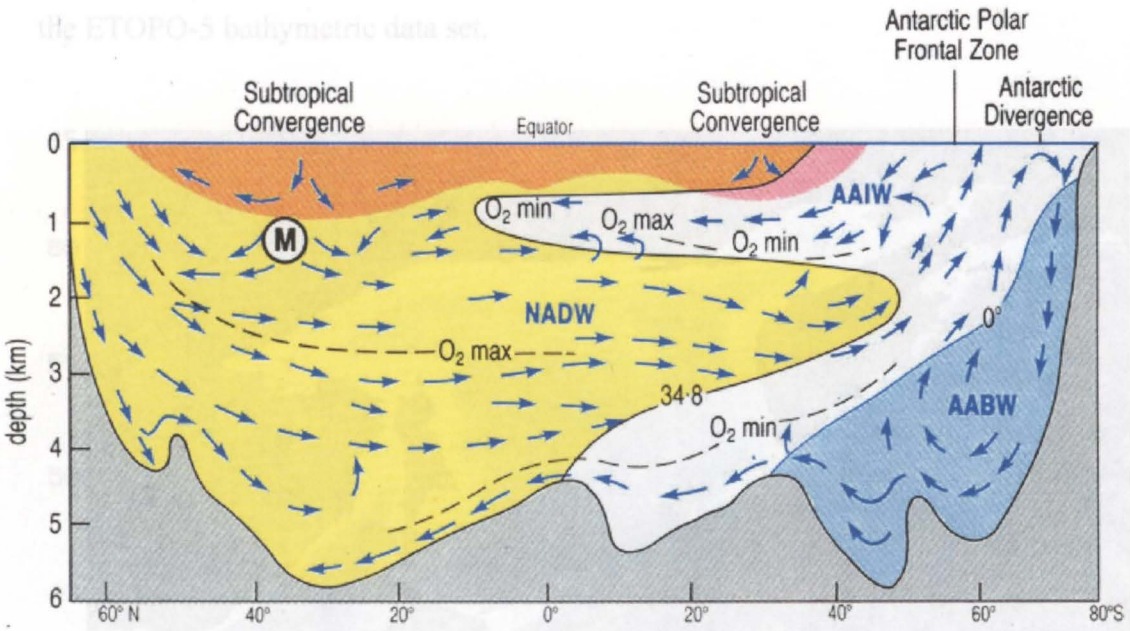

Figure 1.2. This schematic of Thermohaline Circulation highlights the differences between the two major ocean basins. Principally, the lack of deepwater formation in the North Pacific. Taken from Schmitz (1995)

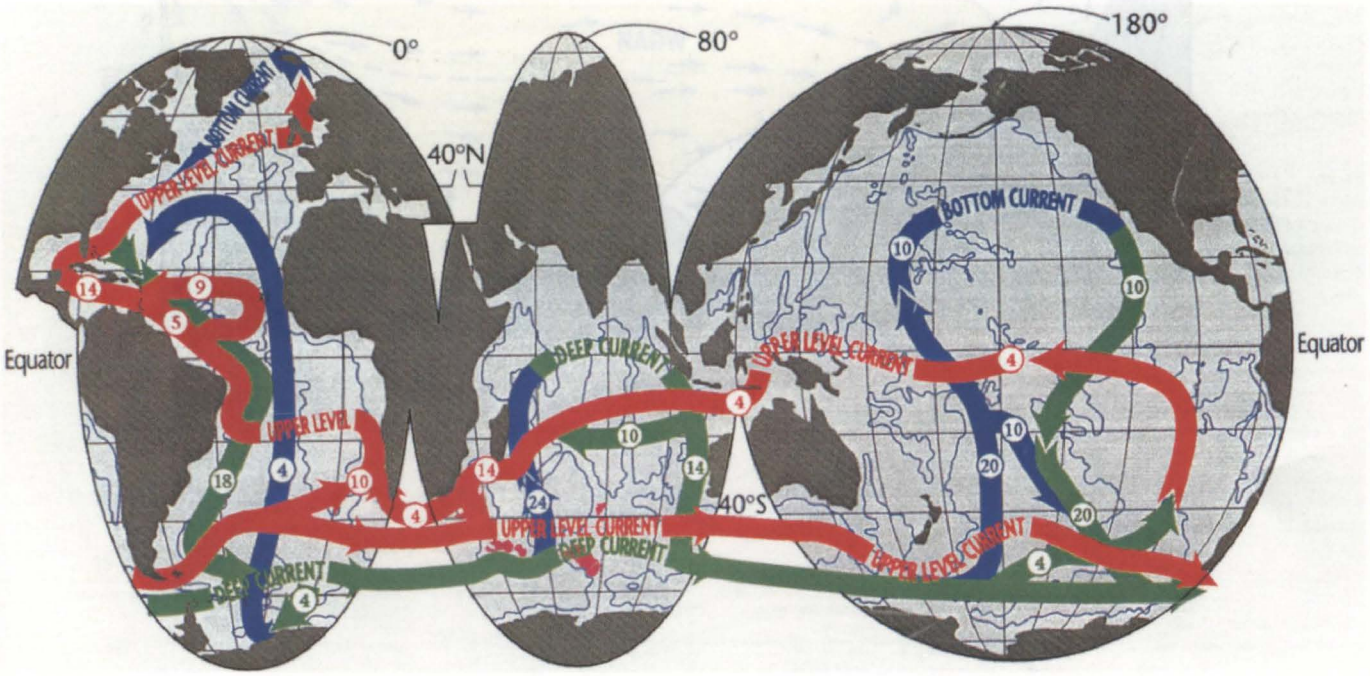

Figure 1.3. Meridional Transect of the Atlantic Basin, which contains the world's major deep-water formation zones, in addition to the Antarctic Intermediate water (AAIW). Taken from Bearman (1995)

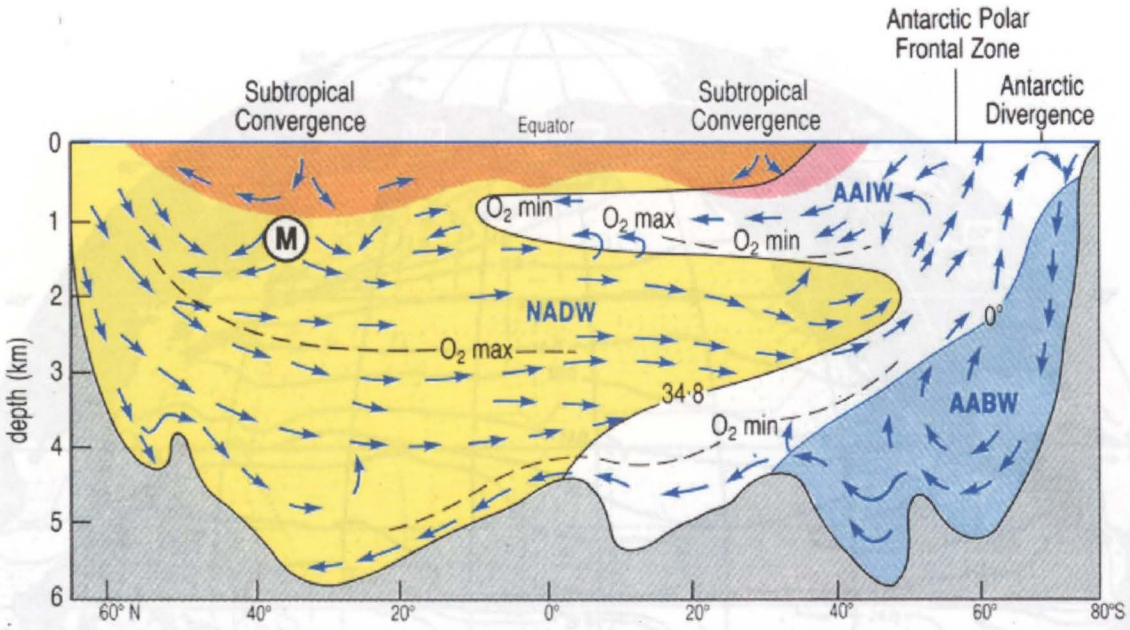

Figure 1.4a. Pacific Surface Temperature (°C). There is a clear east-west transition in the North Pacific, with the coolest waters found in the northwest around the Pacific/Okhotsk interface.

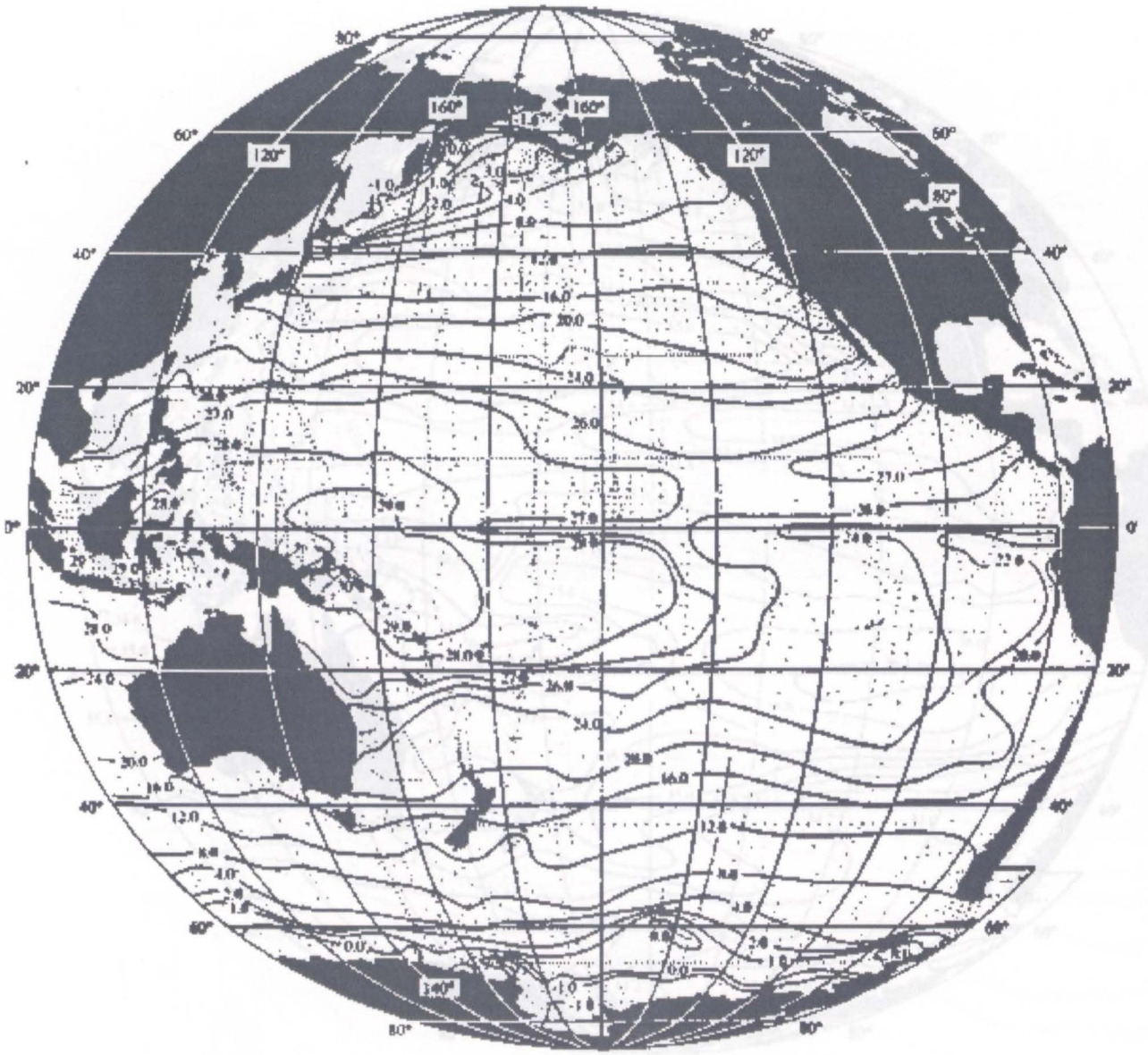

Figure 1.4b. Pacific Surface Salinity (psu). There is a clear transition to fresher waters moving north through the Pacific basin. Taken from Reid *et al* (1997)

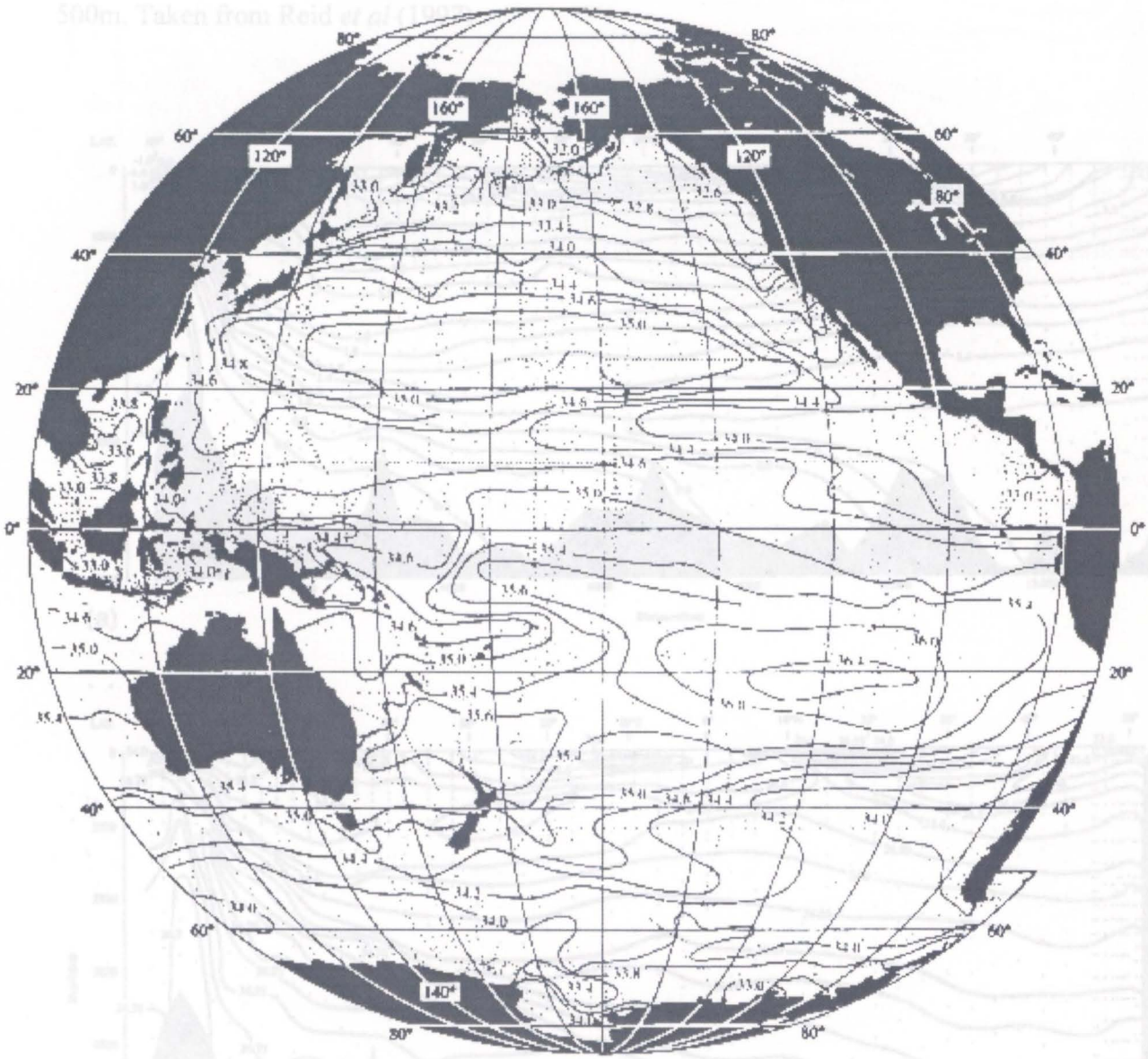

Figure 1.5. Meridional transects through the Pacific of a) Temperature, b) Salinity & c) Potential Density. The shoaling of isolines to the south of the basin in each case is a clear indication of deep convection. In the salinity plot, a tongue of fresher water can be identified, spreading from the north of the basin at intermediate depths centred around 500m. Taken from Reid *et al* (1997)

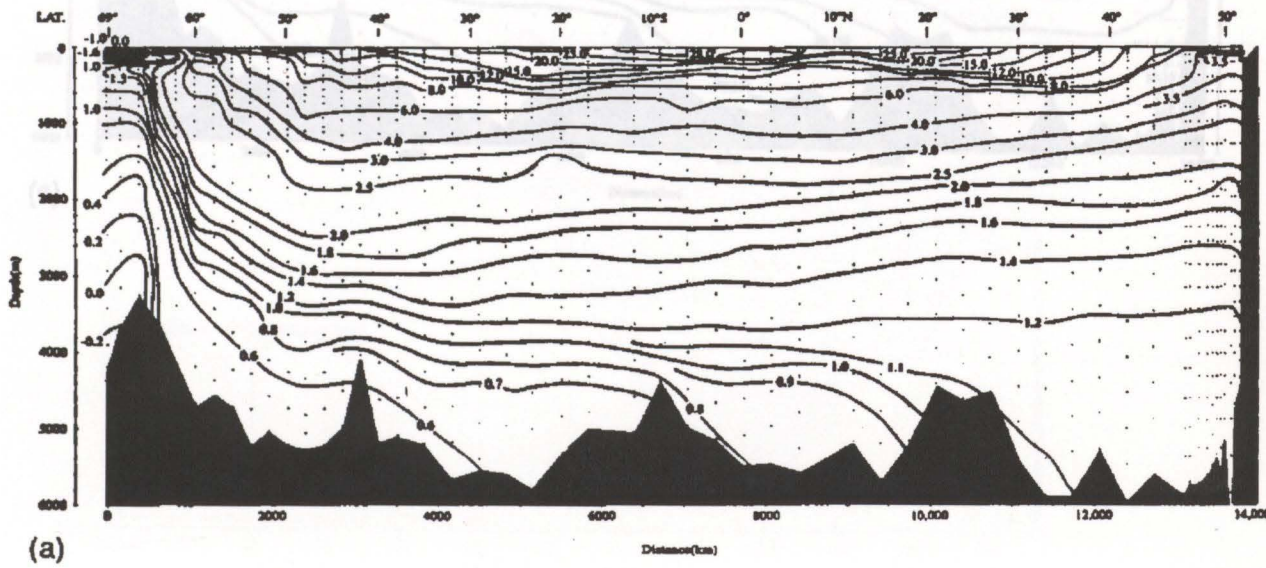

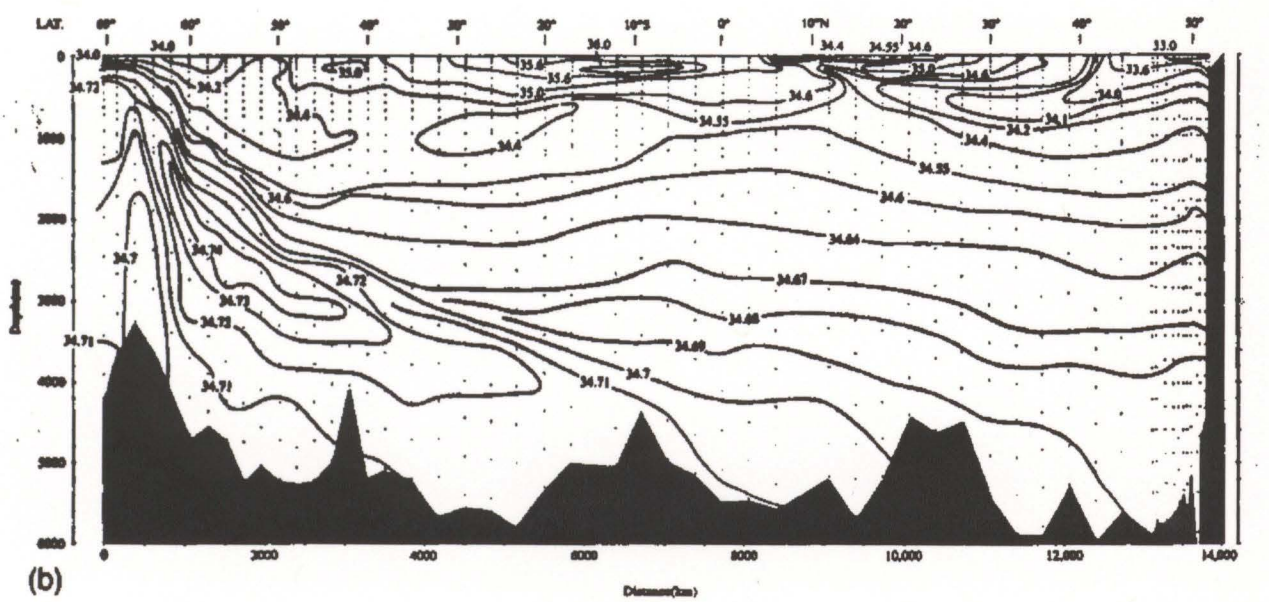

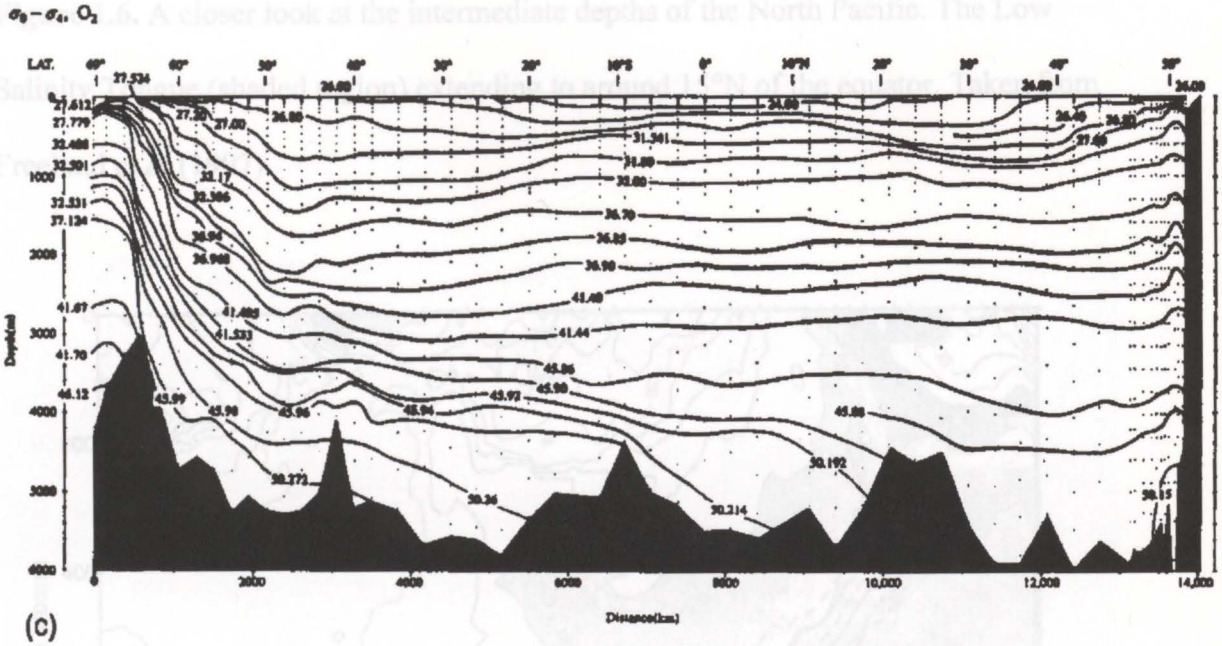
LAT.
Depth(km)
Distance(km)
0
1000
2000
3000
4000
5000
6000
2000
4000
6000
8000
10,000
12,000
14,000

(c)

Figure 1.6. A closer look at the intermediate depths of the North Pacific. The Low Salinity Tongue (shaded region) extending to around 15°N of the equator. Taken from Freeland *et al* (1997).

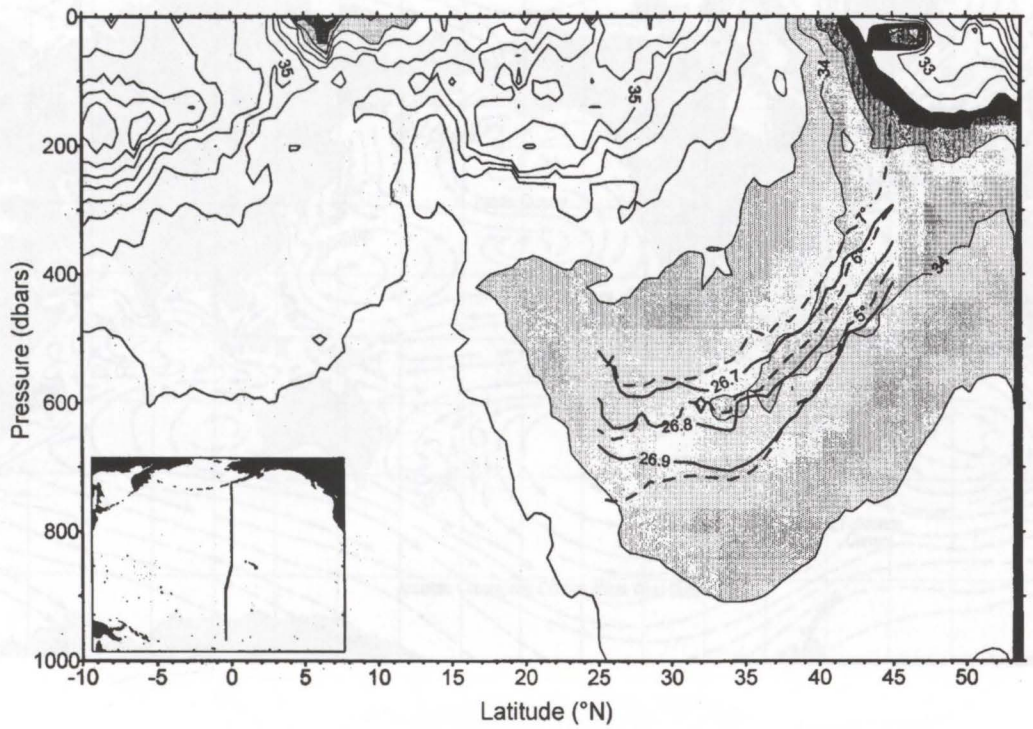

Figure 1.7. Major currents of the World. Of specific interest is the Oyashio and Kuroshio confluence in the northwest Pacific. Taken from Bearman (1995)

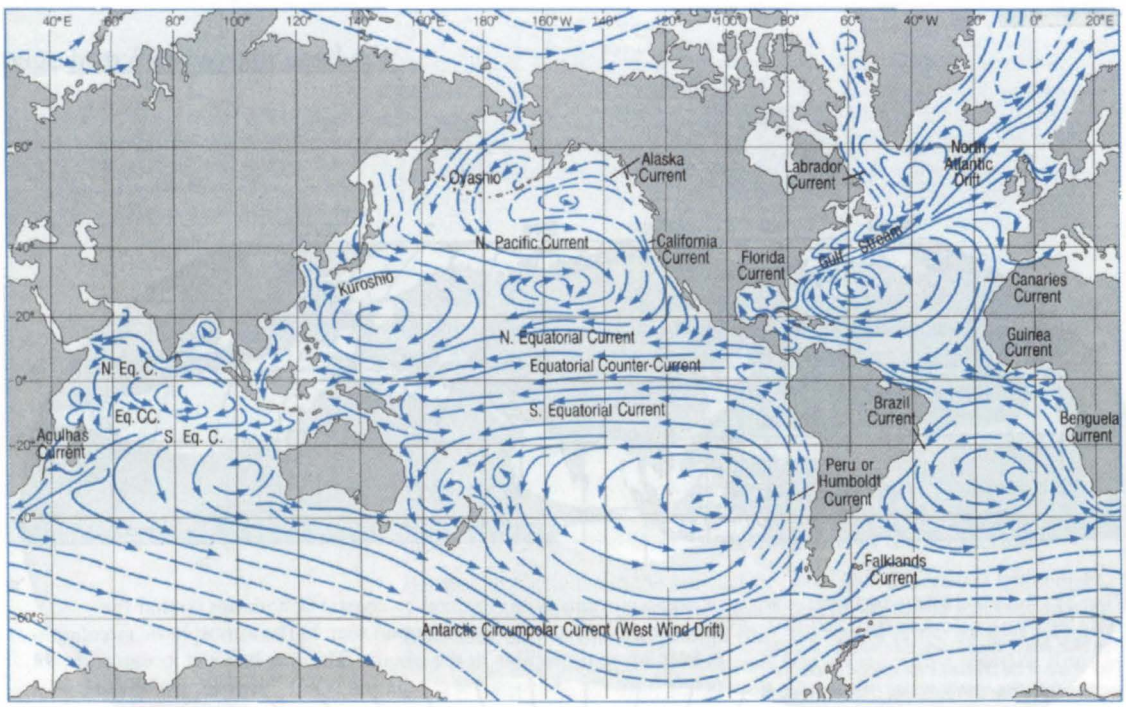

Figure 1.8. Global occurrence of intermediate water masses. Labrador Sea Water (Blue), Antarctic Intermediate Water (dark green) and North Pacific Intermediate Water (light green). Red crosses mark formation regions. The Oyashio and Kuroshio provide the route for the transport of Okhotsk Water into NPIW. Taken from Scripts Institute web page http://www.sam.ucsd.edu

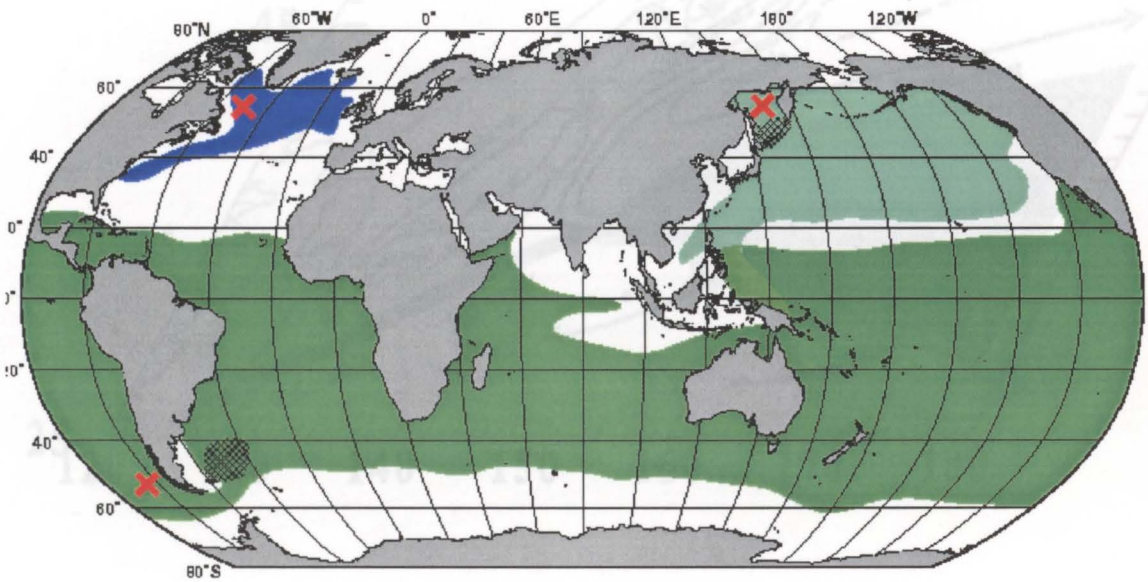

Figure 1.9. A closer look at the Kuroshio-Oyashio Frontal Mixing Zone commonly considered the main region for the formation of NPIW. Outflow from the Sea of Okhotsk is transported to the frontal zone by the Oyashio current. Taken from Yasuda *et al* (1997).

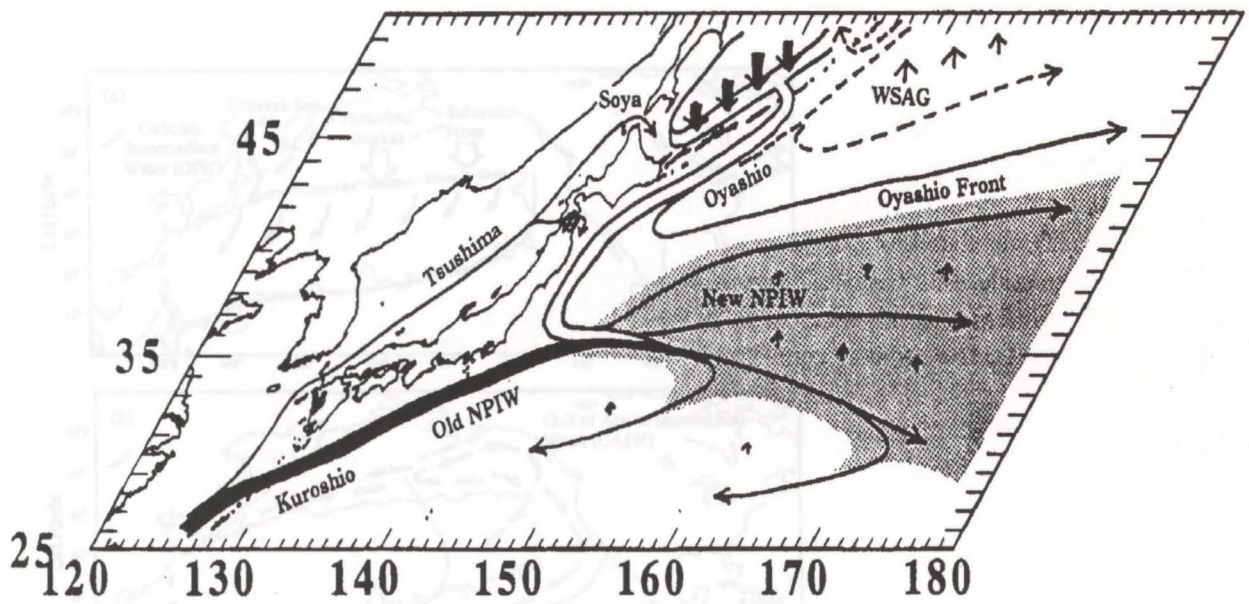

Figure 1.10. Formation of (a)OIW and (b)GAIW and their roles in the formation of North Pacific Intermediate Water (c), according to You *et al* (2000).

You *et al* argue that the formation of NPIW, by combination of these two water masses, actually occurs closer the Pacific's eastern boundary, rather than the Kuroshio/Oyashio frontal zone as discussed by Yasuda *et al* (figure 1.9). Taken from You *et al* (2000)

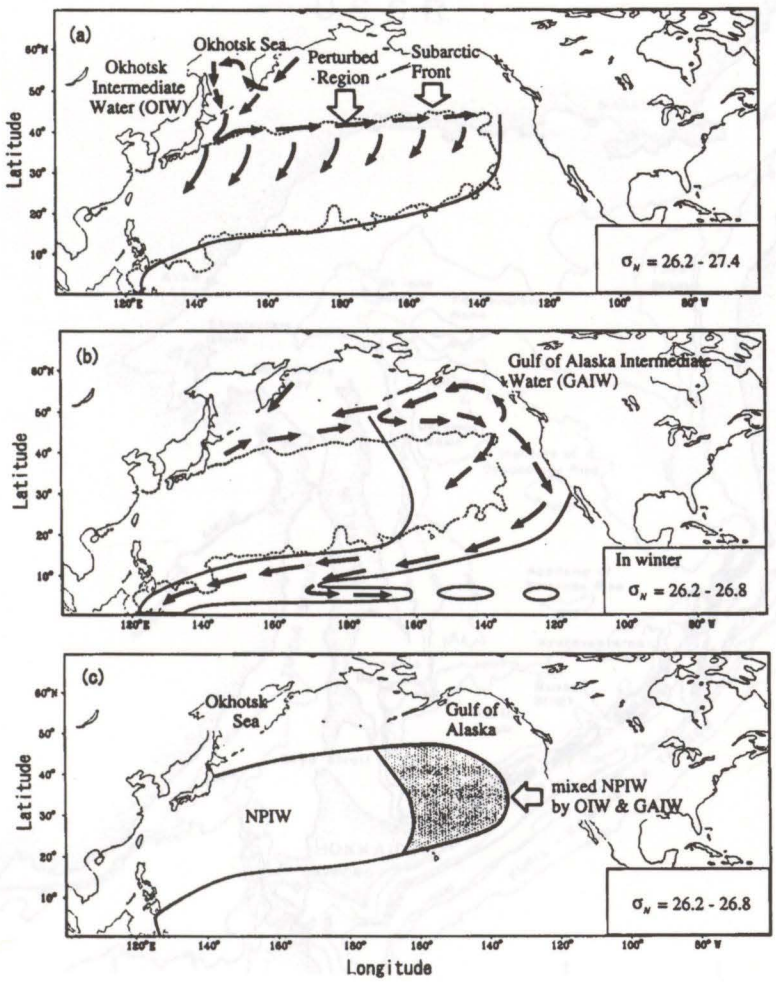

Figure 1.11. Map of the Sea of Okhotsk and relevant place names. Of specific interest are the Bussol and Kruzenstern straits through the Kuril Islands. Taken from Alfultis and Martin (1987)

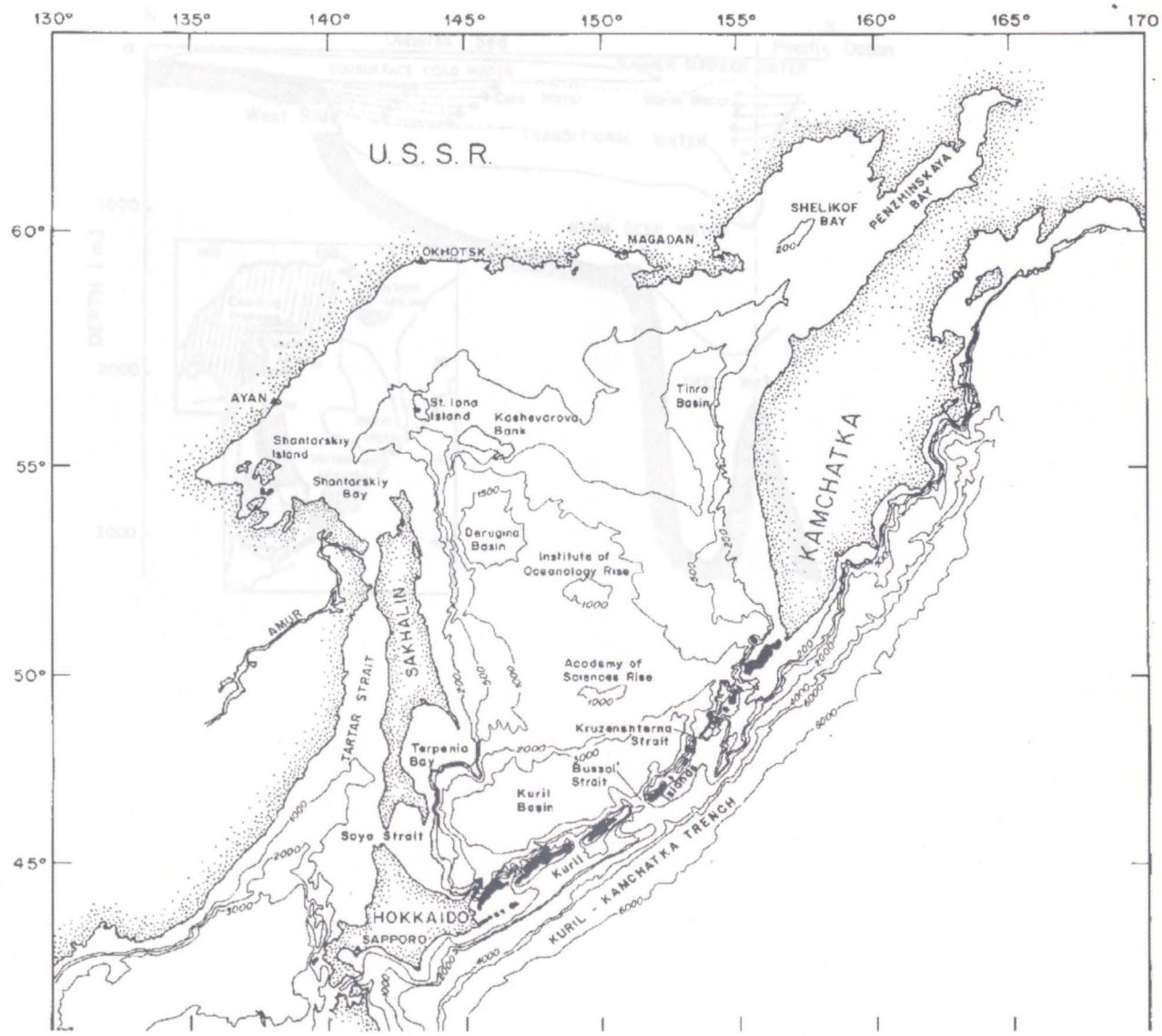

Figure 1.12. The water masses of the Sea of Okhotsk. When considering the role of the Sea of Okhotsk in the formation of NPIW, Transitional water is of particular interest. Taken from Kitani (1973)

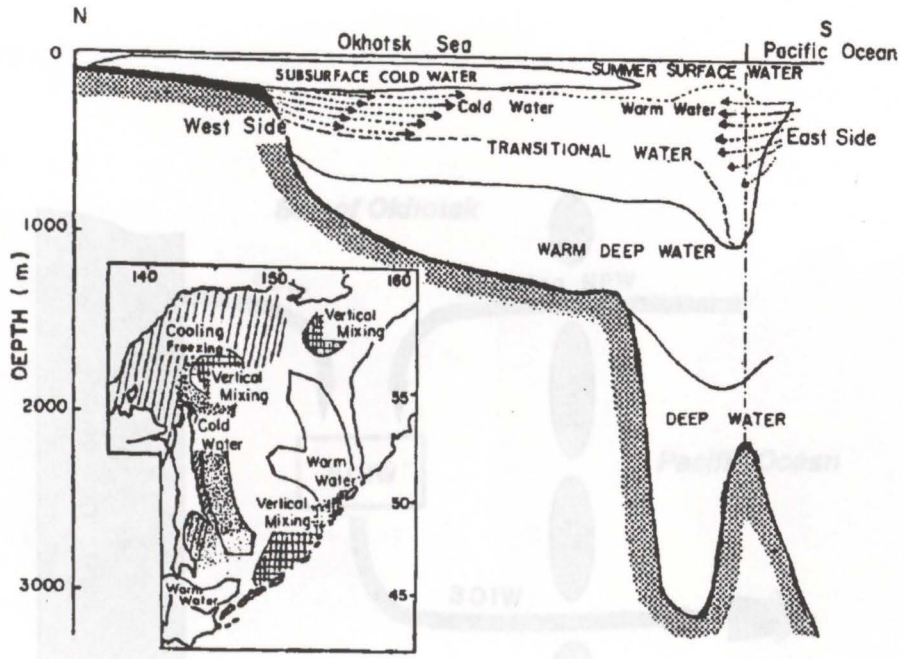

Figure 1.13. Schematic showing geography of mixing in the Sea of Okhotsk at intermediate depths. Wong concluded that Shelf Water from the Northern Shelf meets with Pacific water flowing in through the Kruzenstern Strait and mixes in the central Kuril Basin, before flowing out through the Bussol Strait. Taken from Wong *et al* (1998)

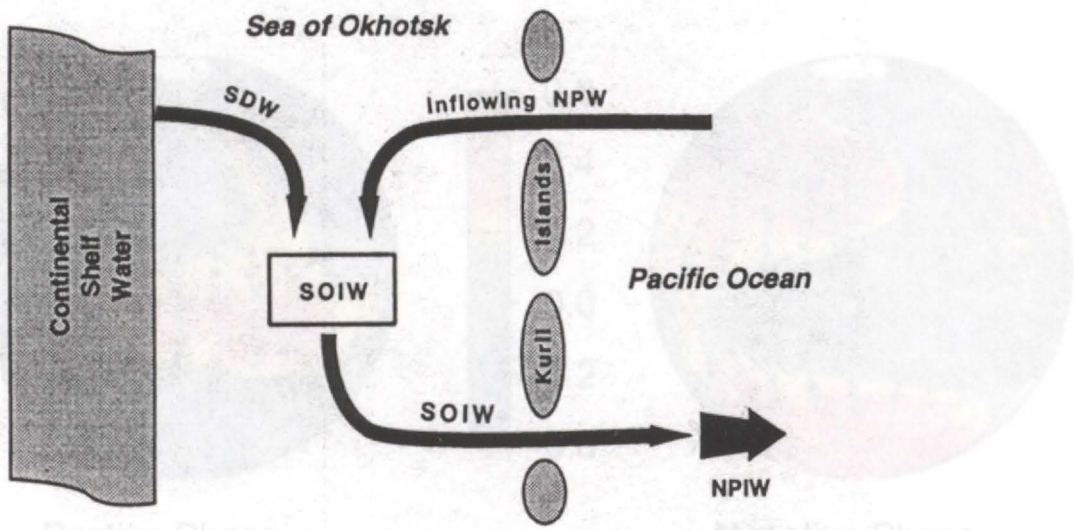

Figure 1.14. a. Temperature anomalies during the phases of the Pacific Decadal Oscillation. This clearly shows a northwest-southeast dipole relationship, which likely to manifest a temperature signature in the Sea of Okhotsk (far Northeast corner of the Pacific). Taken from the University of Washington web page

http://tao.atmos.washington.edu/pdo

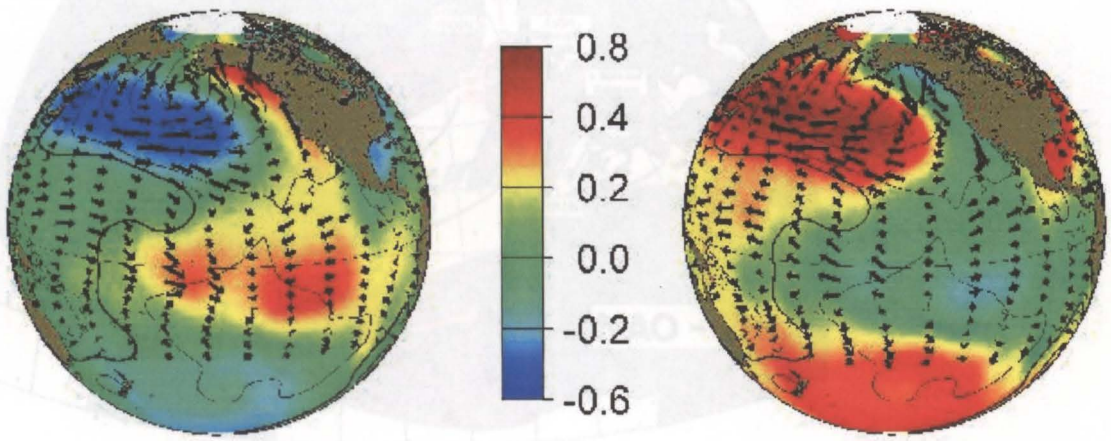

b. PDO Time series.

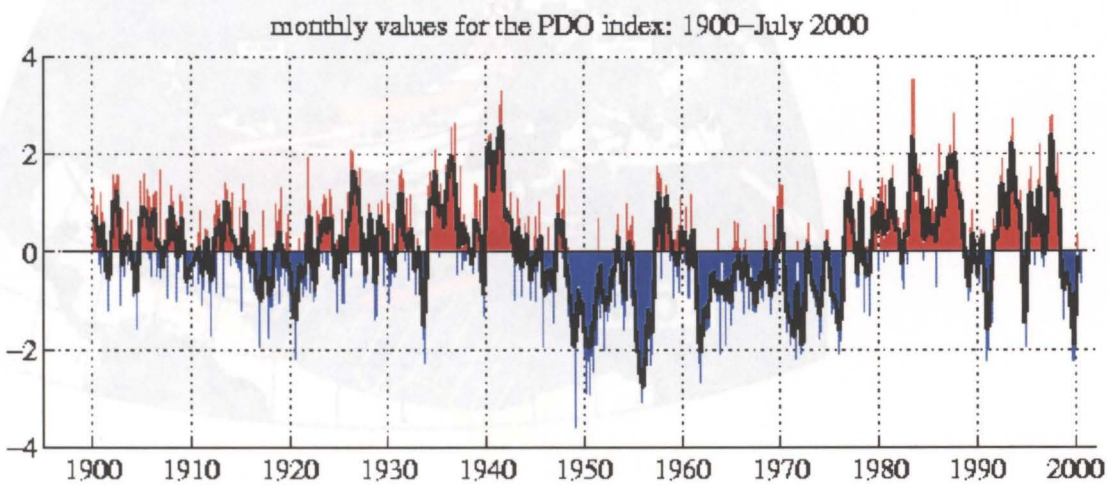

Figure 1.15.a. Phases of the North Atlantic Oscillation influences high latitude precipitation, and therefore modifies the freshwater budget. In such a significant region of convection, this can have far reaching consequences. Taken from University of Reading dept. Meteorology web site.http://www.net.rdg.ac.uk/cag/NAO/index.html

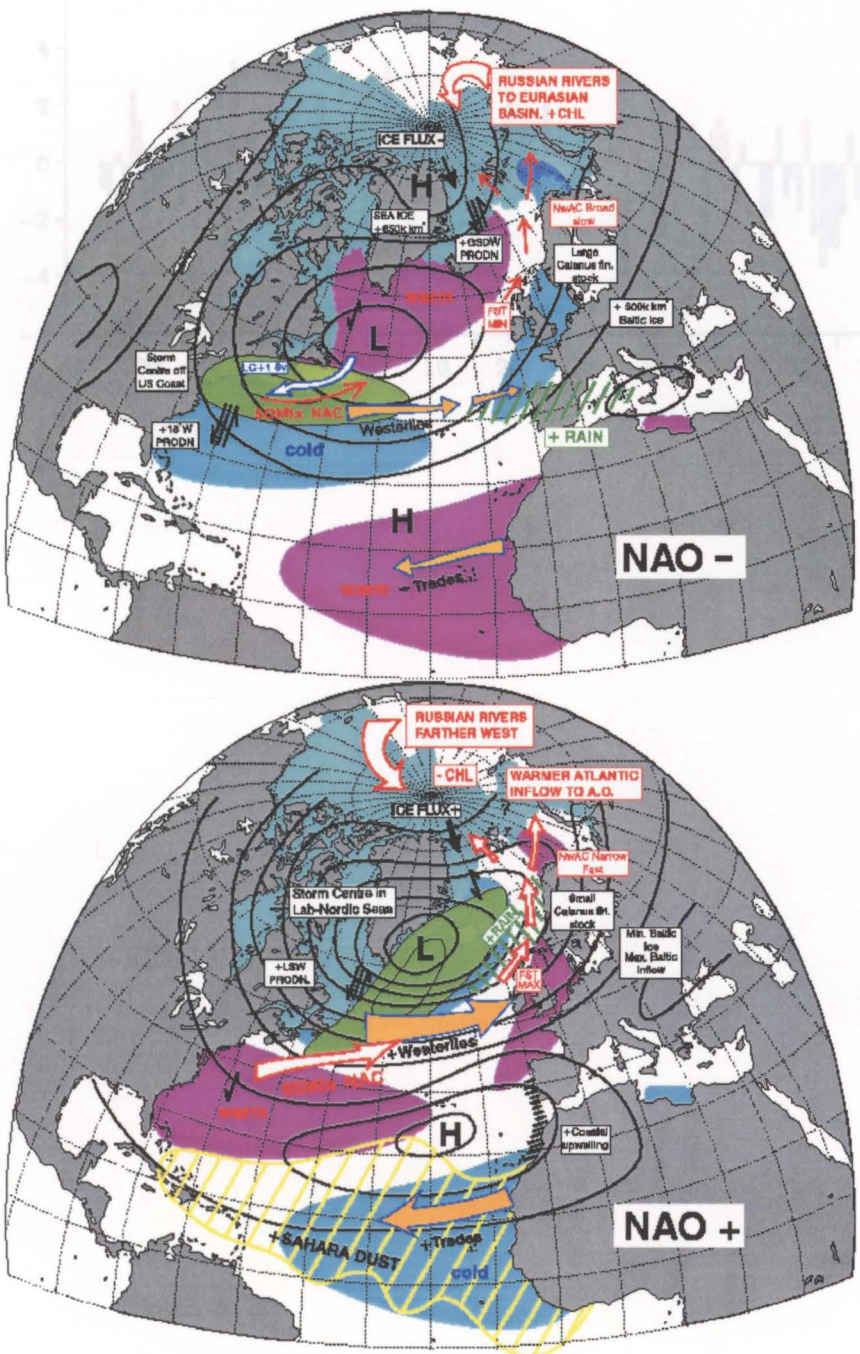

b. The NAO Time series. The NAO has been predominantly positive in the 1980's and 1990's.

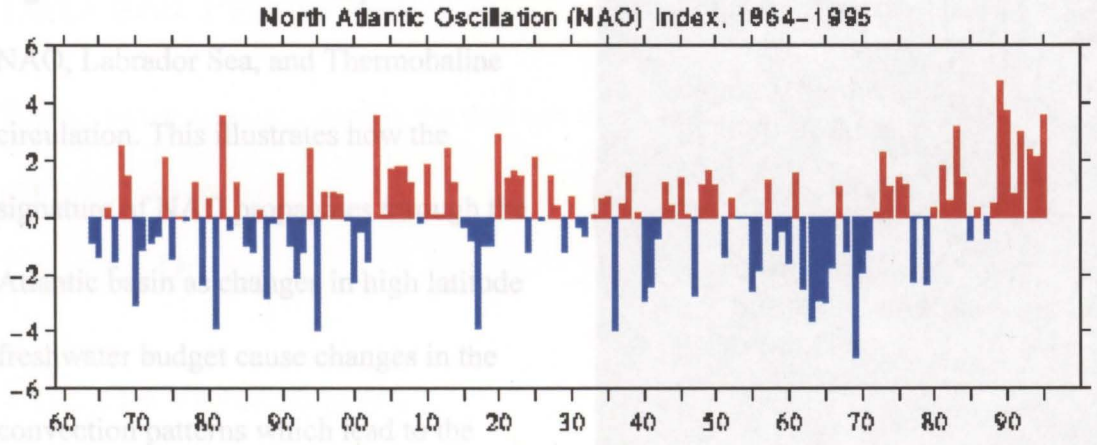

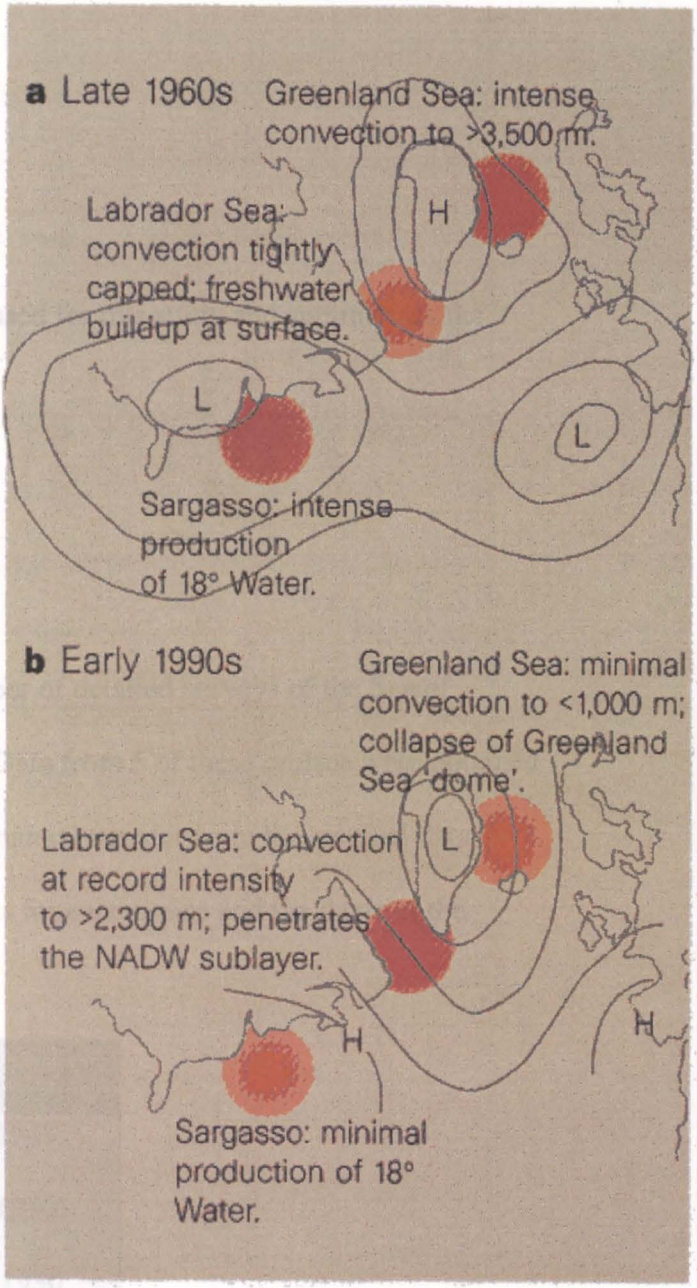

Figure 1.16. The relationship between the NAO, Labrador Sea, and Thermohaline circulation. This illustrates how the signature of NAO propagates through the Atlantic basin as changes in high latitude freshwater budget cause changes in the convection patterns which lead to the formation of NADW and LSW. Taken from Dickson (2000).

Chapter 2

Data and Processing

The following section describes the data sets used for this study and summarises the analysis methods used.

2.1. The Data.

2.1.1. The Vityaz data set.

The Russian ship the *Vityaz* undertook a number of detailed surveys of the Sea of Okhotsk in the late 1940's and early 1950's. Data from 5 of these cruises were obtained in the form of Excel spreadsheets, following manual transfer from the original data transcripts. Figure 2.1 shows the station points for each cruise and the dates of the cruises are summarised in table 2.1:

CRUISE NUMBER	DATES
02:	**09/08/1949 - 16/10/1949**
04:	**21/05/1950 - 01/07/1950**
07:	**03/06/1950 – 26/07/1950**
09:	**11/11/1951 - 29/12/1951**
12:	**19/09/1952 - 31/10/1952**

Table 2.1. The Russian ship the *Vityaz:* Cruise numbers and dates of the survey data obtained for this thesis.

The station data includes measurements of temperature, salinity, oxygen, and various nutrients. It must be noted, however, that as the data were obtained in absence of the ship logs, information on the precise measuring and positioning techniques are not available.

2.1.2.The WOCE P1W data set

From the 3rd to the 12th September 1993 a transect through the Sea of Okhotsk was surveyed in a joint Canadian-Russian venture as part of the World Ocean Circulation Experiment, (Freeland 1998). A transect of 30 CTD casts was obtained at the station positions shown in figure 2.2. The transect ran from the mainland Russian coast, through the middle of the Sea of Okhotsk, and out through the Bussol Strait, the largest opening between the Okhotsk and the North Pacific.

2.1.3.The NOAA-AVHRR data

The advent of satellite observations has opened the doors to detailed repeatable snapshot of the surface properties of a region. Satellite SST data are available in ASCII format at 9km resolution from the Pathfinder website for downloading by ftp. Monthly means were downloaded for the region of study from January 1987 to December 1998: totalling 12 years.

2.2. Data Processing

2.2.1.Vityaz Data

Profiles of temperature and salinity were plotted for each station for quality control. Unrealistic looking profiles were identified, and numbers were checked for obvious keypunch errors, such as salinities of 335.0 instead of 33.50. Those clearly suspect values that could not be rectified by such methods were excluded from this study. The data were first vertically interpolated to Levitus standard depth levels, and then regridded horizontally onto regular co-ordinates using *Objective Analysis* (Bretherton *et al* 1976, Wunsch, 1996). The objective analysis is based on the *Gauss-Markov Theorem*, which provides a least squared error estimate of physical data, given a limited number of data points. This allows for a quantitative assessment of the accuracy of interpolation, so that correlation parameters can be adjusted accordingly.

Maps of temperature and salinity were produced for each Levitus standard depth level to establish regional climatology. In addition, to form a picture of the general circulation, geopotential anomaly fields were calculated, and used to compute the geostrophic velocity field for the basin following equation 2.1. Full details in Pond and Pickard (1983), see also figure 2.3.

$$(V_1 - V)_2 = \frac{1}{L2\Omega\sin\phi}\left[\int_{p2}^{p1}\delta_B dp - \int_{p2}^{p1}\delta_A dp\right]$$

$$= \frac{1}{L2\Omega\sin\phi}\left[\Delta\Phi_B - \Delta\Phi_A\right] \qquad \text{(eq. 2.1)}$$

In order to allow direct comparison with the WOCE P1W transect, the WOCE track was recreated from the temperature and salinity data using Gaussian interpolation with a sphere of influence of 200km around the co-ordinates of each WOCE station. Potential temperature and potential density fields (referenced to the surface and 2000dbar) were also calculated. In addition, a transect across the Bussol Strait (see map in figure 1.11) was obtained from the gridded data. This facilitated the calculation of geostrophic velocities through the strait, and therefore allowed an estimation of volume transport to be calculated.

2.2.2.WOCE P1W data

The CTD data from each station were interpolated to Levitus standard depth levels using cubic splines for direct comparison with Vityaz data. In order to determine changes in the mean physical properties of the basin, the vertically integrated heat and salt content were also calculated for WOCE and Vityaz data.

2.2.3. Calculating flux through Bussol Strait.

Bussol Strait is the largest connection between the Sea of Okhotsk and the open ocean. The flux through the strait dictates the role of the Okhotsk in Pacific intermediate water production, and any changes in this will significantly affect the character of intermediate waters in the North Pacific.

a. A question of geostrophy

Initially flow was calculated by the geostrophic method using the Vityaz data (section 2.2.1). A reference depth of 1200 m was identified as the level of no motion from the potential density data. The results of these calculations produced flow rates much lower than expected for this region. When previous studies by Garrett *et al* (1981, 1987) are considered, a number of likely reasons come to light. In Garrett's studies of the Strait of Belle Isle off the coast of Newfoundland, he concluded that flows in this region are: "….predominantly geostrophic, with a significant ageostrophic component".

This can be concluded, as there is significant temporal variation in along-shore flows. It would be expected that the same would be true for the Bussol Strait; in the overflow region, where dense water is flowing into the Kuril Basin over the sill, the effects of bottom friction would be significant, leading to considerable non-geostrophic components. Moreover, if the flow is hydraulically controlled then geostrophy does not apply. In addition, the lack of cross channel data from the WOCE project meant that this method could not be used to quantify changes in flow rates between the 2 data sets.

b. Hydraulic control

A procedure has been developed (taken from Whitehead, 1998 and Freeland, 2001) to calculate volume flux from the density gradient over the sill (equation 2.2). This procedure assumes hydraulic control of flow. Freeland (2001) suggests tightening of density surfaces, and steepening of density surfaces over the sill are indicative of hydraulic control of flow over a sill. Farmer and Armi (1999) go further in suggesting that solely an asymmetry in the isopycnals at a sill imply that the flow is hydraulically controlled at the sill. Figure 3.14 shows the potential density along the line P1W during

the WOCE cruise. It is clear that there is a tightening and steepening of the isopycnals at the sill, providing satisfactory evidence of hydraulic control. A more detailed discussion of hydraulic control can be found in Whitehead (1998).

Whitehead (1998) showed that density profiles up and downstream of a control section are modified by passage through a control point. The volume flux is calculated by comparing the potential density profile of a station upstream with one downstream of the sill (see figure 2.4):

$$Q = \frac{\Delta\rho / \rho\, g h_u^{\,2}}{2f} \qquad \text{(eq. 2.2)}$$

Here $\Delta\rho$ is the largest difference at or above the sill depth, and h_u is the difference between the sill depth and the depth of bifurcation of the 2 profiles. This calculation was performed for both the WOCE data set (stations 6 & 7), and the Vityaz data, from which, stations 144 and 159 in cruise 2 was chosen. Cruise 2, was the ideal candidate as it was carried out at the same time of year as WOCE, and included a detailed survey of the Bussol Strait region. However, subsurface flow through the Bussol Strait is known to be into the Sea of Okhotsk (Freeland ET al, 1998).

Salt flux balance calculations were also performed using the flow rates calculated above, as well as a null hypothesis that outflow had not changed, and that it had increased over the study period. This was done to determine whether the Sea of Okhotsk would be capable of causing the changes in NPIW noted in section 1.8. Changes in the salt flux through the Sea of Okhotsk over the 50 years, was calculated using equations 2.3, 2.4 and

2.5. This assumes that the change in flow rate and salinity gradient between the Sea of Okhotsk and the North Pacific was linear between 1950 and 1993 (see figure 2.5). Therefore, the total salt flux can be inferred as the area under the graph. If this salt flux is divided by the area of NPIW, then the role of the Sea of Okhotsk played in producing the observed changes in the North Pacific can be explored.

$$\text{Salinity Gradient } (\Delta S) = S_{(\text{Okhotsk})} - S_{(\text{Open Pacific})} \quad \text{in psu} \qquad \text{(eq. 2.3)}$$

$$\text{Total Flux} = [(Q_{1990} * \Delta S_{1990}) - (Q_{1950} * \Delta S_{1950})] * 43 \text{ years} / 2 \quad \text{in m}^3 \text{ psu} \qquad \text{(eq. 2.4)}$$

$$\Delta S \text{ (NPIW)} = \text{Total Flux} / \text{Vol NPIW}. \qquad \text{(eq. 2.5)}$$

Four test flow rate (Q) scenarios were used. In the first case the change in inflow, calculated from equation 2.2 above, was assumed to equal the change in outflow; in the second case no change in rate of flow was assumed, (remaining at the 5Sv flushing rate discussed by Kurashina, 1967). In the third and fourth cases an increase in flow rate was assumed. Salinity changes were taken from WOCE station 20 in the Deryugin Basin, and station 1 in the open Pacific (see figure 2.2 and figure 2.6) to calculate the salinity gradients (eq 2.3). The volume of NPIW was estimated from the potential density map produced by Talley (1993) (see figure 2.7). Talley defined the boundary of NPIW as $\sigma_\theta 26.6$, with a depth range of typically 300 to 700m. This allows us to draw a rough box around the area occupied by NPIW. This was taken as 20 - 40°N latitude (2222km), and 120°E - 120°W longitude (11548km), giving a volume of $1.027*10^{16}$ m^3.

2.2.4. NOAA-AVHRR data.

Twelve years of monthly mean SST data allow a detailed analysis of seasonal variability and longer-term changes in this region. The mean climatology for each month was calculated and used to calculate monthly anomaly fields for the region, producing a 12-year catalogue of month to month variability in the region. To determine spatially averaged trends in surface temperature, basin wide mean anomalies were plotted as a time series. Only mid-summer (June and July) anomalies were plotted as a time series. The ice surface will always exhibit the same spectral temperature, and therefore does not reflect variability in ocean temperature or surface climate conditions. As the Sea of Okhotsk has considerable ice cover in the winter months, these data were excluded from the study to allow the year to year trends to be established.

The linear trend of the data was then removed, to permit analysis of the low frequency variability. The normalised anomaly data was plotted against the PDO index, and the cross correlation coefficient was calculated.

Figure 2.1. Map showing the station positions from the *Vityaz* cruises (1949-1952).

Table 2.1 summarises the dates of each respective cruise. The spread of data is not seasonally even, with the cruises clustered around the summer/fall/winter.

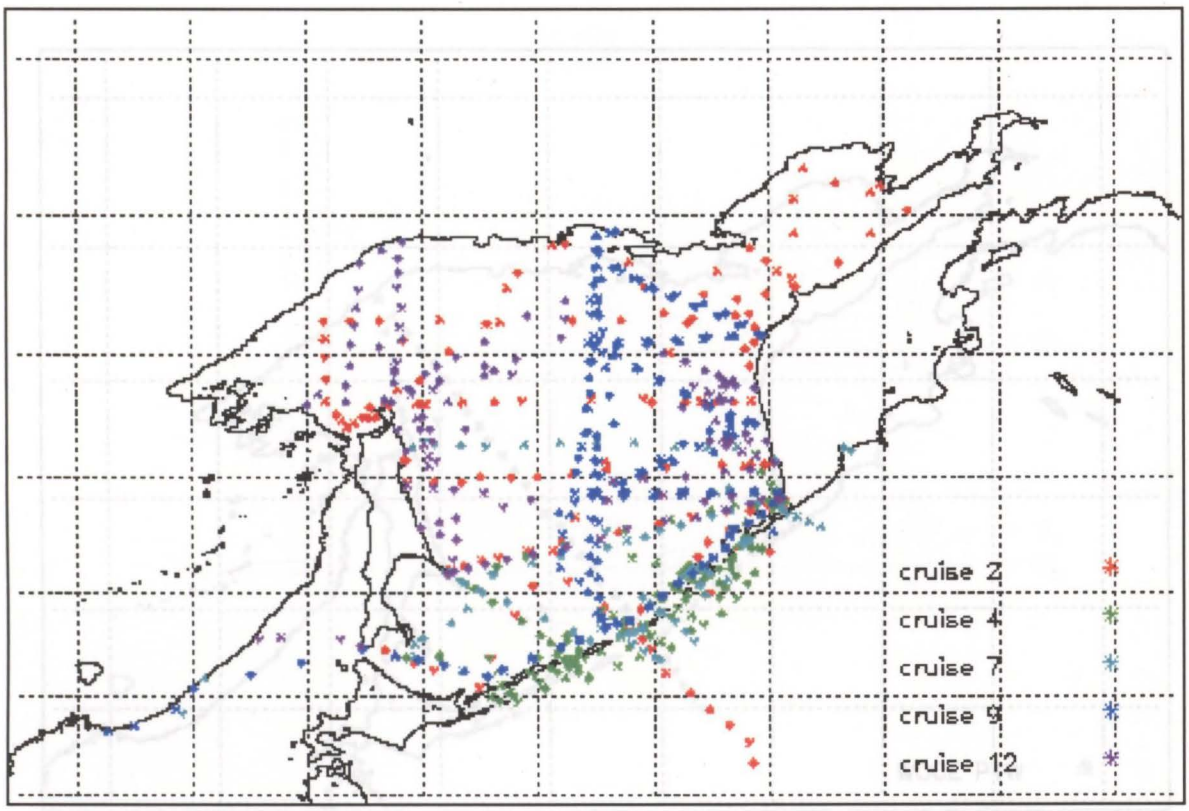

Figure 2.2. Location of Stations from the WOCE P1W cruise (September 1993). The transect bisects the Sea of Okhotsk from the Northern shelf, to the Kuril basin, taking the Bussol Strait through the Kuril Islands, out to the open Pacific.

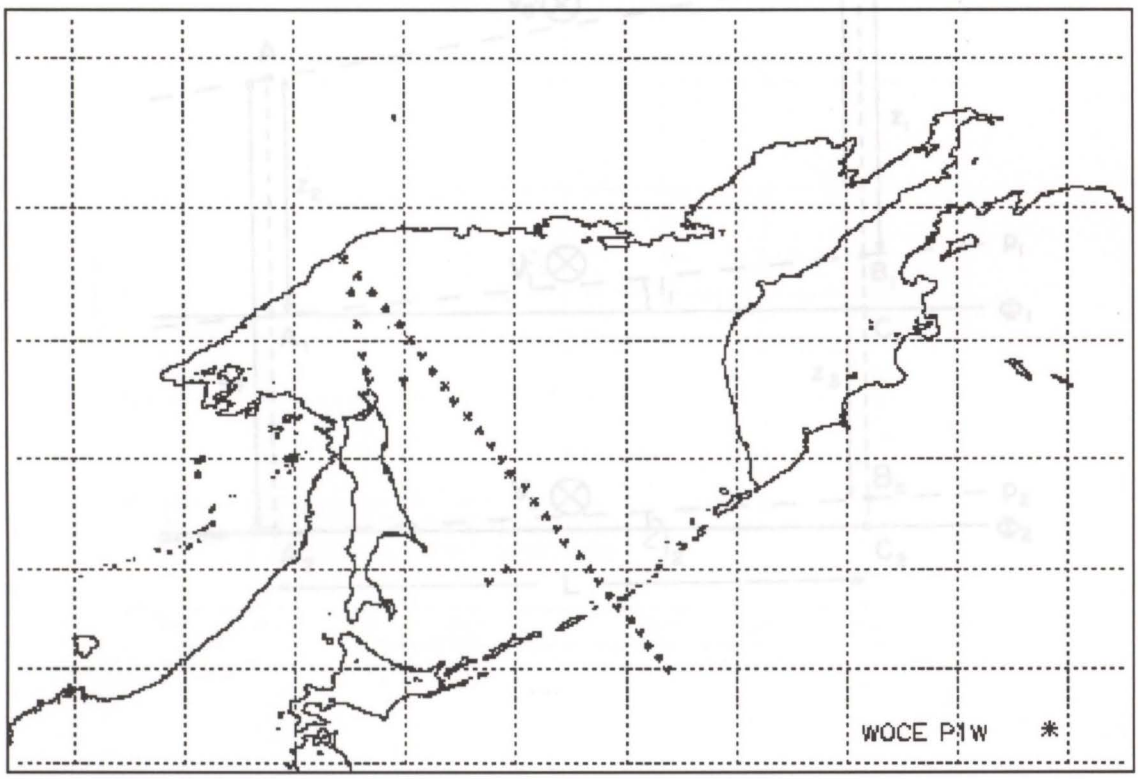

Figure 2.3 Summary of the geostrophic method. Geostrophic flow calculated from the difference in isopycnal height across the flow. See eq. 2.1. Taken from Pond and Pickard (1983).

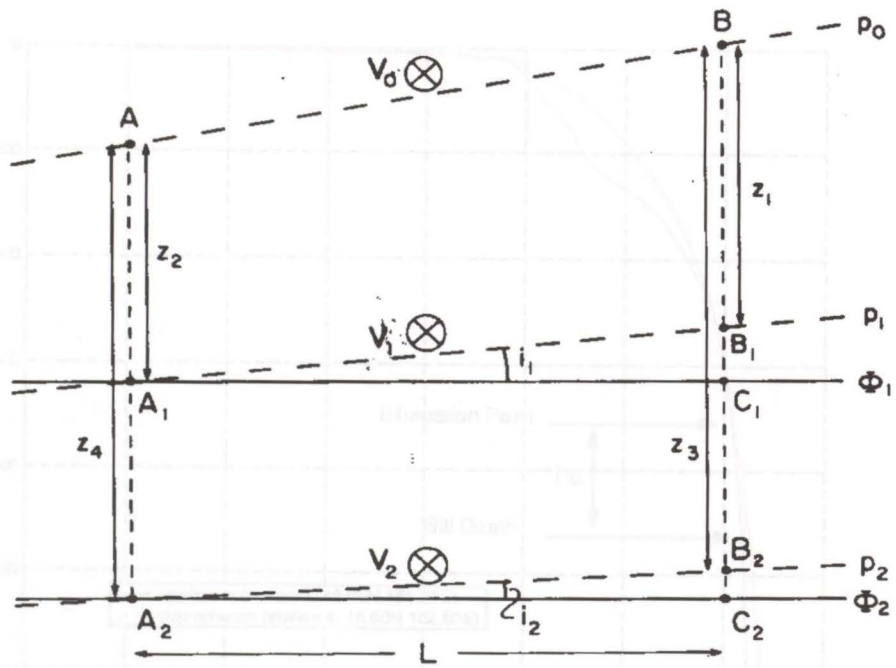

Figure 2.4 Example of Upstream/Downstream potential density profiles used for calculating topographic outflow. The volume flow rate over a sill can be calculated from the maximum difference in density at or above the sill depth, and the difference in depth between the bifurcation point (point at which density profiles separate) and the depth of the sill.

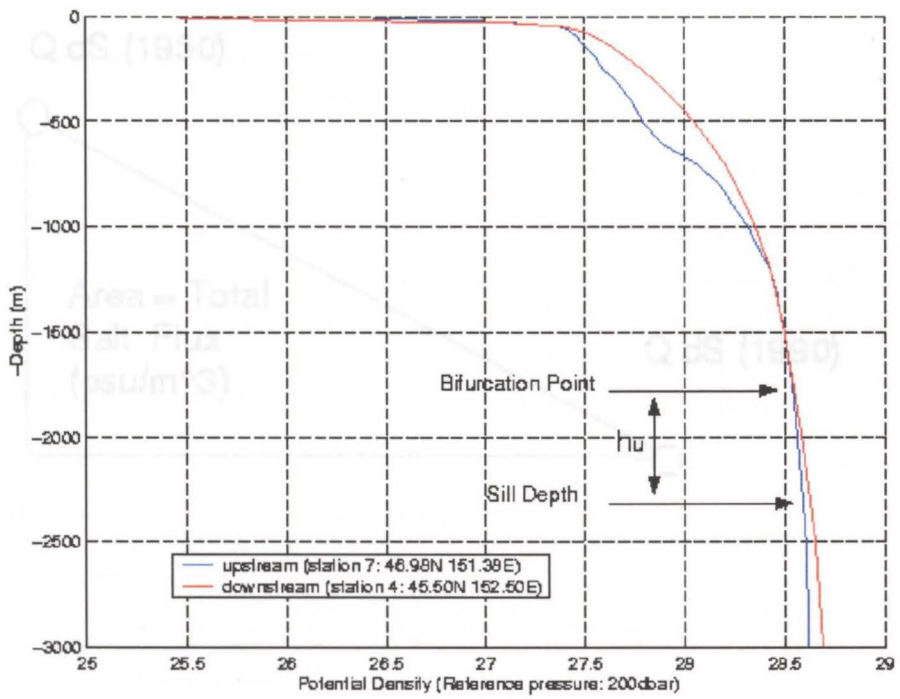

Figure 2.5. Calculating the total salt flux over the 50 years. Volume flow through the Bussol Strait multiplied by the salt gradient across the strait is plotted against time. Assuming a linear change in characteristics, the total salt flux is therefore equal to the area under this graph.

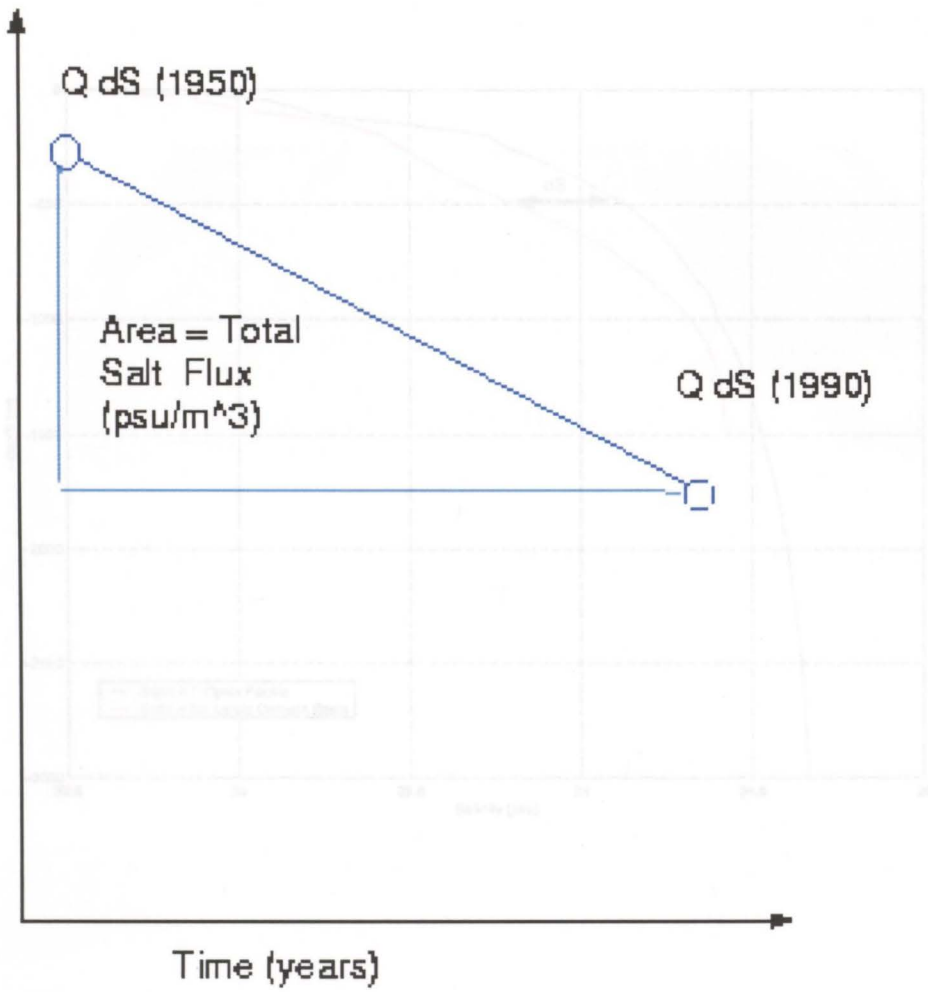

Figure 2.6. Comparing Salinity in the Central Okhotsk to the open Pacific in 1993. The salinity gradient across the Bussol Strait can be approximated by the difference in salinity between the central Sea of Okhotsk and the open Pacific. This was then combined with flow rate scenarios to determine the influence of changes in the Sea of Okhotsk on NPIW.

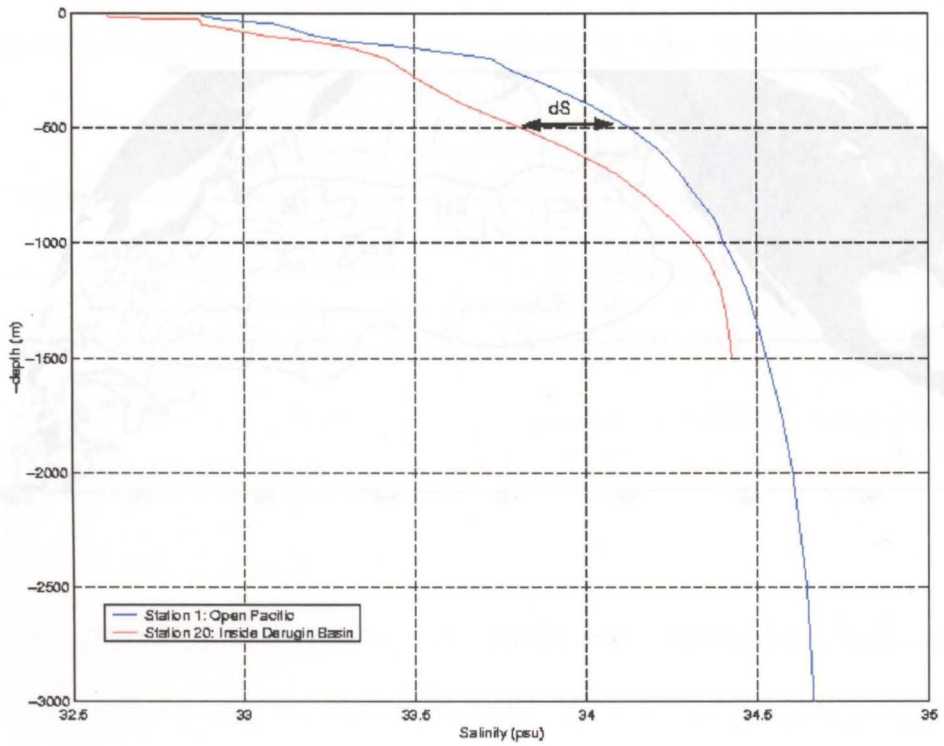

Figure 2.7 Potential Density, δ_θ of NPIW, defined as the salinity minima in the density range 26.6 to 27.0 δ_θ. Talley also defined the depth range at which NPIW occurs, 300-700m. From this data, the volume was estimated to determine the influence of changes in the Sea of Okhotsk on NPIW (section 2.2.3). The NPIW volume was calculated as $1.027*10^{16}m^3$. Taken from Talley (1993).

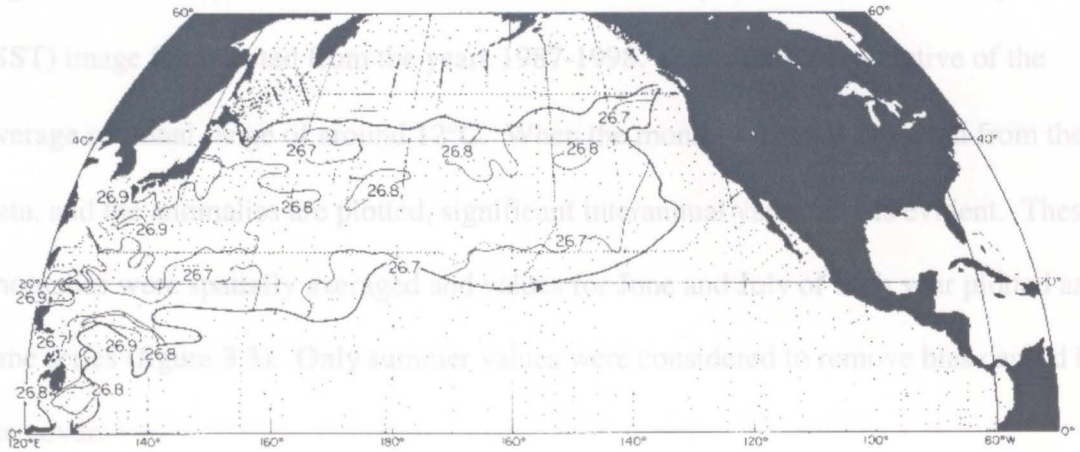

Chapter 3

Results

3.1. Surface properties: AVHRR data.

Figures 3.1 and 3.2 show a winter and a summer monthly mean sea surface temperature (SST) image for selected from the years 1987-1998. These are representative of the average seasonal range of around 12°C. When the monthly mean is removed from the data, and the anomalies are plotted, significant interannual variability is evident. These anomalies were spatially averaged and values for June and July of each year plotted as a time series (figure 3.3). Only summer values were considered to remove bias caused by ice cover.

At first glance a general warming trend can be noted, although this is dominated by a huge warming event in the late 1980's, after which, the temperature falls almost as sharply, before generally climbing more gradually from 1993 onwards. The solid black line represents the first order linear regression of this data, and the broken lines represent the ±50% confidence interval. There is a clear positive trend to these data, despite significant spread. On initial analysis, the trends in surface temperature anomalies correlate with the PDO index (Figure 1.14a). In the late 1980's, the PDO entered into a positive phase until 1993/94 when it entered a short negative phase before returning to a positive phase in 1995. Figure 3.3b shows the detrended SST anomaly plotted against the

PDO index for the 12 years. It is clear by sight that there is a general inverse relationship. When the PDO is in a negative phase, the Sea of Okhotsk exhibits a positive SST anomaly, and when the PDO is in a positive phase, the Sea of Okhotsk exhibits a negative anomaly. The cross correlation coefficient is –0.46, which is not quite significant at the 95% level. A longer data set would be required to establish this relationship more robustly.

3.2. Subsurface: Vityaz ship data.

The temporal distribution of the Russian ship data is insufficient to describe the seasonal cycle, with cruises clustered around summer, fall and winter. With such a large seasonal cycle of around 12°C in this region as discussed above, it was decided to exclude the surface data from this study as the spread of data did not facilitate correction for this effect. Figure 3.4 shows the sea temperature field at 200 metres depth. It is clear that the Okhotsk water is up to 2°C cooler than the neighbouring North Pacific waters at this depth. The Okhotsk water is also significantly fresher (figure 3.5). There is an east-west contrast in the basin, with cooler shelf waters travelling south along the western boundary, and the warmer Pacific waters moving north along the western boundary. The exchange between these water masses is mediated by the Kuril Islands. The plume of cooler water moving from the Bussol Strait into the North Pacific clearly marks outflow from the Sea of Okhotsk at this depth. Conversely, the Kruzenstern Strait further north exhibits a dominant inflow at this depth, shown by the plume of warmer Pacific water intruding into the Sea of Okhotsk. This effect can also be noted in the salinity field.

The geostrophic flow field illustrated in figure 3.6 shows a dominant counter clockwise flow structure in the central basin, with a clockwise regime to the south, in the Kuril Basin. One must, however, be cautioned against taking the representation of flow characteristics around the Kuril Islands literally, as frictional/mixing effects are likely to play a significant role in the dynamics of this region.

The plots of temperature, salinity and potential density across the Bussol Strait (figures 3.7, 3.8, 3.9) clearly show a two layer structure; a cooler fresher upper layer found down to between 500m in the south-west and less than 200m in the northeast. This overlies a warmer more saline intermediate-deep layer, which occupies the region down to 1500m. The cooler layer exhibits temperatures dropping below 1°C and salinities around 33psu, whereas the intermediate warmer layer contains temperatures up to 2.4°C, with salinities reaching 34.5psu. In the potential density field, the isopycnals in this surface region (down to around 500m) shoal towards the northwest, suggesting a geostrophic outflow. The region around 1000-1200 m exhibits virtually horizontal isopycnals, suggesting close to zero geostrophic flow at this depth. Below this depth, there is a slight slope to the isopycnals, which shoal to the southwest, indicating very weak inflow through the strait. Such weak characteristics could also suggest significant portions of the strait dynamics are not in geostrophic balance.

3.3. Comparing Vityaz with WOCE along line P1W.

Figures 3.10, 3.11 show temperature and salinity along the WOCE transect. The cool fresher near surface plume spreading offshore from the northern shelf is clear, with a temperature minimum dipping below 0°C in the region of ~100-200m. It is also important to note that these characteristics terminate rather abruptly on entering the Kuril Basin from the Deryugin Basin, with a warmer plume intruding in from the Pacific over the Bussol sill at mid depths of ~300-1200m. In the salinity transect, this intrusion is best identified at 500m where a horizontal increase of around 0.5psu is visible. When compared with same geographic transect recreated from the Vityaz data (figures 3.12 & 3.13), it is apparent that the large-scale characteristics and behaviour of this region have not changed in the 40 years between these cruise projects. Both clearly exhibit the cool fresher surface pool of water, and a warmer intrusion at intermediate depths from the North Pacific. Figures 3.14 & 3.15 show the potential density for the WOCE and Vityaz cruises along this transect. Again, the large-scale patterns are very much the same, considering the smoothing caused by regridding the Vityaz data for figure 3.15. The signature waters with potential density of around 27-27.5 occur around the 500m-depth contour. One feature to note is the increased density of deeper waters. Water denser than 27.6 are found below the Kuril sill in the Vityaz data, whereas this contour occurs above the sill in the WOCE data set.

To quantify any changes that may have occurred, the temperature and salinity transect data from the Vityaz cruises were subtracted from the WOCE data. The resulting

anomaly images can be seen in figures 3.16 and 3.17. In the temperature anomaly image, the biggest feature to note is a large positive anomaly of around 1°C around the region of the Bussol Strait, and into the Kuril Basin, between 200 and 800m. This suggests that warmer waters are entering the Sea of Okhotsk from the North Pacific. This warming can be seen clearly when depth averaged anomalies were plotted (figure 3.18). A minimum positive temperature anomaly of around 0.1°C is found close to the shelf and close to the open Pacific and a maximum of 0.3°C at station 12 in the Deryugin Basin. The average anomaly is around 0.2°C

The salinity anomaly plot shows consistent freshening throughout the water column along the transect. Significant regions of note are the Kuril Basin between 300 and 800m, which shows a freshening of 0.3psu, and in the open Pacific just south of the Kuril Islands between 200 and 700m, which exhibits a freshening of around 0.4psu. In addition, a significant region of subsurface freshening is apparent in the Deryugin Basin at around 200m exhibiting freshening of over 0.4psu, which is connected to a deeper, larger anomaly of around 0.16psu. This deeper anomaly occupies the region between 300 and 800m. On plotting the depth averaged salinity anomalies (figure 3.19), there is a clear basin wide freshening of around 0.1-0.2psu. However, the pattern of variability almost exactly mirrors that of the temperature anomalies, with a minimum freshening at station 12, of around 0.04psu, and a maximum at the shelf slope of 0.15psu.

3.4. Flux calculations.

As mentioned earlier, the flow in the Bussol Strait is considered to be a 2-layer flow system. Using the topographic flow calculations discussed in the previous chapter, the inflow over the Bussol Sill was calculated as being 6Sv around 1950 (from the Vityaz data), and 3.6Sv in 1993 (from the WOCE data). If this is representative of the total input into the Sea of Okhotsk, it points to a significant reduction in water flushing through the Sea of Okhotsk. However, we are measuring deep *inflow* through the Bussol Strait, when we require surface outflow in order to quantify the role of Okhotsk outflow on NPIW. The other major inputs include the Kruzenstern Strait to the north, considered to be the dominant oceanic input into the Sea of Okhotsk, and outflow from the shelf regions in the northern Sea of Okhotsk.

It was therefore decided to calculate the change in salt flux between the 2 data sets under 3 outflow scenarios. 1) assumes that the reduction in inflow through the Bussol Strait calculated above was equal to the reduction in outflow, and thus a decrease in outflow of 2.4Sv had occurred over the 43 years; 2) assumes that there had been no change in flow rate, and flushing had stayed consistent at 5 Sv (Kurashina et al, 1967); 3) assumes that outflow has increased by 1 Sv; 4) assumes outflow increased by 2Sv. The results are summarised in table 3.1.

The salinity gradients were calculated as follows:

ΔS = S (Okhotsk) – S (Pacific)

ΔS_{1990}= 33.81 – 34.13 = -0.32 psu

ΔS_{1950}=33.96 – 34.19 = -0.23 psu

	Scenario 1	Scenario 2	Scenario 3	Scenario 4
Change in outflow rate (Sv)	**-2.4 Sv**	**0 Sv**	**+1 Sv**	**+2 Sv**
Change in NPIW (psu)	**+0.014 psu**	**-0.028psu**	**-0.044psu**	**-0.061psu**

Table 3.1. Results of salt flux calculations under different flow change scenarios calculated from equations 2.3, 2.4 and 2.5. This demonstrates that small changes in the salinity gradient and flow rates between the Sea of Okhotsk and the North Pacific can make a significant contribution to the observed changes in NPIW discussed in section 1.8.

The changes in salinity for the Central Okhotsk and open Pacific over the 40 years show that the Okhotsk has freshened by about twice the magnitude of the open Pacific. In terms of salt balance, there is a salt flux into the Sea of Okhotsk. This gradient has increased between 1950 and 1990, from –0.23psu to –0.32psu. When this is considered in relation to possible flow scenarios over this period, such small changes in the salinity gradient in an enclosed basin, are clearly capable of contributing significantly to changes in open ocean properties.

Figure 3.1. An example of winter SST from satellite AVHRR. Unfortunately, the winter months are dogged with cloud cover problems.

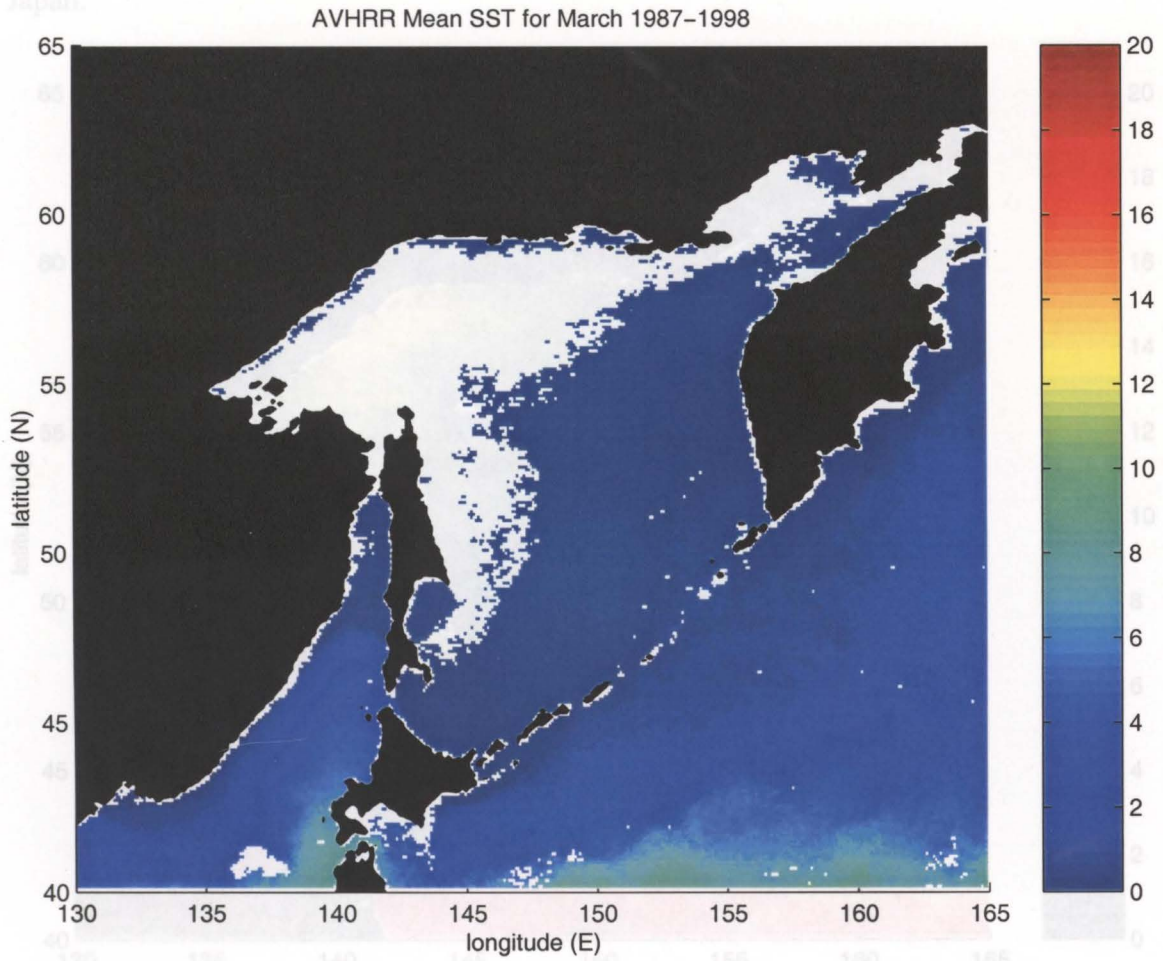

Figure 3.2. An example of summer SST from satellite AVHRR. Coastal Okhotsk surface temperatures reach in excess of 12°C in this image. There is also a clear transition to warmer temperatures on entering the North Pacific, which reaches 20°C around northern Japan.

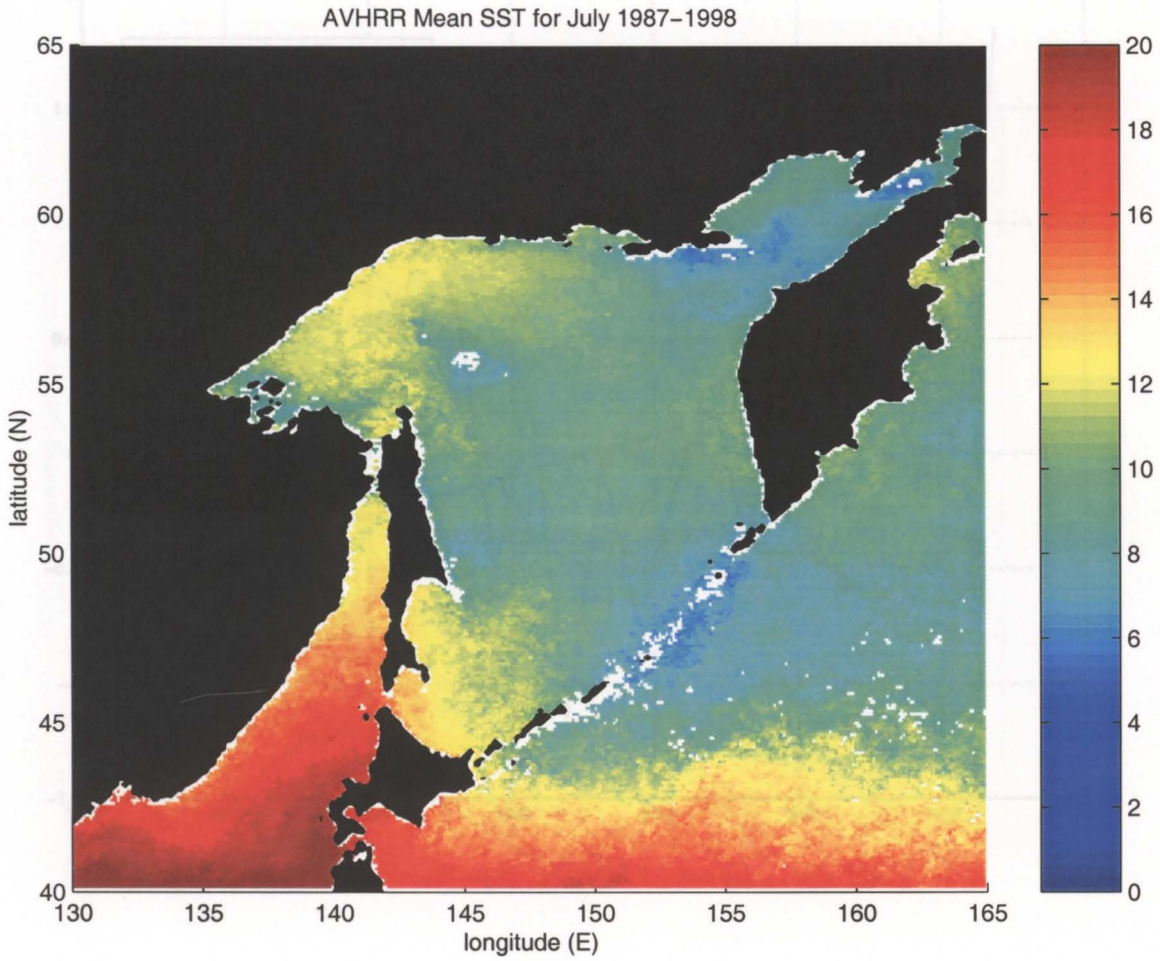

Figure 3.3.a. Time series of summer anomalies from AVHRR data. A clear positive trend is evident in the Okhotsk surface temperature, although significant variability is superimposed on this.

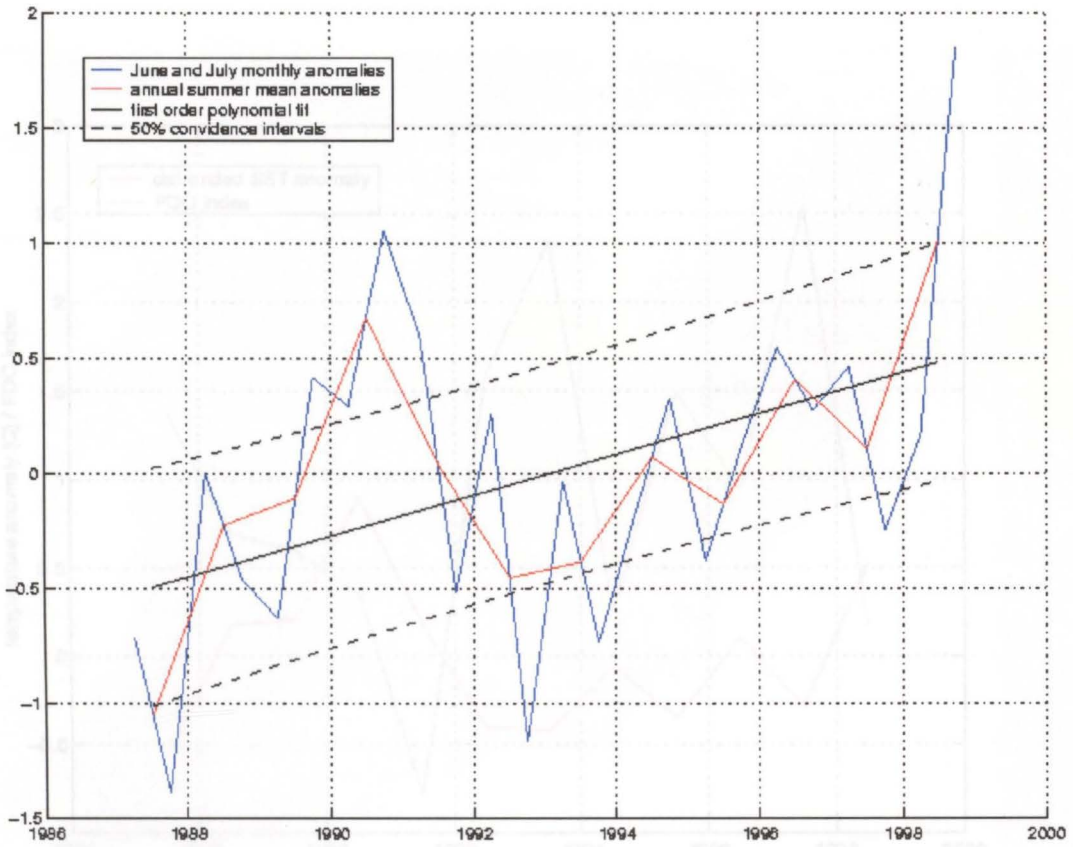

Figure 3.3.b. The above annual summer mean temperature anomalies, after removing the linear fit, plotted against the corresponding summer mean PDO time series. A general inverse correlation is apparent.

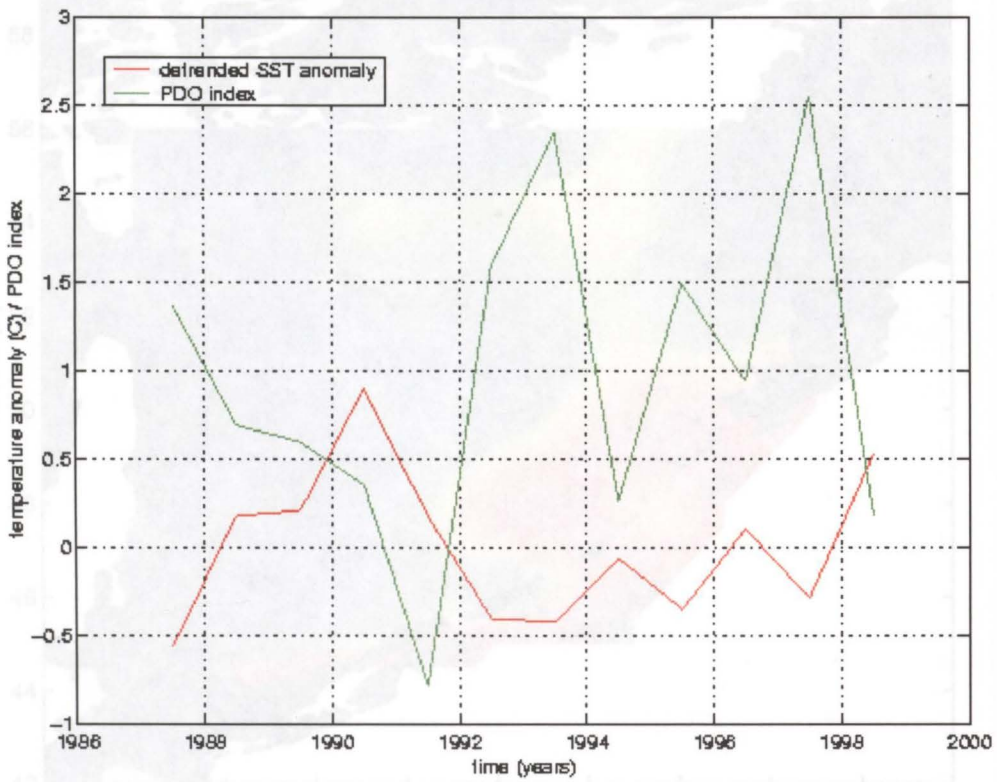

Figure 3.4. Temperature at 200m produced by regridding Vityaz station data using Objective analysis. A deformation radius of 200 km was used to smooth the field. Areas shaded in black are land, and those in grey represent regions under 200m deep.

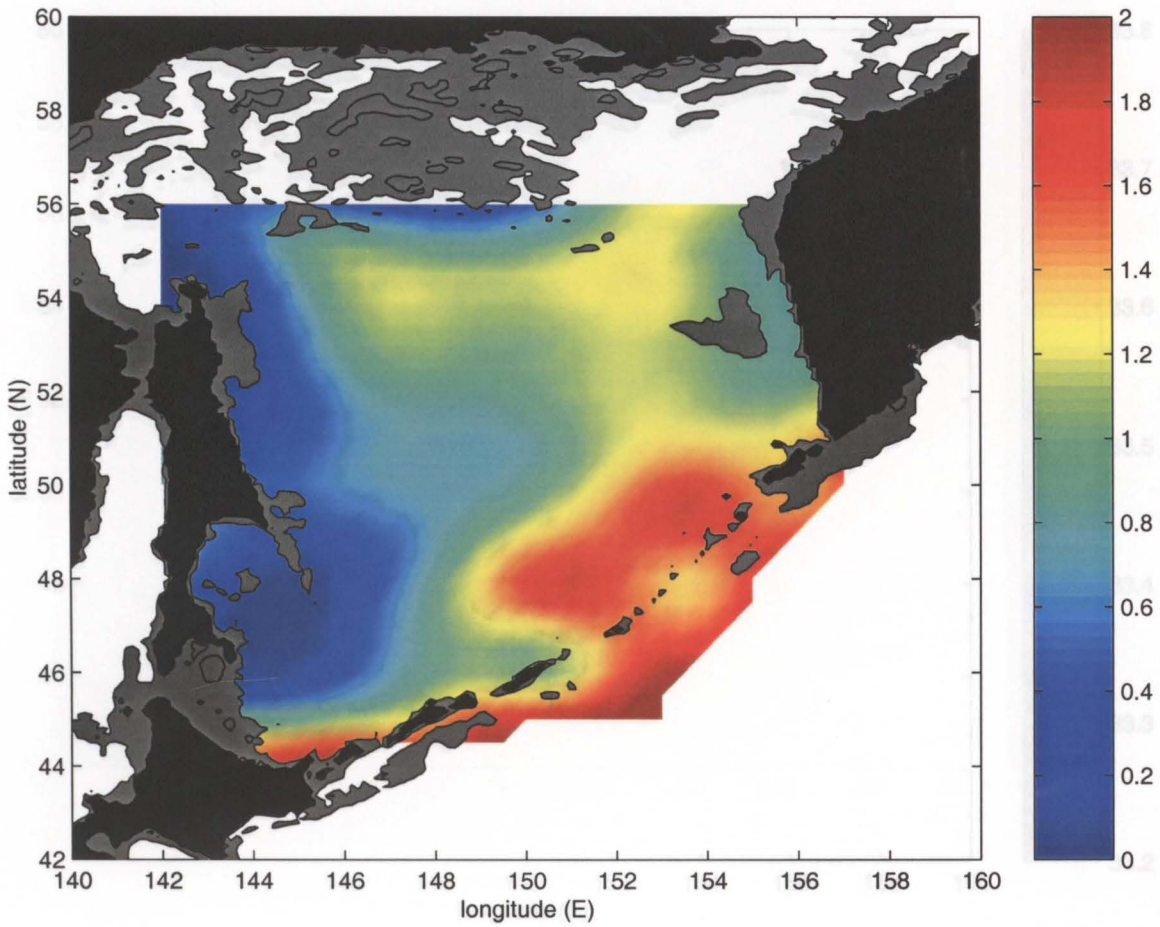

Figure 3.5. Salinity climatology at 200m depth from regridded Vityaz data using Objective Analysis. Again, a deformation radius of 200km was used to smooth the field.

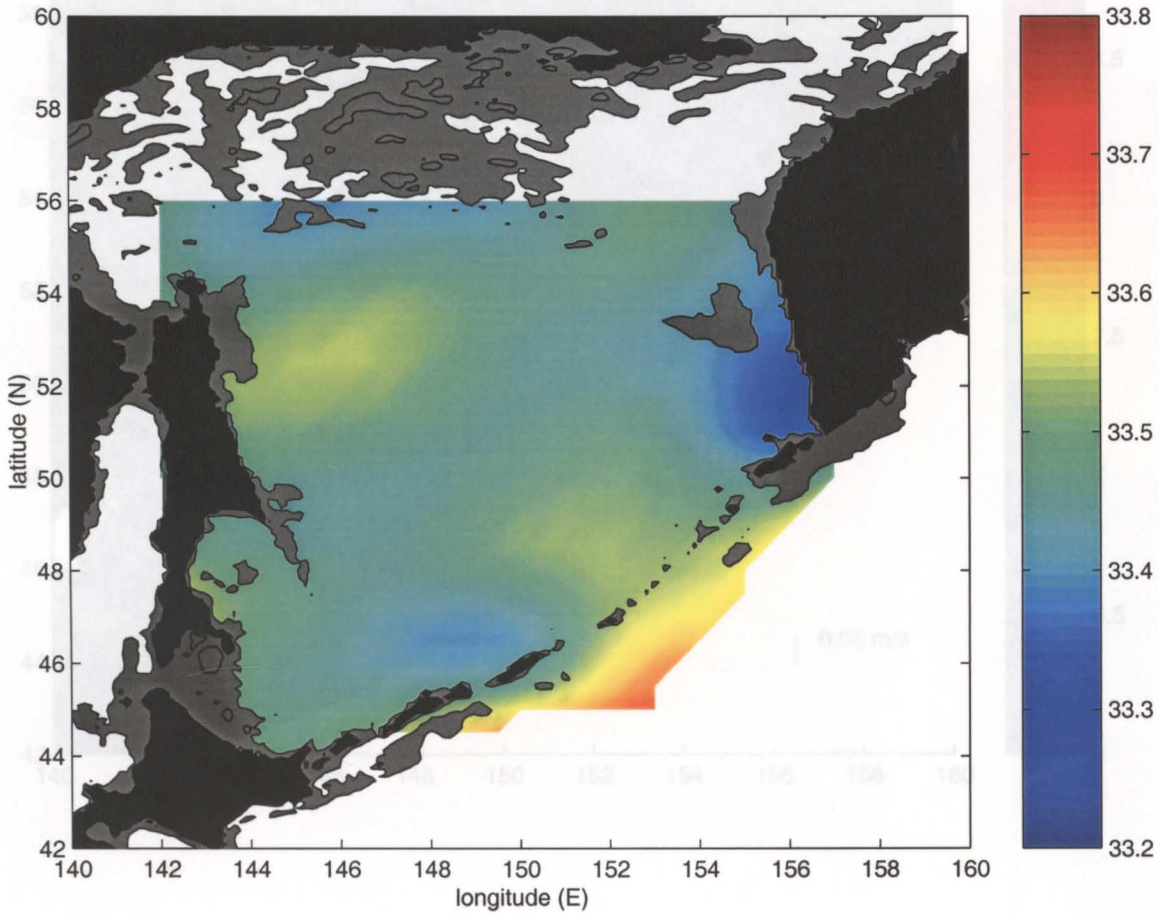

Figure 3.6. Mean geostrophic flow velocities plotted over the geopotential anomaly field, calculated from Vityaz data (for calculation method see figure 2.3, and eq 2.1).

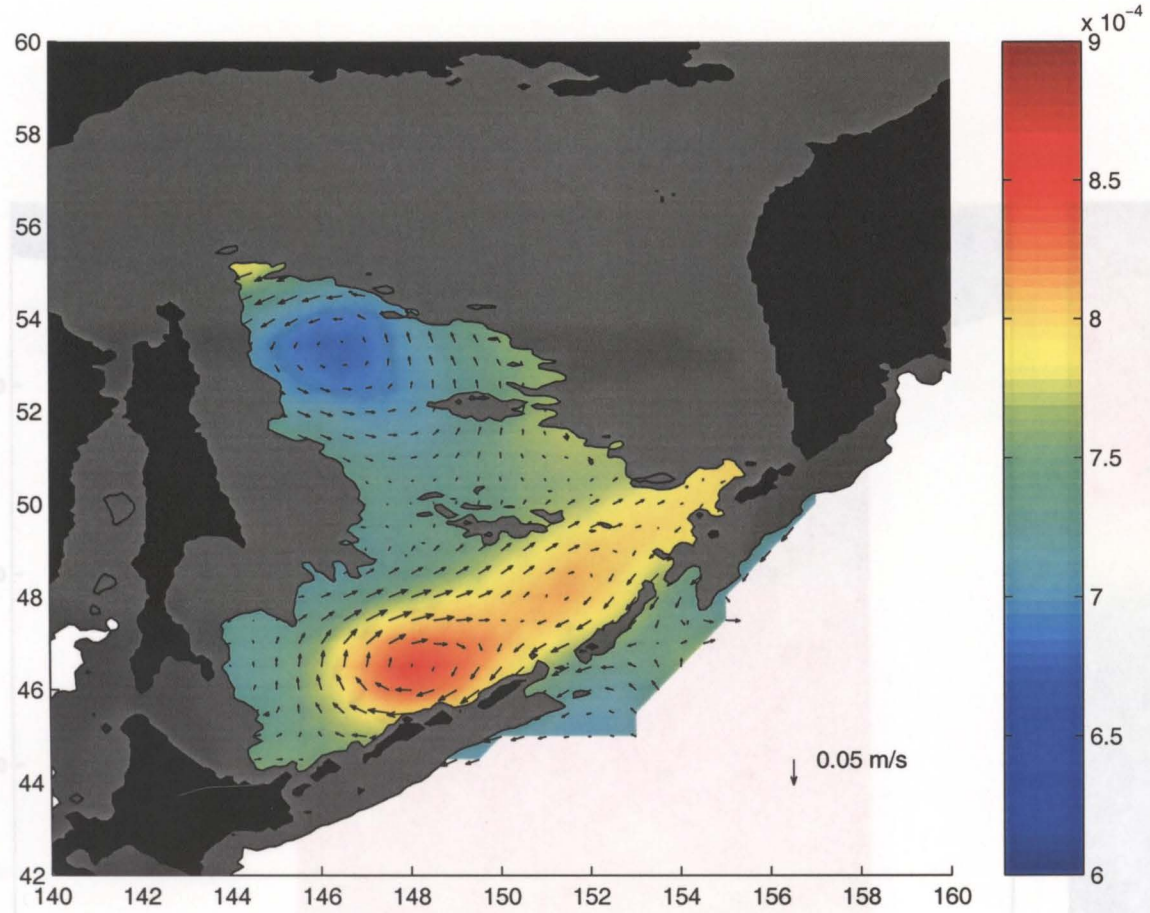

Figure 3.7. Temperature transect across Bussol Strait from Vityaz cruises. This is an impressive representation of the vertical structure in this region. Temperatures range from less than 1°C (dark blue) to around 2.3°C (dark red).

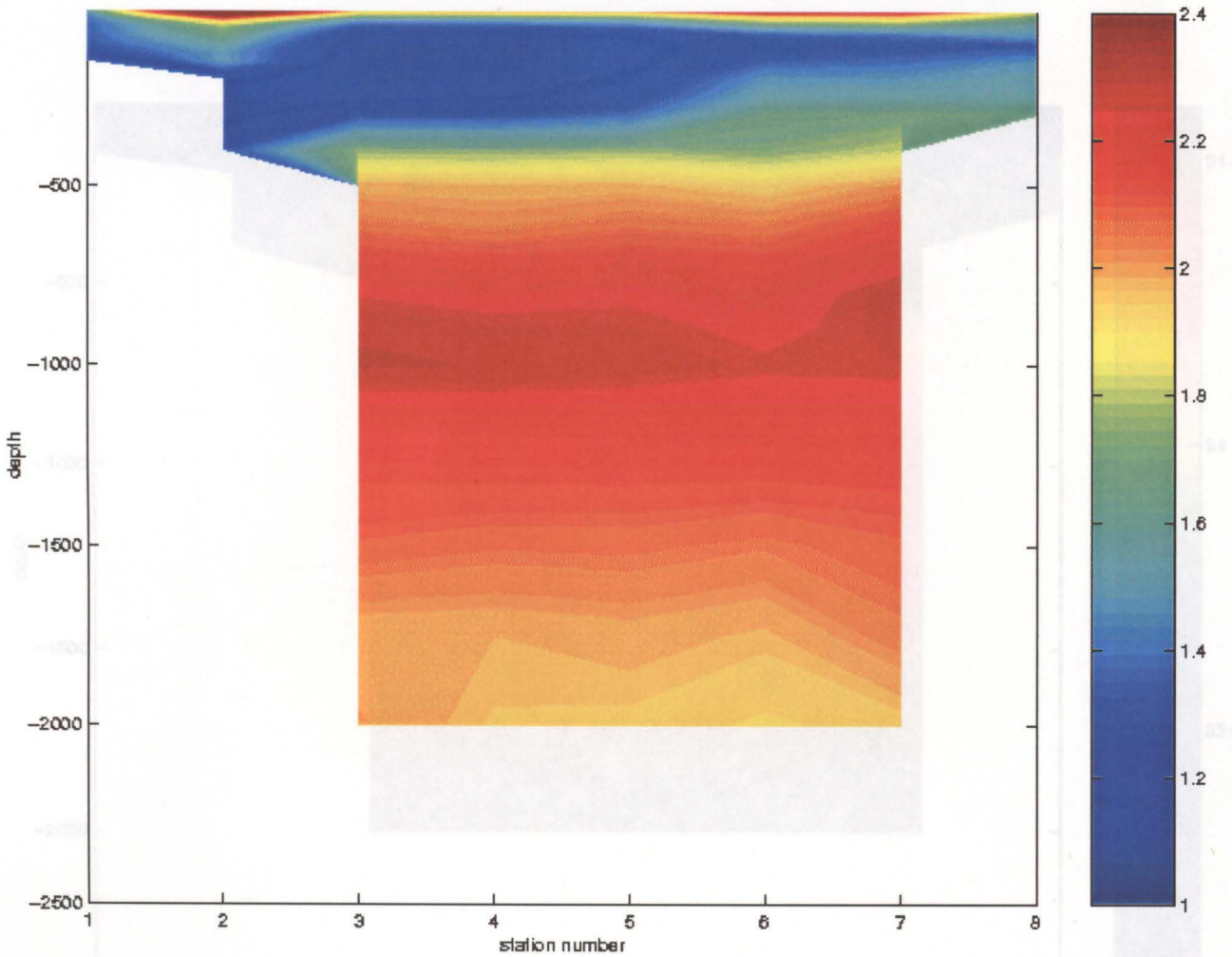

Figure 3.8. Salinity transect across the Bussol Strait from Vityaz cruises. This shows a very strong salinity gradient, ranging from 33psu at the surface to in excess of 34.5psu at depth.

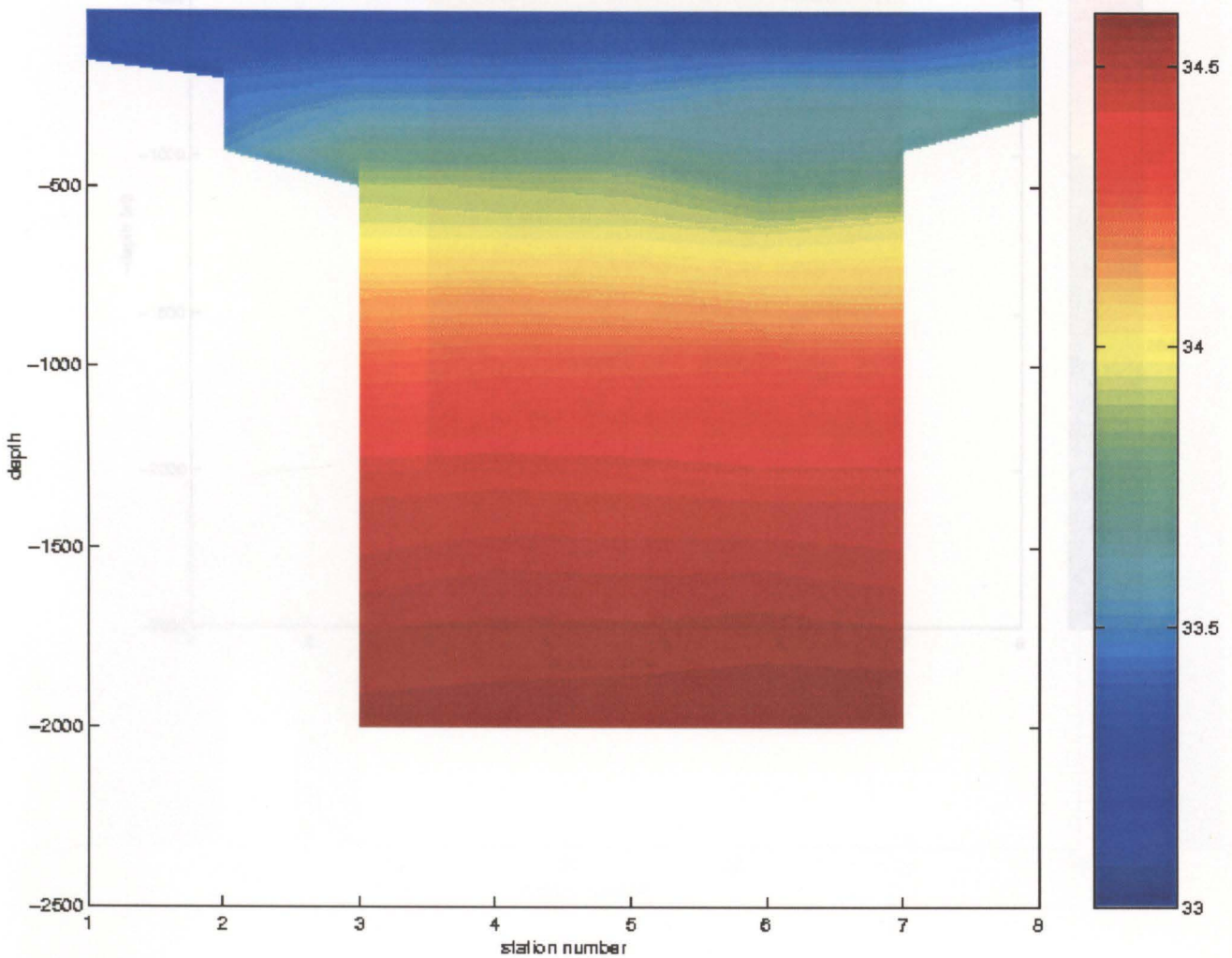

Figure 3.9. Potential density across the Bussol Strait from Vityaz cruises. Reference depth: surface. The sloping of isopycnals give clues to the geostrophic flow characteristics.

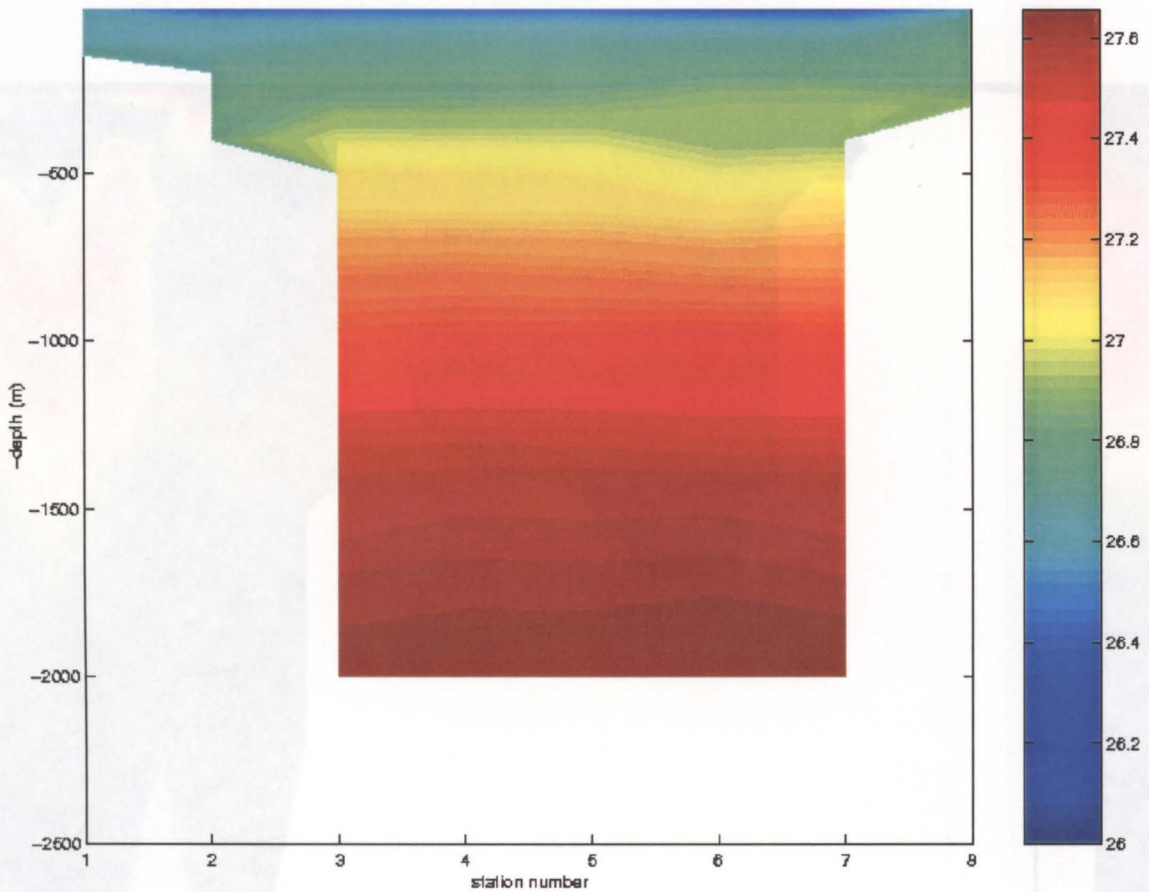

Figure 3.10. Temperature along the P1W transect 1993: Survey was part of WOCE. The main water mass features discussed by Kitani (1973) can be identified in this image. Compare with figure 1.12.

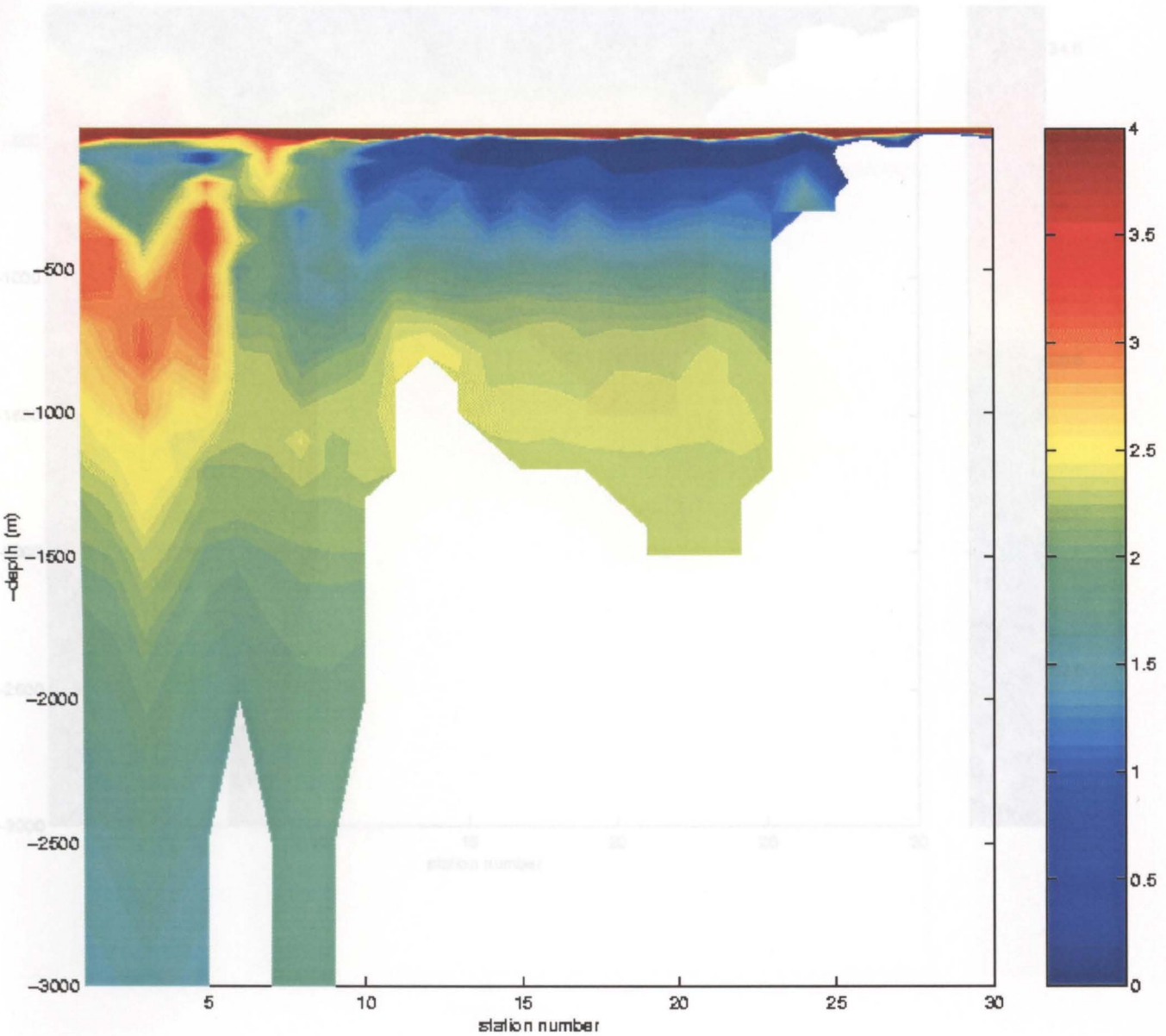

Figure 3.11. Salinity along the P1W transect 1993. When this information is combined with the temperature section, a clear picture of the Okhotsk properties can be inferred.

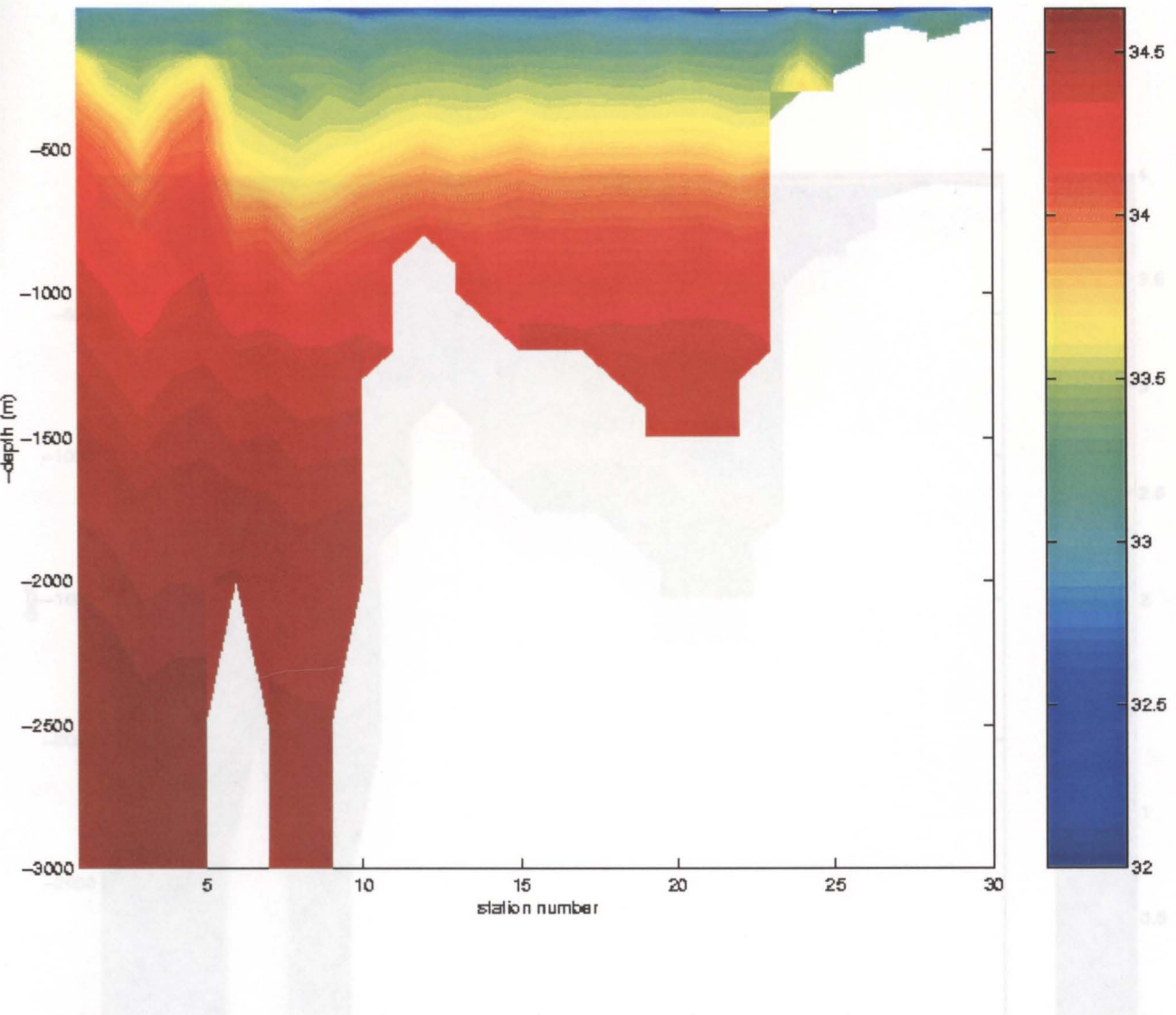

Figure 3.12. Temperature along the P1W transect 1949-52. In the main, the same structural features can be identified as in figure 3.10. Use of Gaussian interpolation means contouring appears smoothed compared to that from WOCE.

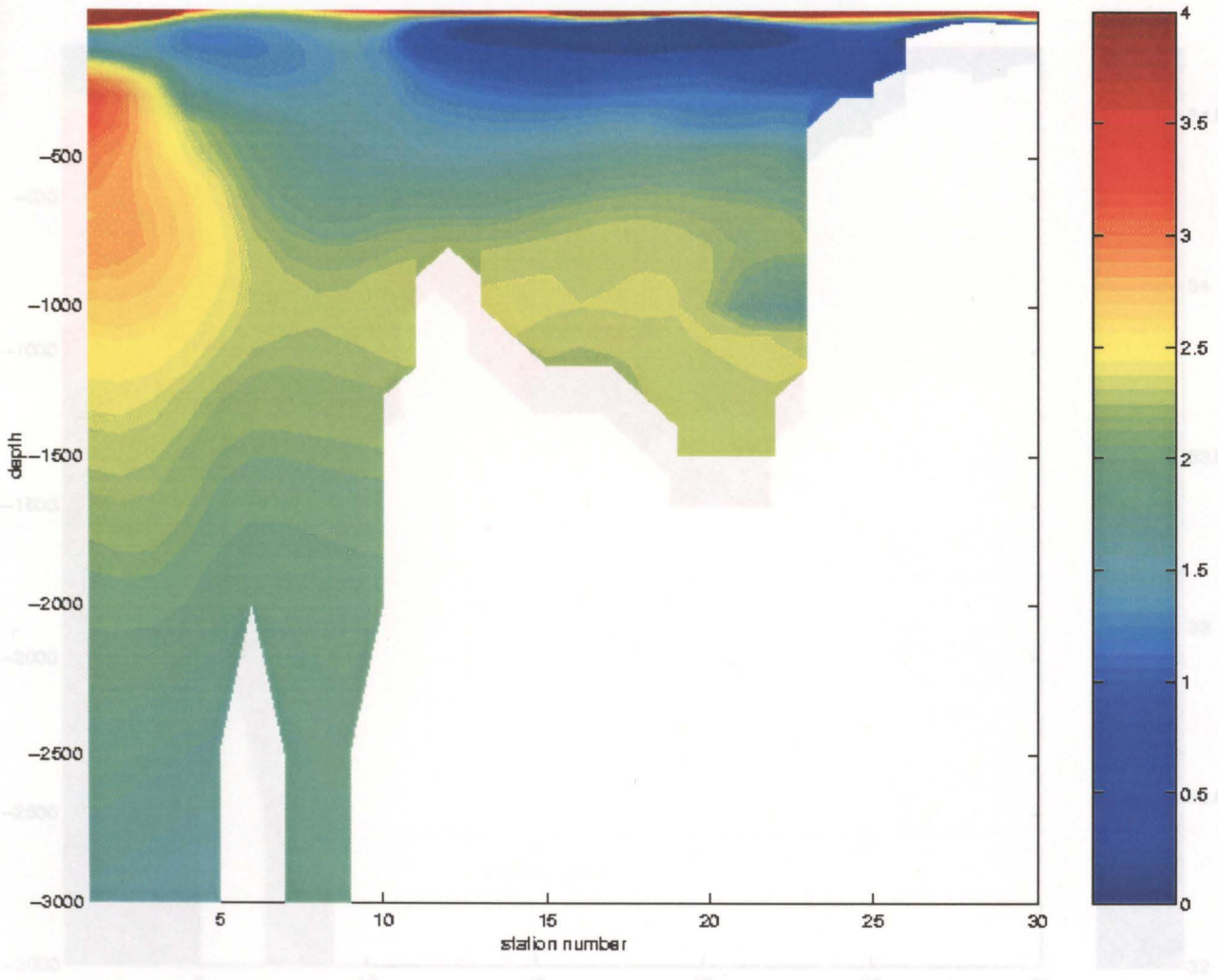

Figure 3.13. Salinity along the P1W transect 1949-52. Compare with figure 3.11 to determine changes over the 40 years.

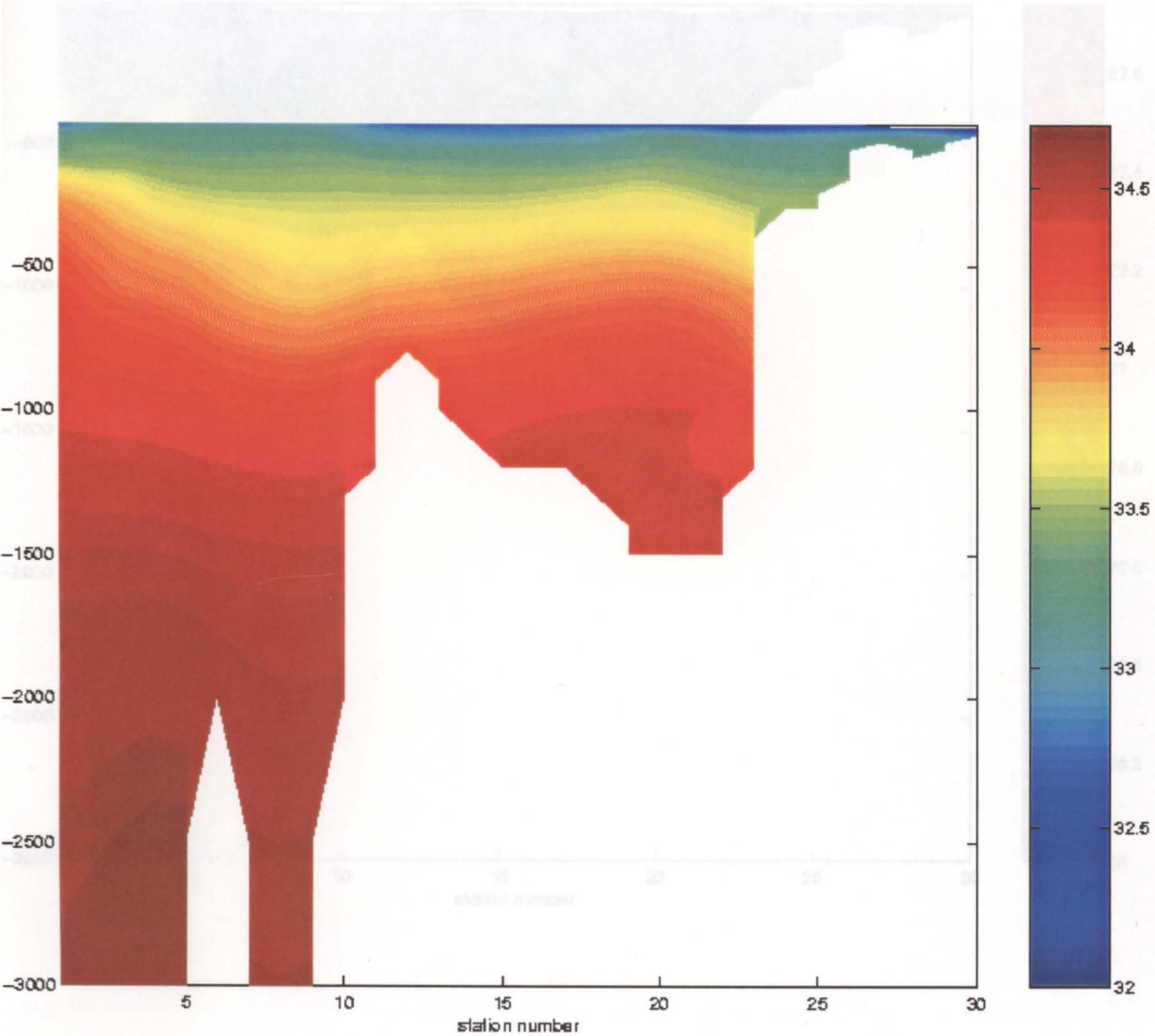

Figure 3.14. Potential Density along the P1W transect in 1993 (referenced to surface). Signature densities of 26.7-26.9 δ_θ are found to outcrop at the surface on the Northern Shelf, and occupy the region above 500m throughout the basin.

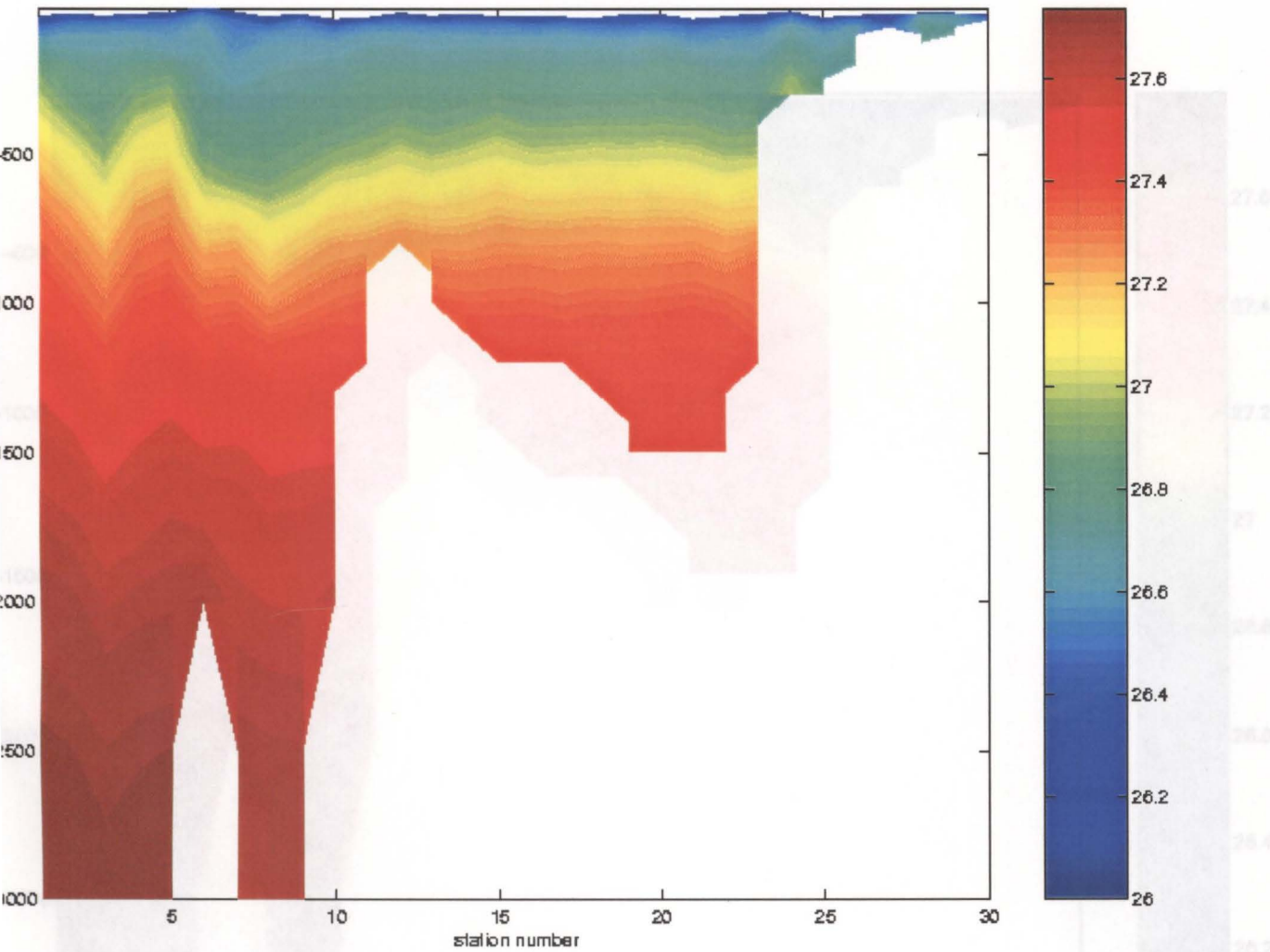

Figure 3.15. Potential Density along the P1W transect 1949-52 (referenced to surface). Density contours appear to be deeper, lacking a 26.8δ_θ outcrop at the surface.

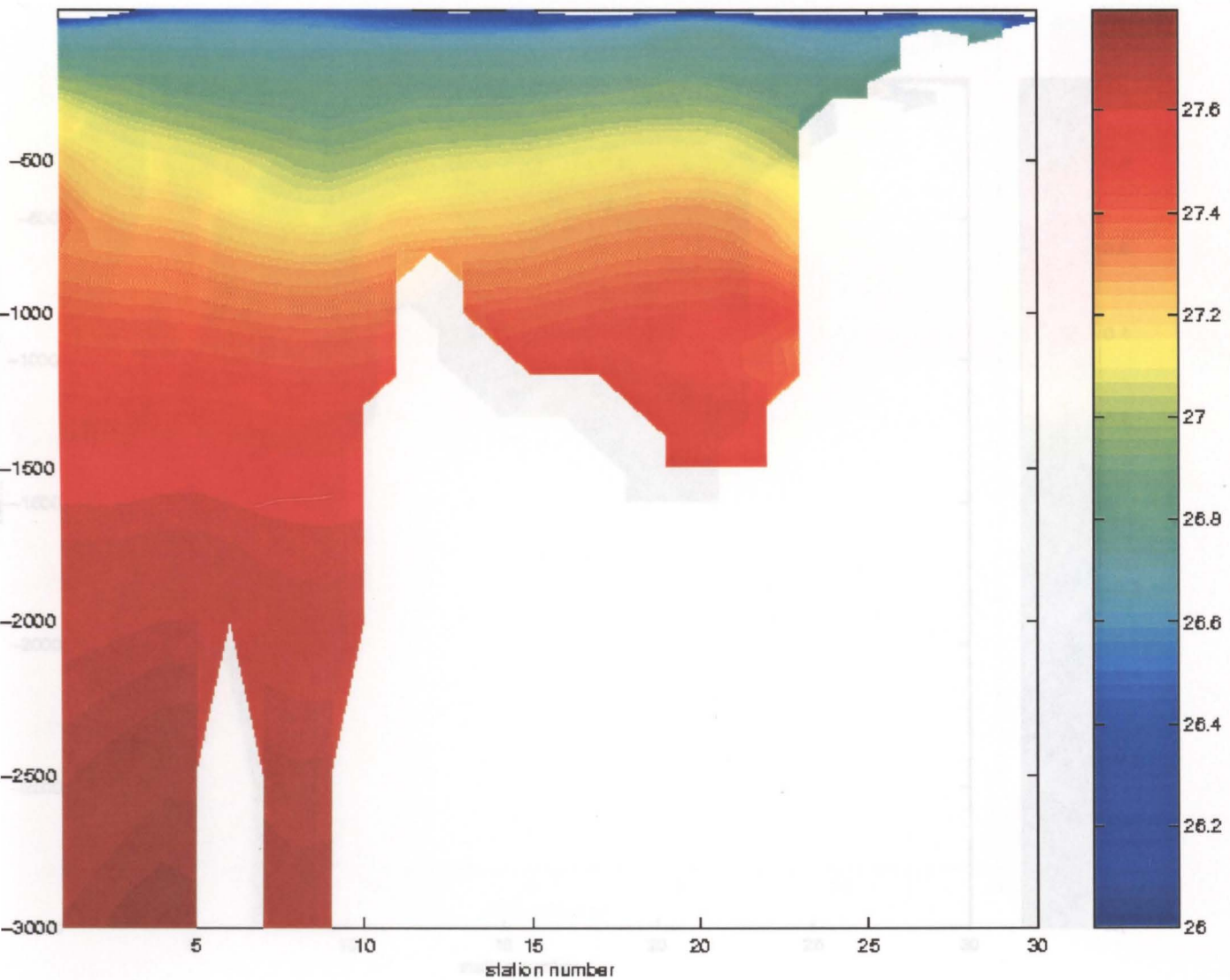

Figure 3.16. Temperature change between 1949-52 and 1993 along line P1W. This shows significant warming at the surface, and down to 800m through the Bussol Strait and either side. Isolated positive and negative anomalies are evident in the region below the surface, down to around 500m.

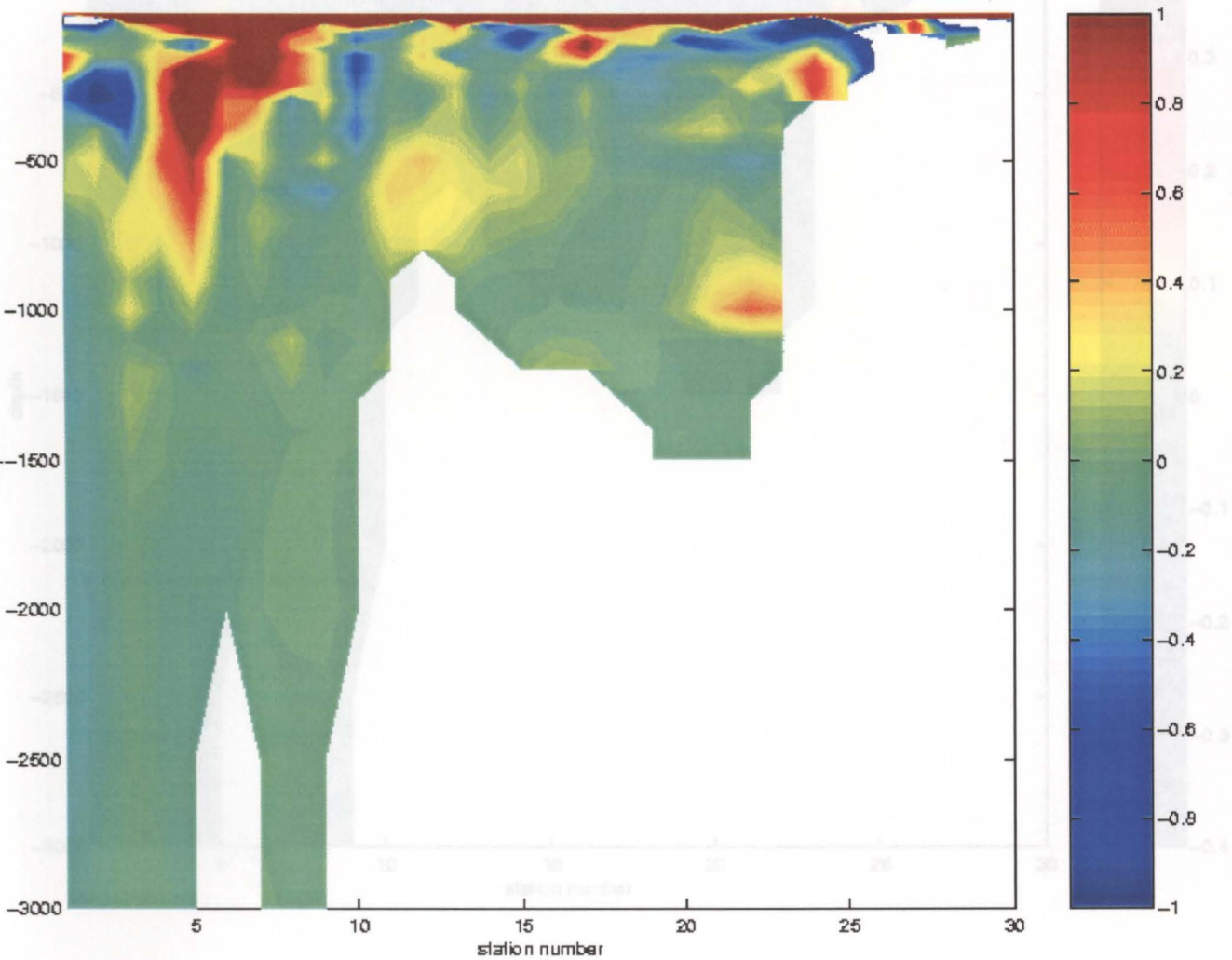

Figure 3.17. Salinity change between 1949-52 and 1993 along line P1W. This shows a clear basin wide freshening of between 0.1 and 0.4 psu. Little evidence of regions of positive anomalies to counteract this.

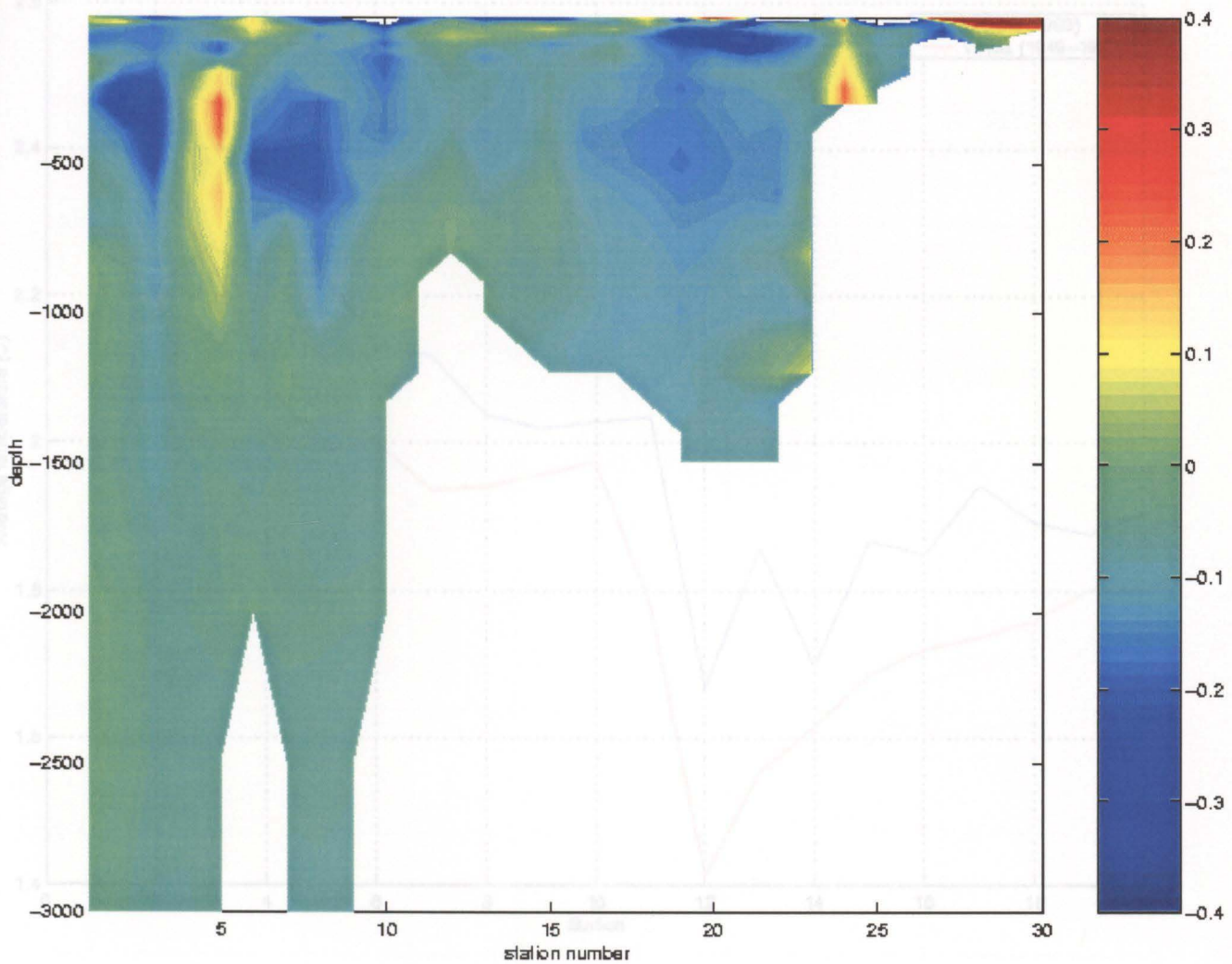

Figure 3.18. Depth averaged temperature anomaly along line P1W. This clearly shows a basin wide warming of 0.1 to 0.2 °C, apart from at the entrance into the open Pacific, which seems to have experience a general cooling of around the same magnitude.

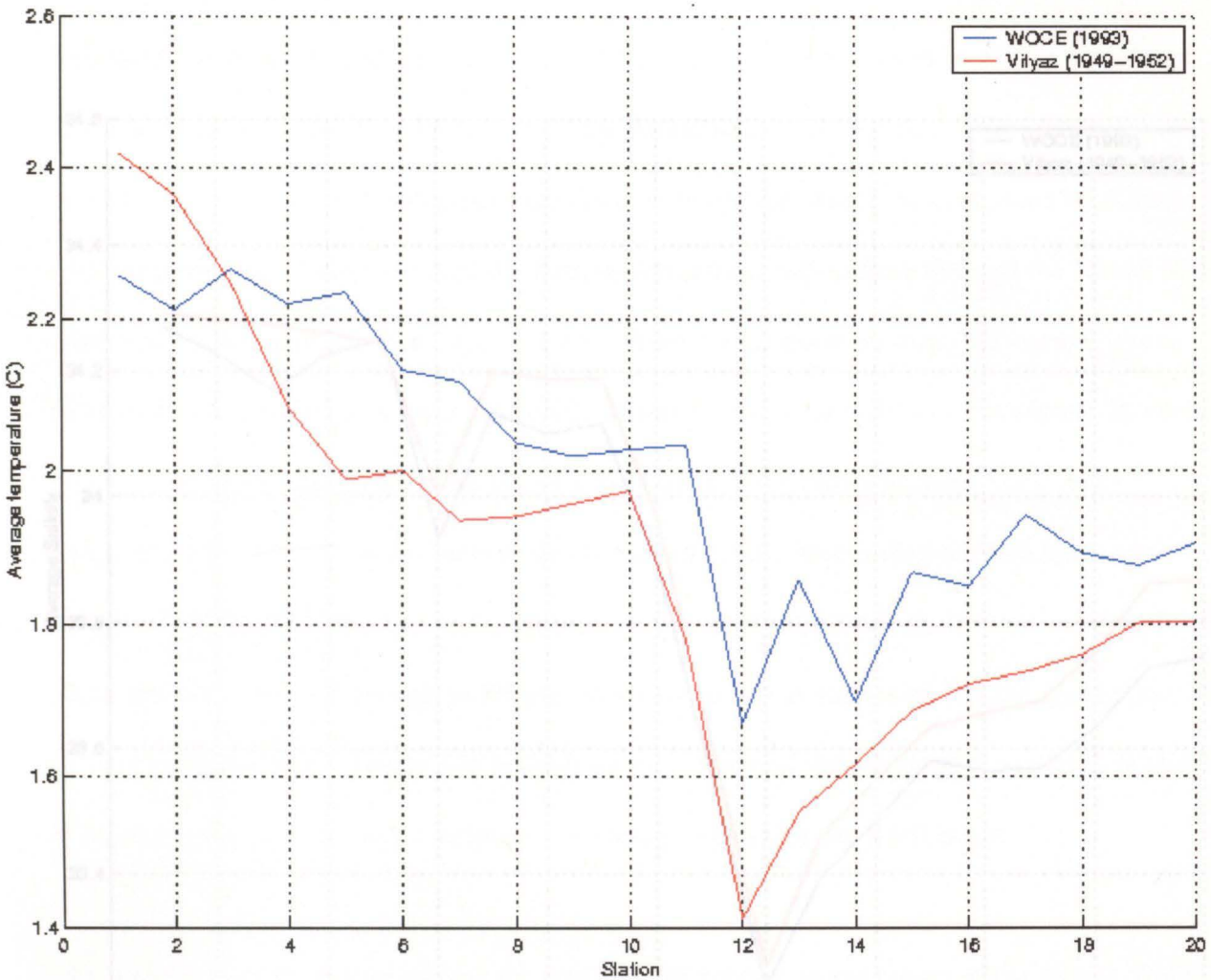

Figure 3.19. Depth averaged salinity anomaly along line P1W. This plot confirms evidence in the anomaly section of a basin-wide freshening of around 0.1psu. The minimum freshening is found between stations 9 and 12, where the Academy of Sciences Rise descends into the Kuril Basin.

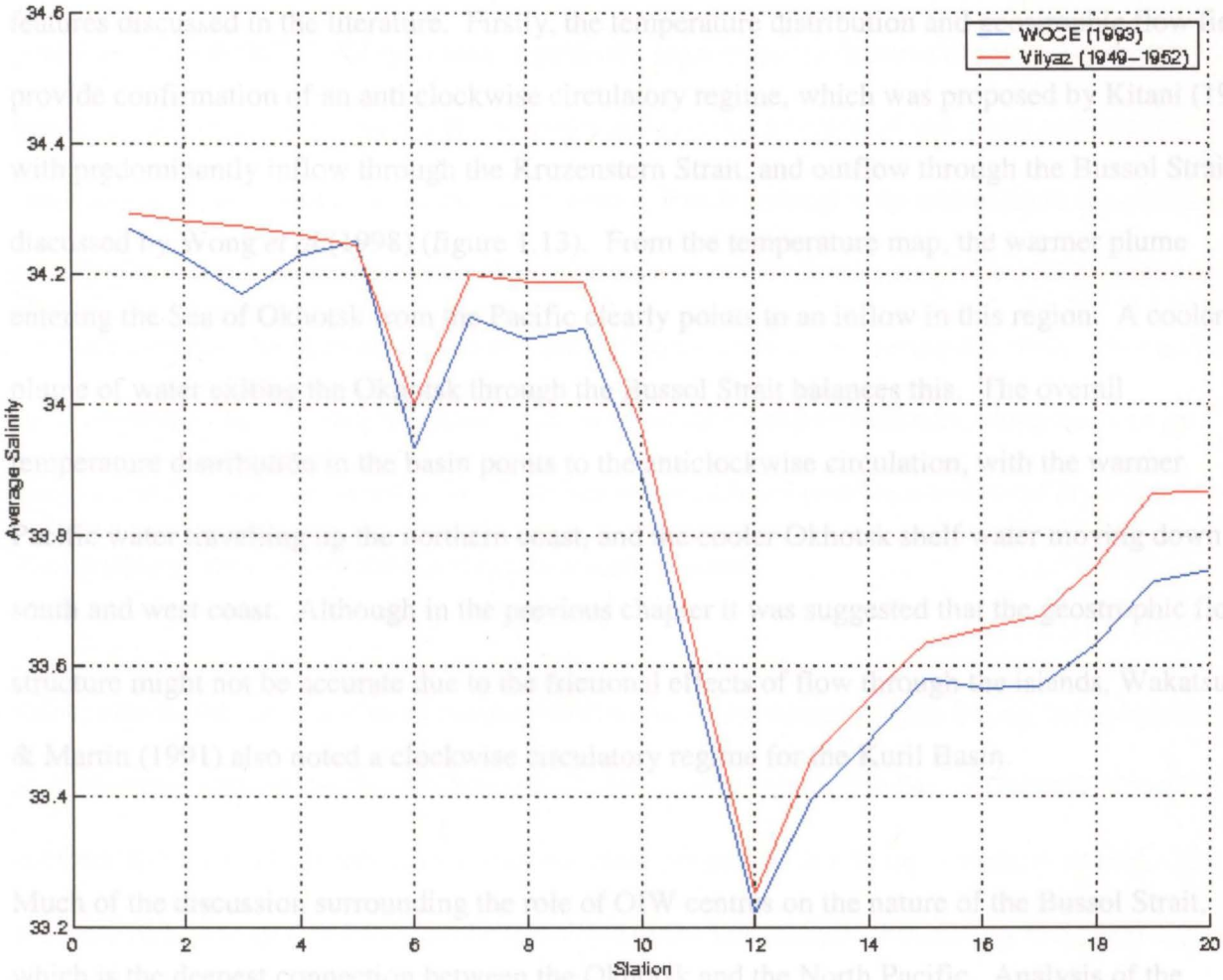

Chapter 4

Discussion

4.1. The Climatology of the Sea of Okhotsk.

The basin climatology produced from the 1949-52 data set allowed us to identify a number of features discussed in the literature. Firstly, the temperature distribution and geostrophic flow field provide confirmation of an anti clockwise circulatory regime, which was proposed by Kitani (1973) with predominantly inflow through the Kruzenstern Strait, and outflow through the Bussol Strait, discussed by Wong *et al* (1998) (figure 1.13). From the temperature map, the warmer plume entering the Sea of Okhotsk from the Pacific clearly points to an inflow in this region. A cooler plume of water exiting the Okhotsk through the Bussol Strait balances this. The overall temperature distribution in the basin points to the anticlockwise circulation, with the warmer Pacific water travelling up the northern coast, and the cooler Okhotsk shelf water moving down the south and west coast. Although in the previous chapter it was suggested that the geostrophic flow structure might not be accurate due to the frictional effects of flow through the islands, Wakatsuchi & Martin (1991) also noted a clockwise circulatory regime for the Kuril Basin.

Much of the discussion surrounding the role of OIW centres on the nature of the Bussol Strait, which is the deepest connection between the Okhotsk and the North Pacific. Analysis of the temperature, salinity and potential density cross sections of the channel (figures 3.7 to 3.9) confirm Freeland *et al's* (1998) suggestion of a two layer flow, which was inferred from nutrient

measurements. In particular, the temperature transect neatly separates the two flow components, with the cooler outflow overlying the warmer inflow.

4.2. Okhotsk structure in cross section.

Kitani (1973) was the first to publish a schematic of the vertical structure of the sea of Okhotsk, and it's transition from the shelf to the open Pacific (figure 1.12). Again, the temperature transect produced from WOCE P1W data almost perfectly represents the features described (figure 3.10). Below the defined near-surface layer of seasonal warming, a region of minimum temperature is clear, which Kitani named subsurface cold water. This is formed from waters from the northern shelf region, which maintains vertical homogeneity by convective mixing. This cold saline water is formed in winter, and moves towards the deeper regions along the continental shelf. On reaching the continental shelf it spreads horizontally on a surface of ambient density, along the western margin. As it travels south the cold subsurface water diffuses into the transitional layer below. This feature is well represented in the temperature transect.

Kitani also noted the densities of mesothermal water in the western North Pacific were equivalent to the bottom water in the Sea of Okhotsk. However, on entering the Sea of Okhotsk through the northern Kuril Islands, it rapidly loses its signature properties due to rapid vertical mixing. The southern remnants of this input can be identified in the temperature transect, by the warm intrusion in into the Okhotsk Transitional waters at around 500-1000m. This signature is abruptly weakened on reaching the Kuril Shelf. Kitani concluded that this North Pacific Transitional Water (NPTW) spreads northwards in the eastern Okhotsk with significant decreases in temperature and salinity,

and an increase in dissolved oxygen. A highly dynamic transitional layer is produced. This picture of subsurface mixing correlates well with the discussion of an anti-clockwise circulation above.

4.3. Changes along the P1W transect.

When comparing the temperature and salinity transects from the *Vityaz* Surveys around 1950, to WOCE in 1993, no large-scale changes in structure are evident. However, on subtracting the Vityaz transect from the WOCE transect, a consistent cooling and freshening was apparent. The temperature changes tend to be more localized but more extreme, whereas the changes in salinity appear to be more widespread. A depth-averaged warming of 0.1 - 0.3°C and a freshening of 0.04 – 0.15psu were noted. No similar studies have been performed for this region: however, Wong *et al* (1999) noted a consistent basin wide decrease in salinity at intermediate depths in the Pacific. The cause, it was suggested, was likely to be an intensification of the hydrological cycle in the high latitude source regions. This would point to the Sea of Okhotsk, which has been established as a major contributor to the NPIW. At first sight, our findings tie in very convincingly with those of Wong *et al* (1999), and provide fuel to the mounting evidence of change in the ocean-atmosphere system, and more clues to the response of the intermediate/deep ocean to surface changes. However, there is one question that still springs to mind: would such a confined region be capable of causing the observed large scale freshening?

4.4. Fluxes through the Sea of Okhotsk.

Salt flux calculations, summarised in table 3.1, allow us to explore the possible influence of the Sea of Okhotsk on NPIW under different flow scenarios. Wong *et al* (1999) noted a 0.1psu freshening between 1930 and 1985 along 47°N. Results show that with an increase in Bussol Strait outflow, the changes in the Pacific could largely be caused by changes in the Okhotsk basin. From our calculations, a linear increase in outflow between 1950 and 1993 of 2Sv would cause a reduction in salinity of 0.061 psu. Interestingly, we noted a change of 0.06psu at the outermost station (station 1 of the WOCE transect) over the same time period. These findings are significant as they quantitatively correlate the changes noted by Wong *et al* in the Open Pacific, with the changes we have seen in the Sea of Okhotsk. It also establishes the importance of the Sea of Okhotsk in mediating changes in the intermediate North Pacific. As noted in section 1.8, the physics of the Mediterranean and the Sea of Okhotsk could be classed as opposite in terms of their climate and mixing dynamics. Nevertheless, similarity can be identified in terms of changes in such a small, enclosed volume having a significant influence on the behaviour of the open ocean.

We can also tie our findings in with theories presented by Levitus (2000), who identified a global mean warming of 0.06°C in subsurface waters (300-1000m). This was attributed to convection communicating surface changes to the deeper water masses, citing regions such as the Labrador Sea as an example. Like the Labrador Sea, the Sea of Okhotsk is likely to respond quickly to external forcing, such as enhanced atmospheric warming, and hydrological cycle, due to it's high latitude, and enclosed geography. These changes are communicated to the deeper open ocean through the interaction of Okhotsk Intermediate Water with the inflowing Oyashio Water.

4.5. Caution: Long term change or variations?

When infering change from two snapshots in time such as this, we must caution against automatically infering the differences being a result of long term change. In section 1.8, the role of low frequency variability was discussed, and figure 3.3b shows a relationship between the PDO and satellite sea surface temperature anomalies. It cannot be determined with any certainty that the changes identified between 1949-52 and 1993 are solely a result of long term change. However, it is unlikely that the magnitude of change identified in chapter 3 would be as a result of short term variability. In addition, these results tie in nicely with the literature, all of which points to long term warming and freshening of NPIW. With this in mind, it is unlikely that the changes noted are dominated by variations in the system.

The findings summarised above establish the importance of the Sea of Okhotsk in the Global Ocean structure. Such significant changes over the past half-century highlight the need for continued monitoring of such a dynamic region, which is evidently exhibiting significant changes.

References

Alfultis, M.A. & S. Martin (1987). Satellite passive microwave studies of the Sea of Okhotsk ice cover and it's relation to ocean processes, 1978-1982. *Journal of Geophysical Research.* 92(C12) 13 013- 13 028.

Aota, M. (1975) Studies on the Soya Warm Current. *Low-Temperature Science.* A33 151-172 (in Japanese).

Belkin, I.M., S. Levitus, J. Antonov & S-A. Malmberg (1998). "Great Salinity Anomalies" in the North Atlantic. *Progress in Oceanography.* 41 1-68.

Bearman, G. (ed) (1995). Ocean Circulation. *Open University/Pergamon Press.* 238pp.

Bethoux, J.P., B. Gentili, P. Morin, E. Nicolas, C. Pierre & D. Ruiz-Pino (1999). The Mediterranean Sea: a miniture ocean for climatic and environmental studies and a key for the climatic functioning of the North Atlantic. *Progress in Oceanography.* 44 131-146.

Bretherton, F.P. R.E. Davis, & C.B. Fandry (1976) A technique for objective analysis and design of oceanographic experiments applied to MODE-73. *Deep Sea Research* 23 559-582.

Broecker, W.S., T.H. Peng, J. Jouzel, G. Russel (1990) The magnitude of global freshwater transports of importance to ocean circulation. *Climate Dynamics.* 4 79-89

Bryden, H.L. et al (1996) Decadal changes in watermass characteristics at 24N in the subtropical North Atlantic Ocean. *Journal of Climate*. 9 3162-3186.

Delworth, T.L. & K.W. Dixon (2000) Implications of the recent trend in the Arctic/North Atlantic Oscillation for the North Atlantic Thermohaline Circulation. *Journal of Climate*. 13(21) 3712.

Dickson, R., J. Lazier, J. Meincke & P. Rhines. (1996) Long term coordinated changes in the convective activity of the North Atlantic. *NATO ASI series, Vol I 44. Decadal climate variability dynamics and predictability. Ed. D.L.T. Anderson & J. Willebrand.* 211-253.

Dickson, K.W. (2000) From the Labrador Sea to global change. *Nature* 386 649-650.

Farmer, D.M. & L. Armi (1999) Stratified flow over topography: the role of small scale entrainment and mixing in flow establishment. *Proceedings of the Royal Society of London.* A 455 3221-3258.

Favourite, F., A.J. Dodimead & K. Nasu (1976) Oceanography of the subarctic Pacific region, 1960-1971. *International North Pacific Fisheries Commision.* 33 187pp

Freeland, H.J. (in press) Observations of the flow of abyssal water through the Samoa Passage.

Freeland, H.J., A.S. Bychkov, F. Whitney, C. Taylor, C.S. Wong & G.I. Yurasov (1998). WOCE section P1W in the Sea of Okhotsk, 1. Oceanographic data description. *Journal of Geophysical Research.* 103(C8) 15613-15623.

Freeland, H., K. Denman, C.S. Wong, F.Whitney & Renee Jacques (1997) Evidence of change in the winter mixed layer in the Northeast Pacific Ocean. *Deep Sea Research 1.* 44(12) 2117-2129.

Garrett, C.J., M. Bormans & K. Thompson(1987) Is the exchange through the Strait of Gibraltar maximal or submaximal? *Proceedings of the NATO/ONR Workshop on Physical Oceanography of Sea Straits.* ed. L.J. Pratt, Kluwer, 271-294.

Garrett, C.J.& B. Petrie (1981). Dynamical aspects of the flow through the Strait of Belle Isle. *Journal of Physical Oceanography.* 11, 376-393.

Gladyshev, S.V. (1998a) Thermohaline structure of the bottom water on the Northern Okhotsk Sea Shelf. *Russian Meteorology and Hydrology.* 3 39-46.

Gladyshev, S.V. (1998b) Estimation of cold dense water formation of the Northern Shelf of the Sea of Okhotsk. *Russian Meteorology and Hydrology.* 4 53-59.

Gilman, C. & Garret, C. (1994). Heat flux parameterisations for the Mediterranean sea: The role of atmospheric aerosols and constraints from the water budget. *Journal of Geophysical Research.* 99(C3) 5119-5134.

Gordon, H.B. & S.P. O'Farrell (1997) Transient climate change in the CSIRO coupled model with dynamic sea ice. *Monthly Weather Review.* 125 875-907.

Hatakeyama, Y., S. Tanaka, T. Sugimura & T. Nishimura (1985). Surface currents around Hokkaido in the late fall of 1981 obtained from the analysis of satellite images. *Journal of the Oceangoraphy Society of Japan.* 41 327-338.

Kajiura, K. (1949) On the hydrography of the Okhotsk Sea in summer. *Journal of the Oceanography Society of Japan.* 5 19-26 (in Japanese).

Kawasaki, Y. & T. Kono (1995) Distribution and transport of Subarctic waters around the middle of Kuril Islands. *Umi to Sora.* 70(2) 71-84

Kitani, K. (1973). An Oceanographic Study of the Okhotsk Sea- Particularly in respect to cold waters. *Bulletin of the Far Seas Fisheries Research Laboratory.* 9 45-76.

Kono, T. & Y. Kawasaki (1997) Modification of western subarctic water by exchange with the Okhotsk Sea. *Deep Sea Research 1.* 44 689-711.

Kovshov V.A. & Y.N. Sinyurin (1982). Permanent spareness of the ice cover in open areas of the Okhotsk Sea. *Meteorol. Gidrol.* 11 76-81.

Kurashina, S., K. Nishida & S. Nakayashi (1967) On the open water in the southeastern part of the frozen Okhotsk Sea and the currents through the Kuril Islands. *Journal of the Oceanographical Society of Japan.* 23 57-62.

Kuz'mina, N.P. & V.E. Skylarov (1984) Drifting ice as a tracer for the study of the general circulation of marginal seas. *Issled. Zemli Kosm.*1 16-25 (in Russian).

Leonov, A.K. (1990) The Sea of Okhotsk. *NTIS AD 639 585.* National Technological Information Service, Springfield, Va., 95pp.

Levitus, S., J.I. Antonov, T.P. Boyer, C. Stephans (2000). Warming of the world ocean. *Science* 287 2225-2229.

Manabe, S., K. Bryan & M.J. Spelman (1990) Transient response of a global ocean atmosphere model to a doubling of carbon dioxide. *Journal of Physical Oceanography* 20 722-749

Manabe, S., R.J. Stouffer, M.J. Spelman & K. Bryan (1991) Transient responses of a coupled ocean-atmosphere model to gradual changes of atmospheric CO_2. Part 1. annual mean response. *Journal of Climate* 4 785-818.

Martin, S., R. Drucker & K. Yamashita (1998) The Production of ice and dense shelf water in the Okhotsk Sea polynias. *Journal of Geophysical Research,* 103(C12) 27 771-27 782.

Miller, G.R. (1966) The flux of tidal energy out of the deep ocean. *Journal of Geophysical Research.* 71 2485-2489.

Moroshkin, K.V.(1966) Watermasses of the Sea of Okhotsk. U.S Department of Commerce; Clearinghouse for Federal Scientific and Technical information, Joint Publication Research Service 43 942 98pp.Translation of *Vodnyye Massy Okhotskogo Morya,* Nauka Publishing House, Moscow, 66pp.

Murphy, J.M., & J.F.B. Mitchell (1995) Transient response of the Hadley Centre coupled climate model to increasing carbon dioxide. Part 2. Spatial and temporal structure of response. *Journal of Climate.* 8 57-80.

Myers, P.G. & A.J. Weaver (1997) On the circulation of the North Pacific Ocean: climatology, seasonal cycle, and interpentadal variability. *Progress in Oceanography.* 38(1) 1-49.

Overland, J.E. & S. Salo (1999). Salinity signature of the Pacific Decadal Oscillation. *Geophysical Research Letters* 26(9) 1337-1340.

Pond, S. & G.L. Pickard. (1983). Introductory dynamical oceanography. 2nd Ed. *Butterworth Heinman.* 329pp.

Preller & Hogan (1998) Oceanography of the Okhotsk and the Japan /East Sea. *The Sea.* 11 429-482.

Read, J.F. & W.J. Gould (1992) Cooling and freshening of the subpolar North Atlantic Ocean since the 1960's. *Nature.* 360 55-57

Reid J.L. (1965) Intermediate waters of the Pacific Ocean, *John Hopkins Oceanography Studies.* 5 96pp.

Reid, J.L (1973) The shallow salinity minima of the Pacific Ocean. *Deep Sea Research.* 20 51-68.

Reid, J.L. (1973) Northwest Pacific Ocean waters in winter. *John Hopkins Oceanography Studies.*

Reid, J.L. (1997) On the total Geostrophic circulation of the Pacific Ocean: Flow patterns, tracers, and transports. *Progress in Oceanography.* 39 263-352.

Riser, S.C., Exchange of water between the Okhotsk Sea and the North Pacific Ocean through the Kurile Straits. *Proceedings of the International Workshop on the Okhotsk Sea and the Arctic.* T. Takizawa, ed. Science and Technology Agency of Japan. 205pp.

Rogachev, K.A. (2000) Recent variablility in the Pacific western subarctic boundary currents and the sea of Okhotsk. *Progress in Oceanography.* 47 299-336.

Ruddick, B.R. (1983) A practical indicator of the stability of the water column to double diffusive activity. *Deep Sea Research. Part A.* 30 1105-1107.

Sekine, Y., (1988) Anomalous southward intrusion of the Oyashio east of Japan. 1. Influence of the seasonal and interannual variations in the wind stress over the North Pacific. *Journal of Geophysical Research.* 93 2247-2255.

Suzuki, K. and S. Kanari (1986) Tidal Simulation of the Sea of Okhotsk. *Kaiyo Kagaku.* 18 455-463 (in Japanese).

Talley, L.D. (1997) North Pacific water transports and the mixed water region. *Journal of Physical Oceanography.* 27 1795-1803.

Tally, L.D. & Y. Nagata (1995) The Okhotsk Sea and Oyashio region. *PICES Scientific Report.* 2 227pp

Talley, L.D., Y. Nagata, M. Fujimura, T. Iwao, T. Kono, D. Inake, M. Hirai & K. Okuda (1995). North Pacific Intermediate Water in the Kuroshio/Oyashio mixed water region. *Journal of Physical Oceanography.* 25 475-501.

Talley, L.D. (1993) Distribution and formation of North Pacific Intermediate water. *Journal of Physical Oceanography.* 23 517-537.

Talley L.D. (1991) An Okhotsk Sea anomaly: Implications for ventilation in the North Pacific. *Deep Sea Research. Part A.* 38 S171-S190.

Toulany, B., B. Petrie and C. Garrett (1987). The frequency-dependant dynamics of flow fluctuations in the Strait of Belle Isle. *Journal of Physical Oceanography* 17 185-196.

Tragou, E. & C. Garrett (1997) The shallow thermohaline circulation of the Red Sea. *Deep Sea Research I* 44(8) 1355-1376.

Vanin, N.S.& G.I. Yusasov (1998) Water exchange between the Okhotsk Sea and Pacific Ocean in Bussol and Krusenstern Straits. *Russian Meteorology and Hydrology.* 7 62-68.

Van Scoy, K.A., D.B. Olson & R.A. Fine (1991) Ventilation of the North Pacific Intermediate Waters: The role of the Alaskan Gyre.*Journal of Geophysical Research.* 96 C9 16 801–16 810.

Wakatsuchi, M. and S. Martin (1991) Water circulation of the Kuril Basin of the Okhotsk Sea and its relation to eddy formation. *Journal of the Oceanograpy Society of Japan.* 47 152-168.

Warren, B.A. (1981) Deep circulation of the World Ocean. In: *Evolution of Physical Oceanography,* ed B.A. Warren & C.Wunsch. p.6-41. Cambridge MA. pp620.

Weaver, A.J., J. Marotzke, P.F. Cummins & E.S. Sarachik (1993) Stability and variability of the Thermohaline Circulation. *Journal of Physical Oceaography.* 23(1) 39-60.

Whitehead, J.A. (1998) Topographic control of oceanic flows in deep passages and straits. *Reviews of Geophysics.* 36(3) 423-440.

Wong, A.P.S., N.L. Bindoff & J.A. Church (1999) Large-scale freshening of intermediate waters in the Pacific and Indian Oceans. *Nature* 400 440-443.

Wong, C.S., R.J. Matear, H.J. Freeland, F.A. Whitney & A.S. Bychkov (1998) WOCE line P1W in the Sea of Okhotsk. 2. CFC's and the formation rate of intermediate water. *Journal of Geophysical Research.* 103(C8) 15625-15642.

Wunsch,C.(1996) The ocean circulation inverse problem. *Cambridge University Press* 442pp.

Wüst, G. (1930) Meridionale Schichtung und Tiefenzirkulation in der Westhalften der drei Ozeane. *Journal du Consei, Conseil Internationale pour l'Exploration de la Mer.* 5 21pp.

Yasuda, I. (1997) The origin of North Pacific Intermediate Water. *Journal of Geophysical Research.* 102(C1) 893-909.

Yasuda, I., K. Okuda & Y. Shimizu (1996) Distribution and modification of North Pacific Intermediate Water in the Kuroshio-Oyashio interfrontal zone. *Journal of Physical Oceanography.* 26 448-464.

Yasuoka T. (1967) Hydrography of the Okhotsk Sea – (1). *The Oceanographical Magazine.* 19 61-72.

Yasuoka T. (1968) Hydrography of the Okhotsk Sea – (2). *The Oceanographical Magazine.* 20 55-63.

You, Y., N. Suginohara, M. Fukasawa, I. Yasuda, I. Kaneko, H. Yoritaka & M. Kawamiya (2000) Roles of the Okhotsk Sea and the Gulf of Alaska in forming the North Pacific Intermediate Water. *Journal of Geophysical Research*. 105(C2) 3253-3280.

VITA

Surname: Hill Given Names: Katherine Louise

Place of Birth: Leicester, Leicestershire, United Kingdom

Educational Institutions Attended:

University of Victoria	1999-2001
University of Southampton	1995-1998

Degrees Awarded:

B.Sc. (Honours) University of Southampton 1998

Publications:

Extratropical planetary wave propagation characteristics from ATSR global Sea Surface Temperature Record.
K.L. Hill, I.S. Robinson and P. Cipollini.
Journal of Geophysical Research - Oceans. 105(C9) 21 927 - 21946, September 2000

Global characteristics of Rossby wave propagation from multiple satellite datasets.
P.G. Challenor, P. Cipollini, D. Cromwell, K.L. Hill, G.D. Quartly and I.S. Robinson.
Submitted to: *International Journal of Remote Sensing*, January 2001.

UNIVERSITY OF VICTORIA PARTIAL COPYRIGHT LICENSE.

I hearby grant the right to lend my thesis (or dissertation) to users of the University of Victoria Library and to make single copies only for such users or in response to a request from the library of any other university, or similar institution, on its behalf or for one of its users. I further agree that the permission for extensive copying of this for scholarly purposes may be granted by me or a member of the University designated by me. It is understood that copying or publication of this thesis for financial gain by the University of Victoria shall not be allowed without my permission.

Title of Thesis:

Evidence of change in the Sea of Okhotsk between 1949-1952 and 1993 from Hydrographic Data: Implications for the North Pacific.

Author: [redacted]

Katherine Louise Hill

December 12, 2001